The c-Myc/TBX3/nucleolin/Hsc70 signalling axis in breast cancer

By Stephanie Maria Ncube

(NCBSTE003)

Submitted to the University of Cape Town

In fulfilment of the requirements for the degree

MSc (Med) in Medical Cell Biology

Department of Human Biology

Faculty of Health Sciences

University of Cape Town

23 January 2019

Supervisor: Professor Sharon Prince

Declaration

I, Stephanie Maria Ncube, hereby declare that the work on which this dissertation/thesis is based is my original work (except where acknowledgements indicate otherwise) and that neither the whole work nor any part of it has been, is being, or is to be submitted for another degree in this or any other university.

I empower the university to reproduce for the purpose of research either the whole or any portion of the contents in any manner whatsoever.

Signed by candidate

Stephanie Maria Ncube
23 January 2019

Acknowledgements

I would like to express my deep gratitude to the following people for their continued support throughout my Masters:

My supervisor, **Professor Sharon Prince**, for her constant support throughout my MSc. Her constant encouragement and faith in me have pushed me to strive to become a better scientist and researcher. I feel so privileged to have been under her tutelage and I am grateful for the skills that I have gained throughout this experience. I would also like to thank **Dr Tarryn Willmer** for her support and input with this project.

The **T-box lab members** for their continued support and advice. Many thanks to **Alexis, Rehana, Dr Jade Peres and Dr Arul Jothi** for dedicating their time to assist me with several technical aspects of this project and for help with proof-reading my thesis. Thank you **Alexis** for your constant words of wisdom and upliftment- I will miss them dearly. The members of the Blackburn lab also must be thanked, in particular **Dr Clemens Hermann** for cheerfully assisting me with my mass spectrometry experiments and data analysis.

A special thanks to my friends for their support throughout my studies. To my best friend **Anesu**, thank you for your endless love and encouragement and for being by my side through the highs and the lows. **Lihle** and **Luqmaan**, thank you for being a constant source of much needed comic relief along the way. To my siblings, **Loraine**, **Charmaine** and **Dumi**, thank you for being my cheer-leaders since day one. I love you guys.

My parents, **Stephan and Kate**, to whom this thesis is dedicated. I am eternally blessed to have parents that believe in me and constantly pray and intercede for me. Words cannot fully describe my gratitude. None of this would have been possible without their sacrifice, love and support. I love you mom and dad.

I am thankful to the almighty God for His grace and favour throughout this journey.

This work was generously supported by NRF and CANSA. Thank you for the funding and financial support that enabled this project.

Research outputs from this Masters

Oral presentations:

Willmer T, **Ncube S**, Smuts D, Smiley S, Prince S: The c-Myc/TBX3/nucleolin/Hsc70 signalling axis in oncogenesis. SASBMB- FASBMB (South African Society of Biochemistry and Molecular Biology in conjunction with the Federation of African Societies of Biochemistry and Molecular Biology) Conference, North-West University, Potchefstroom, 8-11 July 2018

Willmer T, **Ncube S**, Smuts D, Smiley S, Prince S: The c-Myc/TBX3/nucleolin/Hsc70 signalling axis in oncogenesis. Human Biology Research day, University of Cape Town, 12 September 2018

Table of contents

Abbreviations

DMEM: Dulbecco's-modified Eagle medium

DNA: deoxyribonucleic acid

EMT: epithelial-to-mesenchymal transition

FBS: fetal bovine serum

FGF: fibroblast growth factor

G-418: geneticin

Hsc: Heat shock cognate

Hsp: Heat shock protein

IP: immunoprecipitation

mRNA: messenger RNA

PBS: phosphate buffered saline

PBS/T: 1X phosphate buffered saline /0.1% Tween-20

PCR: polymerase chain reaction

qRT-PCR: quantitative real-time polymerase chain reaction

RNA: ribonucleic acid

rpm: revolutions per minute

RT: room temperature

SDS-PAGE: sodium-dodecyl-sulphate polyacrylamide gel electrophoresis

SHCTRL: positively transfected stable shCTRL control cell line

shRNA: short hairpin RNA

ShTBX3: positively transfected stable shTBX3 knockdown cell line

siCtrl: positively transfected transient siCTRL control cell line

siRNA: short interfering RNA

TBX: T-box

TGF-β: transforming growth factor beta

UMS: ulnar mammary syndrome

List of tables and figures

Abstract

The T-box transcription factor TBX3, plays critical roles in development including the formation of the limbs, heart and mammary glands. While haploinsufficiency of TBX3 results in ulnar mammary syndrome, its overexpression is linked to several cancers. We and others have shown that TBX3 drives tumour formation, invasion and metastasis of several sarcoma subtypes as well as melanoma, cervical cancer and breast cancer. TBX3 has thus been proposed as a novel therapeutic target to treat these cancers. Direct targeting of transcription factors for therapies however continues to represent a serious challenge and therefore an understanding of the molecular mechanisms that regulate and mediate its oncogenic activity may reveal more amenable anti-cancer drug targets. This project therefore aimed to (1) identify signalling molecules that upregulate TBX3 expression in MCF-7 breast cancer cells as well as (2) identify and characterize protein partners that cooperate with TBX3 to drive its oncogenic functions in these cells.

The overexpression of the basic helix-loop-helix oncogenic transcription factor c-Myc has been widely reported in breast cancer progression and c-Myc-driven pathways are elevated in aggressive drug resistant breast cancer cells and tumours. Our laboratory has previously shown that c-Myc directly binds and activates the TBX3 promoter in several sarcoma subtypes, and it was hypothesised that c-Myc may also activate TBX3 in breast cancer. To investigate this, the impact of transiently knocking down c-Myc on TBX3 mRNA and protein levels was firstly assessed by qRT-PCR and western blotting respectively. Results show that when c-Myc is depleted, TBX3 mRNA and protein levels decrease, suggesting that c-Myc may be transcriptionally upregulating TBX3. To confirm this, c-Myc was ectopically overexpressed in MCF-7 breast cancer cells in the presence or absence of Actinomycin D, an inhibitor of de novo transcription, and TBX3 mRNA and protein levels were measured by qRT-PCR and western blotting respectively. Indeed, results show that when de novo transcription is inhibited, the c-Myc mediated activation of TBX3 expression is abolished.

To identify and characterize TBX3 protein partners, MCF-7 breast cancer cells that stably overexpress FLAG-TBX3 were firstly established to enable effective immunoprecipitation

for mass spectrometry. The overexpression of FLAG-TBX3 was confirmed by western blotting and immunocytochemistry and the anti-proliferative and pro-migratory roles of TBX3 overexpression in breast cancer cells was confirmed using growth curves and scratch motility assays respectively. Through affinity purifications coupled with mass spectrometry a myriad of putative TBX3 protein co-factors were identified and from this list three partners viz nucleolin, Hsc70 and HnRNP K were validated by immunoprecipitation and colocalization experiments. Importantly, results show that the interaction of TBX3 with Hsc70 is required for TBX3 protein stability and that nucleolin and TBX3 cooperate to promote MCF-7 breast cancer cell migration. Furthermore, treatment of MCF-7 cells with the nucleolin targeting aptamer, AS1411, mislocalizes TBX3 and nucleolin to the cytoplasm and causes a reduction in cell viability while having no effect on the viability of normal skin fibroblasts. Together the results from this study show that c-Myc/TBX3/nucleolin/Hsc70 may be an important oncogenic pathway in breast cancer and that AS1411 may be a potentially important aptamer for the treatment of TBX3-driven breast cancer.

CHAPTER 1

Literature review

1.1. Introduction

Cancer is one of the major causes of death worldwide, responsible for approximately 9.6 million deaths in 2018, killing more people than AIDS, tuberculosis and malaria combined (Bray, Ferlay and Soerjomataram, 2018). According to the World Health Organization (WHO), 8.2 million cancer-related deaths and 18.1 million new cancer cases were reported globally in 2018, with approximately 70% of deaths occurring in less developed regions of the world. Of major concern is the prediction that the number of new cancer cases is expected to rise globally to 20 million by 2020 (WHO). According to the National Cancer Registry which was last updated in 2014, almost 38 thousand and 37 thousand new cancer cases were reported in females and males respectively in South Africa. Furthermore, according to Lancet Oncology the number of cancer cases in South Africa is projected to increase by 78% by 2030.

Breast cancer is the second most common malignancy globally with an estimated 20.9 million cases reported in 2018 (WHO) and it is the leading cause of cancer death in women. Furthermore, it is estimated that one in eight women will develop breast cancer in their lifetime (Ferlay *et al.*, 2014, 2015). Based on WHO statistics in 2012, South Africa reported about 9,815 cases of breast cancer (24.5% of all cancers) with 3,848 associated deaths (15.9% of all cancer deaths) (Ferlay *et al.*, 2014, 2015). Moreover, according to the National Cancer Registry which was last updated in 2014, it is projected that South Africa will have about 32,388 cases of breast cancer in the next 5 years. Despite significant progress in the treatment of breast cancer, it remains a global burden due to poor therapy response, cancer cell drug resistance and the debilitating side effects associated with most therapies. There is therefore a need to improve current breast cancer therapy and/or to develop new and efficacious therapeutic drugs. One approach to addressing this has been to elucidate the molecular mechanism(s) underpinning this disease in order to identify key drivers that can be targeted in molecular therapies. In recent years, a

plethora of studies have shown that the developmentally important T-box transcription factor, TBX3, is upregulated in several cancers, including breast cancer, where it contributes to a number of oncogenic processes. Moreover, TBX3 has been validated to be an attractive therapeutic target to treat breast and other cancers where it is overexpressed. This study explores more versatile ways of targeting TBX3 in breast cancer by identifying (1) signalling molecules responsible for upregulating TBX3, (2) protein co-factors that bind to TBX3 to stabilize the protein and (3) protein co-factors that co-operate with TBX3 to drive its oncogenic activity.

1.2. Breast cancer

Breast cancer is a heterogeneous disease with very distinct biological and pathological behaviour. It can be divided into three clinical subtypes based on the status of three key hormone receptors: (i) estrogen receptor (ER) positive, (ii) human epidermal growth factor receptor 2 (HER2) positive and (iii) triple negative (TN) which lacks the ER, HER2 and progesterone receptor (PR). The three subtypes exhibit fundamental differences with regards to biological behaviour thus requiring distinctive therapeutic interventions. ER positive breast cancer makes up nearly 70% of all breast tumours. It utilizes ER-dependent mechanisms to proliferate and thus the first line adjuvant therapies, such as tamoxifen or aromatase inhibitors, target and block the ERs (Gradishar *et al.*, 2015). HER2 positive breast cancers are more aggressive than the ER positive breast cancers and generally have a poor prognosis. They overexpress HER2 which is involved in signal transduction pathways that play key roles in cell proliferation and differentiation (Yarden Y, 2001). HER2 positive breast cancers are normally treated using monoclonal antibodies such as trastuzumab which targets HER2 or combination therapies such as Nerlynx which block the ability of the cancer cells to receive growth signals (Gradishar *et al.*, 2015). TN breast cancers (TNBCs) are the most proliferative breast cancer subtype and because they lack well defined clinical targets their treatment options are limited to standard FDA approved chemotherapy regimens such as anthracyclines, taxanes, anti-metabolites and more recently, epidermal growth factor receptor (EGFR) inhibitors (Gradishar *et al.*, 2015). While ER positive breast cancer has the best prognosis, TNBCs are extremely aggressive with the worst prognosis (Gluz *et al*., 2009).

The three breast cancer subtypes are further classified into five stages (0, I, II, III and IV) based on the TNM system (T = size of tumour, N = absence or presence of regional lymph node metastasis, M = presence or absence of distant metastasis). Stage 0 refers to early non-invasive breast cancer that is confined to the breast; stage I represents breast cancer that has invaded normal surrounding breast tissue; stage II represents invasive breast cancer that has spread to one to three axillary lymph nodes; stage III represents invasive breast cancer that has spread to four to nine lymph nodes near the breast bone; and stage IV, also known as advanced or metastatic breast cancer, represents invasive breast cancer that has spread beyond the breast to other organs of the body such as distant lymph nodes, the liver or the brain (Benson, 2003; Giuliano *et al.*, 2017). The course of treatment is therefore determined by the subtype and stage and it includes surgery, radiation therapy, hormonal therapy, conventional chemotherapy and targeted therapy (Majeed *et al*., 2014).

Treatments for stages 0, I, II and a proportion of stage III breast cancer may include (i) breast conserving surgery, which removes only the cancer cells and surrounding breast tissue, lymph node dissection and radiation therapy; (ii) mastectomy, which removes the cancerous tissue along with the entire breast; (iii) sentinel lymph node biopsy, followed by surgery; and (iv) targeted therapy. Certain stage III breast cancers may be treated with chemotherapy only or chemotherapy followed by surgery which includes lymph node resection followed by radiation therapy. According to the national cancer institute, treatment of stage IV breast cancers may include: (i) hormonal- and/or chemotherapy with or without targeted therapy; (ii) targeted therapy together with chemotherapy or (iii) radiation therapy and/or surgery for pain relief.

The effectiveness of most chemotherapeutic drugs that are currently in clinical use is, by and large, limited by their general toxicity to all proliferating cells, including “normal” cells, which results in debilitating side effects (Higgins and Baselga, 2011; Masoud *et al.*, 2017). This has thus limited the success of these therapies and necessitated the development of novel therapies (Tsuruo *et al.*, 2003). Over the last two decades, the emergence of targeted therapies for breast cancer has become a promising alternative as it has provided advances in treatment efficacy with minimal toxicities to surrounding non-cancerous cells.

1.2.1. Targeted therapy and breast cancer

Targeted therapy differs from the more conventional chemotherapeutics in that it interferes with a specific molecular target, such as a protein, that is believed to have a critical role in promoting tumour growth or progression. Therefore, in disrupting the targets on which cancer cells closely depend, targeted therapy limits the damage to non-cancerous cells. Indeed, in the past two decades, several monoclonal antibodies and small-molecule inhibitors that target components of key signal transduction pathways involved in breast cancer cell growth, survival, angiogenesis, and metastasis, have been developed and are currently in use or in clinical trials (Sawyers, 2004; Munagala, Aqil and Gupta, 2011). These include inhibitors to Raf, insulin-like growth factor, poly ADP-ribose, histone deacetylase, Hsp90, src-family tyrosinase kinases as well as inhibitors to components of the RAS/MEK/ERK, cell cycle, apoptosis, invasion and metastasis pathways (**Figure 1.1**). This section will focus on only inhibitors of HER2, EGFR and VEGF.

Human epidermal growth factor receptor 2 (HER2) receptors are part of a family of transmembrane growth factor receptors that function to activate intracellular signalling pathways in response to extracellular signals. They play pivotal roles in mammalian development and are critically involved in the development of multiple organ systems including the brain, skin, lung, and gastrointestine (Moasser, 2011). In addition, studies have reported the overexpression of HER2 in several cancers including stomach, ovary, uterine cervix, colon, bladder, lung, head and neck, and oesophageal cancers (Iqbal and Iqbal, 2014). Moreover, HER2 is overexpressed in 20–30% of breast cancer where it has been associated with increased tumorigenicity, a poor clinical outcome, and resistance to conventional hormonal chemotherapy (English, Roque and Santin, 2014). Furthermore, a study by Benz *et al.* (1992) reported that HER2 overexpressing MCF-7 breast cancer cells implanted into ovariectomized athymic nude mice, had increased tumorigenicity. HER2 positive breast cancers are currently treated with trastuzumab, a monoclonal antibody that specifically inhibits HER2 by targeted binding to its extracellular domain (Goldenberg, 1999). Trastuzumab has improved clinical outcomes for some women with HER2 positive breast cancer and does not exhibit toxic effects such as nausea and vomiting that are normally associated with chemotherapy (Feldman, Lorell and Reis,

2000). Despite the considerable clinical benefit provided, trastuzumab has been associated with cardiotoxicity events albeit mostly treatable and reversible and a large fraction of HER2 positive tumours displays primary or acquired resistance to this drug (Nahta and Esteva, 2006). However, some clinical trials have shown that combining trastuzumab with anthracycline-taxane-based neo-adjuvant chemotherapy in patients with HER2 positive breast cancer results in high pathologic complete response rate (Untch *et al.*, 2010).

Epidermal growth factor receptors (EGFRs) are transmembrane glycoproteins that contain an extracellular ligand binding domain and an intracellular receptor tyrosine kinase domain (Scaltriti and Baselga, 2006). They activate a number of pathways including Ras/MAPK, PLCγ1/PKC, PI(3) kinase/Akt, and STAT which all play a role in proliferation and migration (Scaltriti and Baselga, 2006). Several studies have reported that EGFRs are overexpressed in all breast cancer subtypes, but it is more frequently observed in TNBCs (Burness, Grushko and Olopade, 2010; Masuda, Zhang and Bartholomeusz, 2012). Moreover, the overexpression of EGFRs is associated with enhanced proliferation and migration in early stage breast cancer subtypes, large tumour size, poor differentiation and poor clinical outcome (Rakha et al., 2007). Preclinical studies involving cetuximab (erbitux), a monoclonal antibody that competitively binds with the extracellular domain of EGFR thereby inhibiting intracellular signal transduction, revealed only minimal activity and failed to show efficacy when tested in combination with paclitaxel in patients with metastatic TNBC (Garland *et al.*, 2006). In addition, several clinical studies involving another EGFR inhibitor, gefitinib, showed that it had low clinical benefit rate and no tumour response in advanced TNBC either as a single agent or in combination with chemotherapy or hormonal therapy (Green *et al.*, 2009). Dual inhibitors of EGFR and HER2 have been extensively studied for their efficacy in the treatment of breast cancer. An example is lapatinib, a potent and orally bioavailable small molecule, has shown promising clinical activity in treatment naive ER positive and HER2 positive breast cancer patients (Liao *et al.*, 2010). Lapatinib has also been shown to have less adverse effects on cardiac function compared to trastuzumab in HER2 positive breast cancer patients (Toxicity and Management, 2007). In a phase I study, a combination of the EGFR inhibitor erlotinib and trastuzumab was well tolerated and

showed preliminary evidence of anti-cancer activity in patients with HER2 positive breast cancer (Britten *et al.*, 2009).

Vascular endothelial growth factor (VEGF) is a member of a sub-family of growth factors, that play important roles in vasculogenesis and angiogenesis (Senger *et al.*, 1983). It has been implicated as a potent inducer of cell migration, invasion and metastasis and plays important roles in angiogenesis in primary invasive breast carcinomas (Weidner *et al.*, 1991). Moreover, overexpression of VEGF has been associated with poor clinical outcomes in a number of patients with different breast cancer subtypes of different stages (Lu *et al.*, 2005). There has therefore been a drive to targeting VEGF as a possible therapeutic treatment option. The VEGF inhibitor, Aflibercept, was found to inhibit tumour growth and metastasis in murine tumour models, however this was not the case in clinical trials (Holash *et al.*, 2002). However, Bevacizumab, another VEGF inhibitor, was shown to inhibit angiogenesis in patients with ER positive metastatic breast cancer and HER2 positive breast cancer patients treated with a combination of bevacizumab and trastuzumab showed encouraging results (Gray *et al.*, 2009).

Despite major advancements in the development of targeted therapy to treat breast cancer, a number of the therapies that are currently in use or in clinical trials either have variable activity, succumb to tumour resistance or in some cases simply fail to perform to expectations when used as single agents or in combination with other chemotherapeutics. There is therefore a need to discover additional effective targets that will reduce rates of relapse and improve clinical outcomes for breast cancer patients (Tsuruo *et al.*, 2003; Munagala, Aqil and Gupta, 2011). In this regard, the developmentally important T-box transcription factor TBX3 is an attractive therapeutic target since its overexpression has been shown to play critical roles in several aspects of breast cancer (Yarosh *et al.*, 2008; Fischer and Pflugfelder, 2015; Krstic *et al.*, 2016).

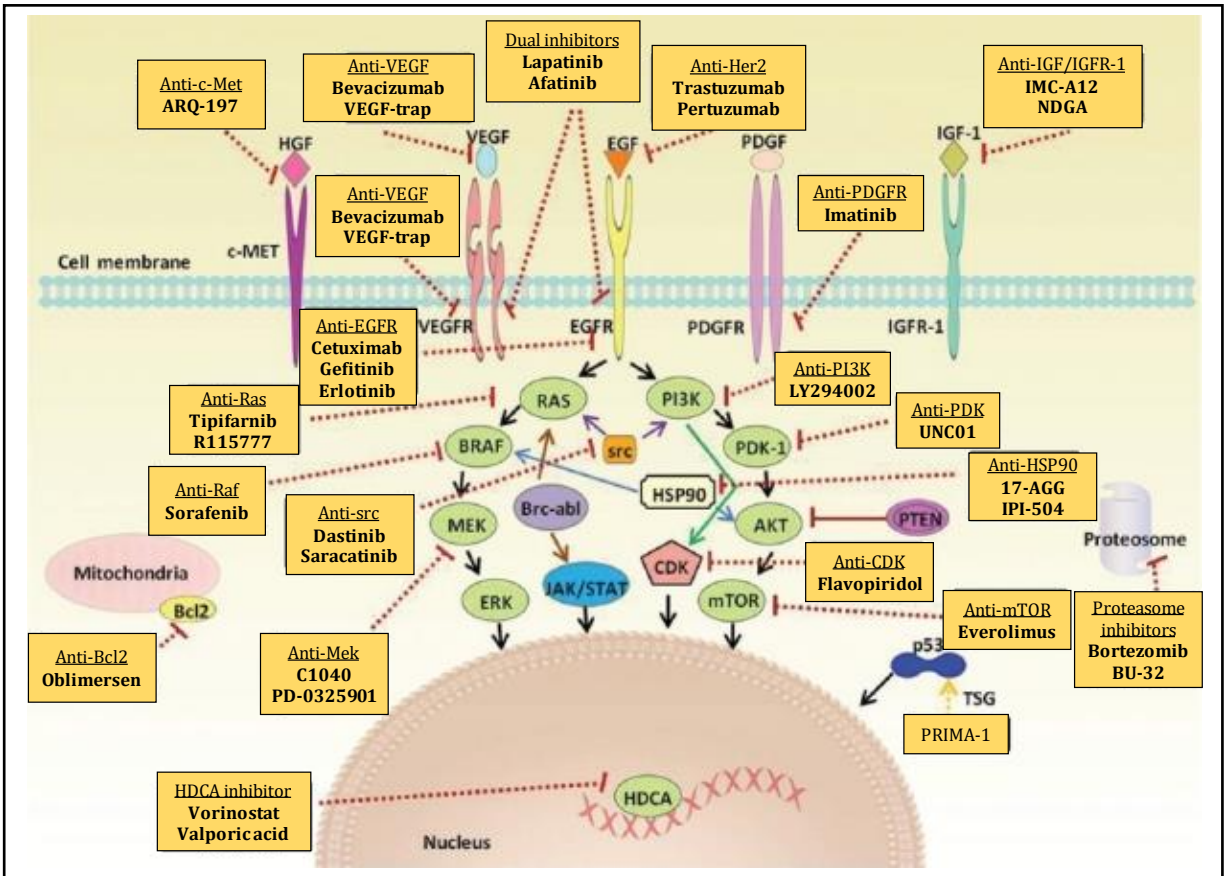

Figure 1.1. Overview of targeted therapy agents in breast cancer (Adapted from Munagala, Aqil and Gupta, 2011)

1.3. T-box transcription factor family

Brachyury is the prototype of the T-box family. It was discovered in 1927 by Nadine Dobrovoskaia-Zavadskaia, who noticed that mice with a heterozygous mutation in this gene experienced stunted tail development, hence the name *Brachyury*, a Greek term that translates to "short tail" (Dobrovolskaïa-Zavadskaïa *et al*., 1927). More than sixty years later, a group of researchers discovered that *Brachyury* exhibits dosage sensitivity as different allelic forms of the gene produced varying protein levels and thus resulted in different severities of the "short-tail" phenotype in mice (MacMurray and Shin, 1988). The *Brachyury* gene was cloned in 1990 and was characterised as a transcription factor with an N-terminal DNA-binding domain which recognizes a palindromic sequence T(G/C)ACACCTAGGTGTGAAATT known as a T-element (Herrmann *et al.*, 1990; Kispert, Koschorz and Herrmann, 1995). The C-terminus of Brachyury was later discovered to

have transactivation and repression domains thereby suggesting that the protein could function as a transcriptional activator and/or repressor (Kispert *et al.*, 1995; E S Casey *et al.*, 1998; Naiche *et al.*, 2005). Since then, several orthologues of *Brachyury* were identified in different species including the fruit-fly *Drosophila melanogaster*, the frog *Xenopus Laevis*, the ascidian *Halocynthia roretzi* and the chick *Gallus domesticus*, where they are fundamental for germ layer specification, cell-fate determination, limb patterning and organogenesis (Smith *et al.*, 1991; Pflugfelder *et al.*, 1992; Kispert *et al.*, 1995; Naiche *et al.*, 2005).

To date, more than fifty T-box family members have been identified, of which 18 are found in humans (Agulnik *et al.*, 1996; Papaioannou, 2014), and they all share a highly conserved DNA-binding motif (T-box) characterised by a 200 amino acid sequence located in their N-termini (**Figure 1.2A**) (Stott, Kispert and Herrmann, 1993; Bollag *et al.*, 1994; Tada and Smith, 2001; Wilson and Conlon, 2002). Phylogenetic analyses revealed that the T-box gene family traced back to a common ancestor and due to several gene duplications diverged along different lineages, thereby giving rise to different paralogues which have been grouped into 5 subfamilies namely: *Brachyury (T)*, *T-brain1 (Tbr1*), *TBX1*, *TBX2* and *TBX6* (Agulnik *et al.*, 1996; Papaioannou, 2014) (**Figure 1.2B**).

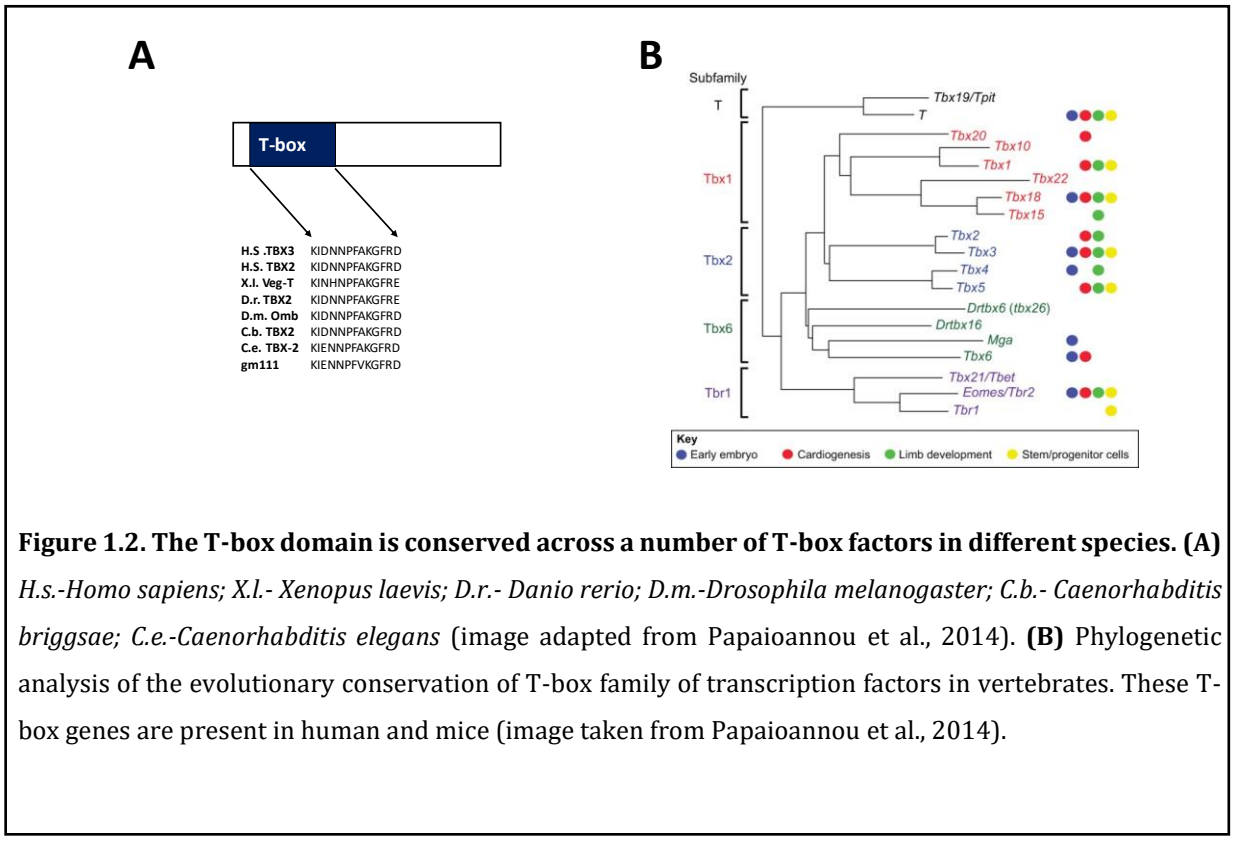

Figure 1.2. The T-box domain is conserved across a number of T-box factors in different species. (A) *H.s.-Homo sapiens; X.l.- Xenopus laevis; D.r.- Danio rerio; D.m.-Drosophila melanogaster; C.b.- Caenorhabditis briggsae; C.e.-Caenorhabditis elegans* (image adapted from Papaioannou et al., 2014). **(B)** Phylogenetic analysis of the evolutionary conservation of T-box family of transcription factors in vertebrates. These T-box genes are present in human and mice (image taken from Papaioannou et al., 2014).

It is worth noting that T-box factors can act as either transcriptional repressors or activators and, in some cases, they can act as either. For example, while TBX15, TBX18 and TBX22 act as transcriptional repressors (Jacobs *et al.*, 2000; Carlson *et al.*, 2001; Prince *et al.*, 2004; Andreou *et al.*, 2007; Farin *et al.*, 2013), TBX1, TBX6 and TBX19 act as transcriptional activators (Elena Silva Casey *et al.*, 1998; Maira *et al.*, 2003; Zaragoza *et al.*, 2004; Ataliotis *et al.*, 2005; Stennard *et al.*, 2005; González *et al.*, 2013). Depending on the cellular context, TBX2, TBX3, TBX5, TBX20 and TBX24 are capable of functioning as either repressors or activators (Carreira *et al.*, 1998; Hurlin *et al.*, 1999; Takeuchi *et al.*, 1999; Carlson *et al.*, 2001; Paxton *et al.*, 2002; Prince *et al.*, 2004; Singh *et al.*, 2005; Stennard *et al.*, 2005; Kawamura, Koshida and Takada, 2008; Sakabe *et al.*, 2012; Tarryn Willmer *et al.*, 2016). Studies have shown that although T-box factors bind the same consensus T-element in vitro as either a monomer or dimer, they frequently bind highly degenerate sites in vivo. Importantly, they regulate different target genes and consequently they have very distinct functions (Kispert and Herrmann, 1993; Papapetrou, Edwards and Sowden, 1997; Hsueh *et al.*, 2000; Jacobs *et al.*, 2000; Papaioannou, 2014). This is thought to result from their interaction with different protein co-factors. Indeed, several co-factors that regulate T-box factor functions during development have been identified and a few examples are described below.

In mouse, *Tbx2*, *Tbx3*, *Tbx5 and Tbx20* interact with the homeobox protein Nkx2-5 resulting in synergistic transcriptional regulation of genes involved in cardiac development (Hiroi *et al.*, 2001; Habets *et al.*, 2002; Hoogaars *et al.*, 2004, 2008; Stennard *et al.*, 2005; Bakker *et al.*, 2008). Lamolet *et al.* (2001) observed that during pituitary development, TBX19 co-operates with the homeoprotein Pitx, where both proteins bind to a regulatory region within the *pro-opiomelanocortin* (*POMC*) gene promoter to drive its expression. Furthermore, through mutational studies, the authors showed that mutations within *Pitx* or its binding sites lead to disruption of POMC transcription, highlighting the importance of this interaction. Miller and Okkema (2011) reported that the nematode T-box factor MLS-1 interacts with UNC-37 through a highly conserved eh1 motif to regulate its target genes during uterine muscle specification. Boogerd *et al.* (2011) have shown that TBX3 requires SOX4 in order to regulate *Connexin43* (*Cx43*) expression during heart development in zebrafish. Kawamura, Koshida and Takada. (2008) reported that Ripply1 interacts with zebrafish T-box proteins, TBX24 and Ntl, and

converts them from activators to repressors during somite segmentation. A study by Murakami *et al.* (2005) reported that TBX5 directly interacts with the co-activator Tafazin (TAZ), and histone acetyltransferases p300 and PCAF, to stimulate TBX5 dependent promoters in cardiac and limb development. In addition, T-box factors have also been reported to interact with chromatin remodelling factors to regulate their target genes at an epigenetic level (Kumar *et al.*, 2014). For example, Tbx3 has been reported to maintain the extraembryonic endoderm differentiation potential of ESCs by direct interaction with, and epigenetic modification of, H3K27-methyltransferase on the Gata6 promoter (Lu *et al*., 2011). A study by Miller *et al.* (2008) reported that Tbx5, Brachyury and Eomesdermin interact with H3K4-methyltransferase and H3K27 demethylase to mediate the activation of target gene expression during cellular differentiation.

1.3.1. T-box transcription factors in development and disease

T-box family members play pivotal roles during early embryonic development including in gastrulation, early limb patterning and organogenesis (Wilson and Conlon, 2002; Papaioannou, 2014). Their importance during embryonic development is underscored by the observations that mutations in a number of T-box genes lead to developmental abnormalities. Loss of *TBX1* due to translocations and/or deletions of the 22q11 chromosomal region lead to DiGeorge syndrome, a disorder characterised by heart abnormalities, palatal defects, thymus hypoplasia and hearing disorders among many other debilitating characteristics (Jerome and Papaioannou, 2001; Merscher *et al.*, 2001; Vitelli *et al.*, 2003; Zhang *et al.*, 2005). Splice, nonsense, missense, or frameshift mutations in human *TBX4* give rise to small patella syndrome, an autosomal-dominant developmental syndrome characterised by limb anomalies and patella hypoplasia (Bongers *et al.*, 2004; Mundlos and Horn, 2014). Recent studies have shown that microdeletions on chromosome 17q23, which affect both *TBX2* and *TBX4*, are associated with an unnamed syndrome that is characterised by microcephaly, retardation in growth, limb abnormalities and heart defects (Ballif *et al.*, 2010; Nimmakayalu *et al.*, 2011). Individuals with haploinsufficiency of TBX5 suffer from Holt Oram syndrome, another debilitating disorder that causes skeletal malformations, heart defects, and disruptions in forelimb patterning (Li *et al.*, 1997; Mundlos and Horn, 2014). *TBX19* is an activator of the *POMC* gene and mutations in *TBX19* have detrimental effects on pituitary

development which results in the isolated adrenocorticotropic hormone (ACTH) syndrome (Liu *et al.*, 2001; Maira *et al.*, 2003; Metherell *et al.*, 2004). Mutations in *TBX22* cause cleft palate, a congenital disorder characterised by craniofacial and speech defects (Braybrook *et al.*, 2001). Lastly studies have reported that haploinsufficiency of *TBX3* due to deletions, frameshifts or missense mutations causes the congenital abnormality known as ulnar mammary syndrome (UMS) (Tada and Smith, 2001; Wilson and Conlon, 2002).
A number of T-box factors including Brachyury, TBX1, TBX2, TBX3, TBX4, TBX5, T-bet (TBX21) and Eomes, are also deregulated in a long list of cancers where they impact a number of oncogenic processes as either tumour promoters or tumour suppressors (He *et al.*, 2002; Atreya *et al.*, 2007; Park *et al.*, 2008; McCune *et al.*, 2010; Reinert *et al.*, 2011; Trempus *et al.*, 2011; Willmer *et al.*, 2016; Prince laboratory, unpublished data).

Brachyury is overexpressed in chordoma, hepatocellular carcinoma, kidney, bladder, uterus, stomach, oesophageal, uterine, prostate and testicular cancer and contributes to cell migration, invasion and metastasis (Palena *et al.*, 2007; Yang *et al.*, 2009; Fernando *et al.*, 2010; Roselli *et al.*, 2012; Sarkar *et al.*, 2012; Shimoda *et al.*, 2012). Studies have reported a direct correlation between Brachyury expression and decreased survival in early colorectal cancer and oral squamous cell carcinoma patients, as well as with poor prognosis and increased metastasis of hepatocellular carcinoma patients (Imajyo *et al*. 2012; Du *et al.*, 2014). Fernando *et al.* (2010) demonstrated that knock down of Brachyury in lung cancer cells decreased their invasive potential in nude mice. In addition, Shimoda *et al.* (2012) showed that when Brachyury is silenced in adenoid cystic carcinoma cells their sphere-forming ability, EMT characteristics and tumorigenicity were reversed. Interestingly, Brachyury is silenced by methylation in lung cancer cell lines and lung adenocarcinoma tissues and is able to block cell-cycle progression, suggesting that it may also have tumour suppressor function (Park *et al.*, 2008; Huang *et al.*, 2013)

Trempus *et al.* (2011) reported that Tbx1[1] is downregulated in mouse skin tumours and it was therefore implicated as a negative regulator of these tumours. Indeed, the authors showed that ectopic overexpression of Tbx1 in a mouse carcinoma cell line, significantly

[1] The accepted convention will be used for human, TBX1, and when referring to both mouse and human, Tbx1/TBX1 will be used.

reduced colony formation and suppressed tumour growth. Moreover, the authors reported that TBX1 expressing cells tend to exhibit a senescent or quiescent cell cycle profile.

Overexpression of TBX2 has been linked to a growing list of cancers including melanoma (Vance *et al.*, 2005; Rodriguez *et al.*, 2008), breast (Jacobs *et al.*, 2000; Sinclair *et al.*, 2002; Fan *et al.*, 2004b; Yarosh *et al.*, 2008; Fillmore *et al.*, 2010), and pancreatic cancer (Mahlamäki *et al.*, 2004; Hansel *et al.*, 2004; Duo *et al.*, 2009). TBX2 has been reported to bypass senescence by directly repressing $p19^{ARF}$ and p21 (Lingbeek, Jacobs and van Lohuizen, 2002; Prince *et al.*, 2004) A study by Redmond *et al.* (2010) showed that TBX2 drives breast cancer cell proliferation through interaction with and recruitment of early growth response 1 (EGR1) resulting in the repression of *N- myc down-regulated gene 1* (*NDRG1*) promoter. A recent study by Du *et al.* (2017) showed that knocking down TBX2 in prostate cancer cells inhibited proliferation while promoting senescence, suggesting that TBX2 has a pro-proliferative role in this cancer. Complimentary to these findings, another study by Nandana *et al.* (2017) showed that inhibiting endogenous TBX2 levels in prostate cancer inhibits proliferation and invasion to local lymph nodes and metastasis to the bone. Moreover, Yu *et al.* (2015) showed that TBX2 is associated with metastasis, invasion and poor prognosis in gastric cancer. A recent study by Khalil *et al.* (2017) suggested that TBX2 may have a tumour suppressor role in non-small cell lung cancer (NSCLC). The authors monitored the expression of TBX2 in human normal tissues compared to NSCLC by in silico analysis of publicly available expression databases. The results showed that suppressed TBX2 expression in cytologically-normal mainstem bronchi significantly distinguished smokers with lung cancer from cancer-free smokers. However, while this study suggests that *TBX2* may function as a tumour suppressor in human NSCLC, future functional studies are required to confirm this.

TBX4 has recently been implicated as a potential tumour suppressor. Increased TBX4 methylation was observed in the aggressive, progressing, non-muscle-invasive urinary bladder tumours (Reinert *et al.*, 2011). Using microarray analysis and validation of targets by PCR and bisulphite sequencing, TBX4 was highlighted as a good candidate marker for disease progression in bladder cancer. Furthermore, Zong, Meng and Li. (2011) reported that low levels of TBX4 correlated with a decrease in the overall survival

of pancreatic ductal cell adenocarcinoma patients. In addition, the authors demonstrated that low TBX4 expression can be used to predict worse prognosis for patients and can also be used a biomarker to predict the stage of intrahepatic cholangiocarcinoma tumours (Zong, Jia and Li, 2013)

A few studies have implicated TBX5 as a tumour suppressor. For example, a study by He *et al.* (2002) reported that ectopic expression of TBX5 in lung cancer cells and in U2OS osteosarcoma cells, led to an increase in apoptosis and a decrease in cell proliferation and colony formation. Yu *et al.* (2010) showed that TBX5 is silenced in the majority of colon cancer cell lines tested, and when TBX5 was ectopically overexpressed in the cells, this resulted in a decrease in cell proliferation and migration and an increase in apoptosis. Moreover, the authors reported that the downregulation of TBX5 was associated with poor survival in colon cancer patients. Interestingly, a study by Rosenbluh *et al.* (2012) reported that TBX5 forms a complex with YAP1 and β-catenin to upregulate anti-apoptotic genes and genes that promote tumour progression and survival in several cancer cell lines including colon cancer and hepatocellular carcinoma. Taken together these studies would suggest that TBX5 may be able to function as either tumour promoter or tumour suppressor which may depend on cellular context.

T-bet (TBX21) overexpression has been reported in ER positive breast cancers. For example, a recent study by McCune *et al.* (2010) showed that T-bet (TBX21) is overexpressed in a subset of ER positive breast cancers where it functions to promote tumorigenesis. Moreover, this study reported that this overexpression leads to resistance to hormone therapy and an unfavourable prognosis. In addition, the study showed that insulin treatment led to the induction of T-bet in MCF-7 breast cancer cells and this resulted in a disrupted ER hormonal network including Gata3 and FoxA1 leading to resistance to hormone therapy. Furthermore, T-bet overexpressing cells were also more resistant to tamoxifen therapy in the presence of insulin and displayed elevated ERK and AKT activation, which is associated with anti-oestrogen resistance.

Eomes plays an important role in immunity and defence by activating effector CD8+ T cells and there is evidence that these cells play an important role in colorectal cancer and anti-tumour immunity (Pearce *et al.*, 2003). Atreya *et al.* (2007) reported a tumour

suppressor role for Eomes. Indeed, the authors showed an inverse relationship between Eomes expression and lymph node metastases in colorectal cancer. Moreover, the authors showed that Eomes reduces lymph node metastasis through the activation of CD8+ T cells via perforin induction, suggesting a tumour suppressor function.

The role of TBX3 in cancer will be discussed in **section 1.4.3**.

1.4. TBX3

1.4.1. Gene and protein structure

TBX3 is a member of the TBX2 sub-family of T-box transcription factors and is situated on chromosome 12 at the 12q23-24.1 locus (Agulnik *et al.*, 1996; Bamshad *et al.*, 1997). It is comprised of 7 exons and the coding region of TBX3 produces a 723-amino acid long protein (Bamshad *et al.*, 1997; Rowley, Grothey and Couch, 2004). Carlson *et al.* (2001), using deletion constructs in luciferase reporter assays, showed that TBX3 contains two repression domains, R2 and R1, in the N- and C- termini respectively and an activation domain (A) in the C-terminus (**Figure 1.2**). Moreover, the authors mapped the DNA binding domain (DBD) (T-box) to the N-terminus between amino acids 104–285. Furthermore, the RREKRK sequence between amino acids 292-297 in the N-terminal region of Tbx3 has been reported to function as the nuclear localization signal (Carlson *et al.*, 2001). Coll, Seidman and Muller (2002) subsequently resolved the crystal structure of the DBD and showed that TBX3 binds to its consensus sequence as a monomer through the "half-site" of the palindromic target sequence. Although alternative splicing between exon two and three of *TBX3* gives rise to four mRNA transcript variants, only two of them, namely *TBX3* and *TBX3+2a*, encode full length functional proteins, with studies showing that *TBX3* is generally the more dominant of the two (Bamshad *et al.*, 1997) (**Figure 1.3A**). The *TBX3+2a* transcript gives rise to a protein with an additional 20 amino acids within the DBD and this has raised the question as to whether TBX3 and TBX3+2a are functionally distinct and whether they regulate different target genes (Bamshad *et al.*, 1999; Fan *et al.*, 2004a) (**Figure 1.3B**). TBX3 has been characterised predominantly as a transcriptional repressor and has been shown to repress *p14/p19* in primary breast tumours, *p21* in chondrosarcoma, *Phosphatase and tensin homolog* (*PTEN*) in head and

neck squamous carcinoma, *E-cadherin* in melanoma, *Nppa* and *Cx40* in heart development and *bmp4* in retina development (Burgucu *et al.*, 2012;Brummelkamp *et al.*, 2002; Lingbeek *et al.*, 2002; Rodriguez *et al.*, 2008; Hoogaars *et al.*, 2008; Hoogaars *et al.*, 2004; Willmer *et al.*, 2016).

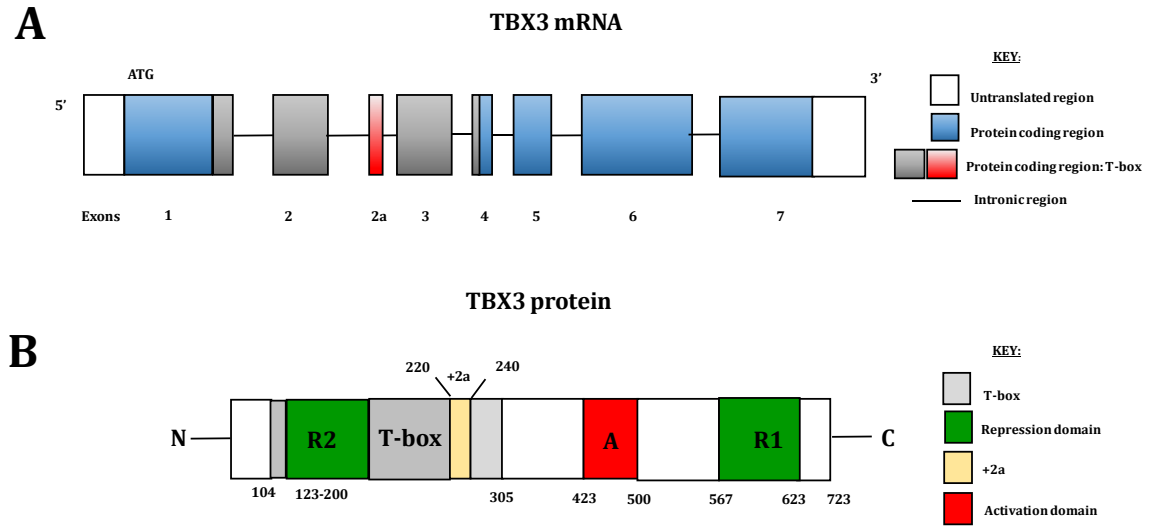

Figure 1.3. TBX3 mRNA and protein structure(A) Schematic of human *TBX3* mRNA. Several alternatively spliced transcripts of *TBX3* are known, however the most commonly investigated are the dominant transcript and the *TBX3+2a* transcript. These transcripts are 7 exons long and are comprised of untranslated sequences (white boxes) and protein coding regions (blue boxes) **(B)** Schematic of human TBX3 protein. The protein is comprised of a T-box (grey boxes), repression domains (green boxes), an additional 20 amino acids in the *TBX3+2a* splice variant (peach box), activation domain (red box) and a highly conserved T-box region. The amino and carboxy termini are indicated by N and C respectively (Adapted from (Bamshad *et al.*, 1999; Carlson *et al.*, 2001).

It is important to note that there is growing evidence that TBX3 can also function as a transcriptional activator in development and cancer contexts. For example, a study by Weidgang *et al.* (2013) showed that TBX3 directly binds and activates the promoters of *Eomes, T* and *Sox17* which are essential for mesoderm differentiation in mouse embryonic stem cells (mESCs). Moreover, TBX3 has been shown to directly bind and activate the *Gata6* promoter in mESCs to promote extra embryonic endodermal differentiation (Lu, Yang and Jin, 2011). Recent studies in the Prince laboratory have also shown TBX3 to be a direct transcriptional activator of *COL1A2* expression in chondrosarcoma and fibrosarcoma as well as of the *inhibitor of DNA binding-1* (*ID1*) in melanoma (unpublished

data). It is important to note that in addition to its function as a transcriptional regulator, TBX3 was also found to regulate mRNA splicing through interacting with a number of splicing and RNA binding proteins (Kumar *et al.*, 2014). While the nuclear localization signal of TBX3 was shown to be critical for this interaction, the T-box and the C-terminal domains were found to be variably required. The same study showed that TBX3 interacts with and recruits splicing factors to RNA containing T-elements to regulate splicing of *Disks large homolog (3Dlg3)* and *Nuclear factor of kappa light polypeptide gene enhancer in B-cells 1* (*Nfκb1*). Interestingly, UMS-associated TBX3 mutations disrupted splicing, suggesting that the pleiotropic effects of TBX3 mutations result from the disruption of transcriptional regulation and pre-mRNA splicing.

1.4.2. TBX3 in development

TBX3 contributes to several aspects of embryonic development, ranging from germ layer specification, maintenance of stem cell pluripotency, all the way through to the development of various human organs and tissues such as the liver, lungs, kidney, heart, small intestine, placenta, ovaries, mammary glands and the thyroid (Bamshad *et al.*, 1999). In mouse development, it is expressed as early as the morula stage in the yolk sac and the extraembryonic tissue and it specifies the ventricular septum, conduction system and the atrioventricles during heart development (Naiche *et al.*, 2005). The critical role played by TBX3 in organ development is underscored by several studies. Firstly, *Tbx3*[2] homozygous mutant mice die in utero due to cardiac abnormalities and deformations of the yolk sac and mice with heterozygous mutations in Tbx3 have failed nipple development and genital abnormalities (Bamshad *et al.*, 1997; Tada and Smith, 2001; Wilson and Conlon, 2002). Frank *et al.* (2013) observed that mutations that result in the deletion of the exons that encode the T-box in *Tbx3* do not necessarily result in a null allele as previously presumed, but rather generate aberrant protein that remains predominantly in the cytoplasm. This is important as it suggests that phenotypes observed in Tbx3 heterozygous mutants are not due to loss of wild type Tbx3, but rather due to the lack of nuclear Tbx3. Importantly, *TBX3* heterozygous mutations in humans, result in the autosomal dominant disorder UMS which is characterised by heart defects

[2] The accepted convention will be used for human, TBX3, and when referring to both mouse and human, Tbx3/TBX3 will be used.

and malformations of the mammary glands, areola, heart, limbs and genitalia (Bamshad *et al.*, 1997). A study by Washkowitz *et al.* (2012) showed that not all tissues that express TBX3 are affected by UMS which suggest that TBX3 is required in different doses in different tissues and organs.

1.4.3. TBX3 in cancer

TBX3 is expressed in adult tissues including the brain, lungs and pancreas but it has no known function in these tissues. Its overexpression has, however, been associated with a number of cancers including melanoma, sarcoma, head and neck, breast, ovarian, lung, liver and bladder cancers and been linked to several oncogenic functions including uncontrolled cell proliferation, bypass of senescence and apoptosis, tumour formation, invasion and metastasis (Fan *et al.*, 2004b; Hoogaars *et al.*, 2008; Yarosh *et al.*, 2008; Burgucu *et al.*, 2012; Willmer *et al.*, 2016). Interestingly, emerging studies have also reported a tumour suppressor role for TBX3. This will be discussed further in **section 1.4.3.3**.

1.4.3.1. TBX3 in senescence, apoptosis and proliferation

Cancer is a disease defined by uncontrolled proliferation. An early event in cancer development is therefore the ability to compromise key cell cycle checkpoints including senescence and apoptotic signals.

Senescence describes a phenomenon where somatic cells irreversibly exit the cell cycle and cease to divide and serves as an important barrier to cancer (Hayflick, 1965). It can occur due to the critical shortening of telomeres or in response to stress signals such as DNA damage (Kuilman *et al.*, 2010; Campisi, 2013). The $p19^{ARF}$/Mdm2/p53 pathway promotes cell cycle arrest and/or senescence and cell death by apoptosis and this pathway has to be bypassed for cancer to occur (Yu and Zhang, 2005; Hanahan and Weinberg, 2011). A study by Brummelkamp *et al.* (2002) showed that TBX3 represses *p19*/*p14* by binding a T-element at position -19 to +54, thereby repressing senescence and thus enabling mouse embryonic fibroblasts (MEFs) and ST.HdhQ111 striatal cells to

gain immortality. Moreover, this occurs through TBX3 recruiting histone deacetylases (HDACs) 1, 2, 3 and 5 to epigenetically silence the *p14*/*p19* promoter (Yarosh *et al.*, 2008). In addition, (Kumar *et al.*, 2014) showed that the CAPERα/TBX3 complex is required to bypass senescence in primary human and mouse cells in vivo by directly repressing transcription of the long non-coding RNA *Urothelial Cancer Associated 1 (UCA1)*, $p16^{INK}$ and other tumour suppressor genes. *UCA1* has been shown stabilise $p16^{INK}$ which in turn negatively regulates the G1/S transition of the cell cycle thereby promoting senescence (Kumar *et al.*, 2014). Together the above studies suggest that TBX3 may bypass senescence to promote cancer by different mechanisms. The importance of the anti-senescence role of TBX3 in cancer have been highlighted by studies that have reported that depleting Tbx3 in advanced melanoma induces senescence (Vance *et al.*, 2005). Moreover, Peres *et al.* (2010) showed that knocking down TBX3 in VGP melanoma cells results in senescence, suggesting that targetting TBX3 in melanomas may be an important pro-senescence therapy.

Apoptosis is a mode of programmed cell death that occurs as a normal part of development and homeostasis. Therefore, it is not surprising that inhibition of this process would result in uncontrolled proliferation, a key hallmark of cancer progression (Schmitt *et al.*, 2007). There are several lines of evidence to show that another mechanism by which TBX3 contributes to oncogenesis is through the evasion of apoptosis. For example, a study by (Carlson *et al.*, 2001) showed that TBX3 transforms primary MEFs by repressing the pro-apoptotic p19/MDM2/p53 pathway. Furthermore, studies have shown that silencing TBX3 in rat bladder cancer cells, human colon carcinoma and osteosarcoma cells, leads to an increase in cell death by apoptosis, suggesting that TBX3 mediates survival of these cells (Renard *et al.*, 2007). Interestingly, another study has shown that silencing Tbx3 in rat bladder carcinoma cells sensitizes them to doxorubicin induced apoptosis (Renard *et al.*, 2007). Moreover, TBX3 overexpression prevents head and neck squamous cell carcinoma cells from undergoing anoikis, a type of programmed cell death that occurs as a result of the loss of normal cell–matrix interactions when anchorage-dependent cells detach from the surrounding extracellular matrix (ECM) (Humtsoe *et al.*, 2012).

TBX3 has also been shown to have a pro-proliferative role in some cancers. For example, (Renard *et al.*, 2007) showed that when Tbx3 was knocked down, this resulted in a decrease in hepatoma cell proliferation and survival. The cooperation of TBX3 and Wnt signalling was confirmed by Arendt *et al.* (2014), who showed that they regulate proliferation in human breast progenitor cells through a possible feedback signalling loop. A study by Ballim *et al*. (2012) showed that upregulation of TBX3 by retinoic acid, enhances the proliferative ability of melanoma cells. In addition, a recent study showed that TBX3 promotes chondrosarcoma cell proliferation by directly repressing the cyclin dependant kinase inhibitor, $p21^{WAF}$, through its DNA binding domain by binding a T-element close to the $p21^{WAF}$ initiator (Willmer *et al*., 2016). Another study has shown that TBX3 promotes proliferation of head and neck squamous cell carcinoma cells through direct binding and repression of the promoter region of the tumour suppressor *PTEN* (Burgucu *et al*., 2012).

1.4.3.2. TBX3 in tumour formation, migration, invasion and metastasis

Anchorage-independent growth is a key hallmark of cancer and it describes the ability of cancer cells to proliferate in the absence of a substrate in order to grow on top of one another to form tumours (Carney *et al.*, 1980; Hanahan et al.,2000). In addition, it enables them to break away from a monolayer, favouring migration, invasion and metastasis which are key mechanisms by which cancer cells escape the primary tumour mass and disseminate. The dissemination of cancer cells is the ultimate cause of death in 90% of cancer patients (Hanahan et al.,2000).

TBX3 has been shown to promote substrate independent growth, tumour formation, migration, invasion and metastasis in several cancers including breast and pancreatic cancer, melanoma and chondrosarcoma (Perkhofer *et al*. 2016; Peres *et al*., 2010; Renard *et al*., 2007; Rodriguez *et al*., 2008; Mowla *et al*., 2010; Willmer *et al.*, 2016). Renard *et al.* (2007) showed that knocking down Tbx3 using an siRNA approach resulted in reduced anchorage-independent growth of hepatoma and colon carcinoma cells. Furthermore, the authors showed that when cells expressing mutant TBX3 were injected into nude mice, tumour formation was abrogated. Studies in the Prince laboratory showed that non-tumourigenic human radial growth phase (RGP) melanoma cells in which TBX3 was

ectopically overexpressed had enhanced anchorage-independent growth and tumour forming ability when injected into nude mice (Peres and Prince, 2013). Similar results were obtained when chondrosarcoma, rhabdomyosarcoma and liposarcoma cells were genetically engineered to overexpress TBX3 (Willmer *et al.*, 2016). Importantly, depleting TBX3 resulted in a reduction in anchorage-independent growth and colony and tumour forming ability in breast cancer and chondrosarcoma cells (Peres *et al*., 2010; Willmer *et al.*, 2016). The mechanism by which TBX3 promotes cancer cell migration would appear to involve, in part, its ability to repress the epithelial marker E-cadherin (Rodriguez *et al*., 2008; Peres *et al*., 2010; Du *et al*., 2014). A study by Peres *et al*. (2015) showed that high TBX3 expression levels correlated with low E-cadherin levels in. Moreover, the study showed that AKT3 directly phosphorylates TBX3, thereby stabilizing the protein thus enhancing its repression of E-cadherin, promoting migration and invasion of melanoma cells. TBX3 has also been found to promote cervical cancer migration through interaction with HPV capsid protein L2 and thus regulating the human papillomavirus lifecycle (Schneider *et al*., 2013). Chen *et al* (2009) has shown that there is a direct correlation between increased *TBX3* mRNA expression and metastasis in breast cancer and a study by Li et al (2013) showed that TGFβ-signalling transcriptionally activate *TBX3* in breast epithelial cells where it mediates TGFβ-induced migration (Li *et al*., 2013). Furthermore, Krstic *et al*. (2016) showed that TBX3 promotes the progression of breast cancer cells from a non-invasive to an invasive phenotype through enhancing EMT.

1.4.3.3. The tumour suppressor role of TBX3

The first studies to suggest a tumour suppressor role for TBX3 were those that showed TBX3 to be silenced via methylation in glioblastoma and uterine cancer and this was associated with increased invasion, metastasis, tumour size and poor prognosis (Etcheverry *et al.*, 2010; Yamashita *et al.*, 2006; Lyng *et al.*, 2006; Etcheverry *et al*., 2010). Moreover, TBX3 was also reported to be methylated and downregulated in bladder cancer and this was associated with a decrease in progression-free survival rates (Kandimalla et al., 2012). A tumour suppressor role for TBX3 was comprehensively investigated in fibrosarcoma using cell culture models in which TBX3 was either knocked down or overexpressed (Willmer et al., 2016). Using in vitro and in vivo assays, this study showed that TBX3 acted as a "brake" to prevent tumour progression in fibrosarcoma.

Indeed, the authors showed that whereas overexpressing TBX3 prevented cell proliferation, migration and tumour formation, depleting TBX3 in fibrosarcoma cells enhanced the cancer phenotype. Taken together, these findings suggest that the ability of TBX3 to exhibit oncogene or tumour suppressor activity may rely on the availability of different co-factors depending on cellular context.

1.4.4. The regulation of TBX3 expression levels and oncogenic activity

Since the deregulated expression of TBX3 plays a pivotal role in several cancers, it is imperative to understand how its levels are regulated and what co-factors it interacts with to carry out its oncogenic functions. This section will focus on (1) signalling molecules that have been identified to upregulate TBX3 levels in cancer and (2) co-factors that mediate the oncogenic activity of TBX3.

1.4.4.1. Signalling molecules that upregulate TBX3 levels in cancer

Fibroblast growth factors (FGFs) are multifunctional signalling molecules that regulate several developmental processes such as mesoderm induction, antero-posterior patterning and limb development (Koga et al., 1999; Bottcher et a., 2003). They act systematically to activate cell surface receptors forming an intricate signalling system. Dysregulation of the FGF signalling system underlies a range of diseases including tumour development and progression (Takahashi et al., 1999). FGF-2 is overexpressed in many malignant tumours including melanomas, astrocytomas, breast, pancreatic, non-small cell lung and bladder cancer (Lindner et al., 1990; Halaban et al., 1996; Bian et al., 2000; Relf et al., 1997; Yamanaka et al., 1993; Berger et al., 1999; Gazzaniga et al., 1999). FGF-19 is thought to promote tumour growth in colorectal cancer and hepatocellular carcinoma through interaction with FGFR4 (Desnoyers et al., 2008). FGFR4 amplification has been found in 10% of primary breast tumours and it has been associated with breast cancer progression (Jaakkola et al., 1993; Jonker et al., 2012). The FGF signalling pathway has also been implicated in the expansion of breast cancer stem cells (CSCs). Indeed, a study by (Fillmore *et al.*, (2010) reported that treatment of a number of ER positive cell lines with β-estradiol resulted in an enrichment of CSC subpopulations. Interestingly,

treatment of ER negative cell lines with conditioned medium from these cells also led to the expansion of CSCs, suggesting that estrogen expands breast CSCs through paracrine-acting factors. Indeed, quantitative assays revealed that estrogen treatment resulted in a significant increase in the secretion of the FGF family members FGF2, bFGF, FGF4, FGF6, FGF7 and FGF9. Moreover, when MCF-7 ER positive breast cancer cells were treated with an inhibitor of FGF signalling, even in the presence of estrogen or conditioned medium, the expansion of CSCs was abrogated indicating that FGF signalling is indeed important for the expansion of CSCs. Importantly Tbx3 has been shown to act both upstream and downstream of the FGF signalling pathway and the authors revealed that Tbx3 mRNA and protein levels were significantly increased in estrogen treated cells. In addition, this promoted the secretion of FGF9. Furthermore, when Tbx3 was knocked down, the expansion of CSCs was lost and tumoursphere formation abrogated. Moreover, while treatment of MCF-7 cells with both an estrogen antagonist and an FGF inhibitor resulted in a corresponding decrease in Tbx3 levels and consequently the loss of CSC induction, co-treatment of the cells with estrogen and FGF9 caused a synergistic increase in Tbx3 levels. This was a key finding, that revealed that estrogen and FGF signalling induces the expression of Tbx3 in breast cancer cells. Taken together, the findings from this study revealed that FGF/FGFR/Tbx3 signalling is critical for the expansion of breast CSCs and the authors suggest that this signalling axis may be a key contributor to anti-hormone therapy resistance in breast cancer.

Transforming growth factor beta 1 (TGF-β1) is a member of the TGF-β family of cytokines which controls cell proliferation, differentiation, apoptosis, wound healing and regulation of the immune system (Assoian et al., 1983; Letterio et al., 1998). Examination of archival tissues from patients with malignant breast and colon cancer revealed that there a correlation between intense immunohistochemical staining for TGF-β1 and increased disease progression and metastasis (Friedman et al., 1995; Go et al., 1999). Moreover, the overexpression of TGF-β1 in human prostate cancer cells significantly stimulated tumour growth and angiogenesis when injected into mice (Stearns et al., 1999; Ueki et al., 1992). TGF-β1 signalling has been reported to inhibit cell proliferation during the early stages of carcinogenesis and promote migration and metastasis in the late stages of the disease (Imamura *et al.*, 2012). It plays an important role in mammary morphogenesis and has been shown to be constitutively activated in breast cancer

(Moses and Barcellos-Hoff, 2011). Li *et al*. (2013) showed that treatment of normal MCF-12A breast epithelial cells and HaCaT keratinocytes with TGF-β1 resulted in increased TBX3 mRNA and protein levels. Moreover, pre-treatment of the cells with a de novo transcriptional inhibitor, Actinomycin D, abolished this activation which indicated that TGF-β1 transcriptionally activates TBX3 expression in these cells. The authors showed that JunB and Smad are the mediators of this regulation. It is worth noting that the authors went on to demonstrate that the anti-proliferative and pro-migratory roles of TGF-β1 in breast epithelial cells are mediated in part by TBX3.

The Wnt/β-catenin pathway is comprised of a group of co-ordinated signal transduction pathways that play important and widespread functions in a myriad of biological and developmental processes such as key cell-cell signalling events during embryonic development (Klaus et al., 2008; Logan and Nusse 2004). Mutations that cause constitutive activation of this pathway have been associated with cancers including 90% of hepatocellular carcinoma (HCC) and colorectal cancers (Krishnamurthy et al., 2017). Furthermore, several studies have reported that mutations that cause constitutive expression of *β-catenin* are found at significant rates in HCC (de la Coste *et al*., 1998; Renard *et al*., 2000; Calvisi *et al*, 2001). A proportion of human breast carcinomas express high levels of WNT-2, WNT-5A, and WNT-7B and there is compelling evidence that suggests that the Wnt/β-catenin may be a therapeutic target in breast cancer (Dale et al., 1996; Huguet et al., 1996; Lejeune et al., 1995). Furthermore, Wnt/β-catenin activation is preferentially found in TNBC and is associated with a poor clinical outcome (Khramtsov et al., 2010; Geyer et al., 2011). Based on the growing body of research implicating the upregulated expression of Wnt/β-catenin in several cancers, targeted inhibition of Wnt/β-catenin signalling provides a promising new approach for the therapy of cancers. The secreted FZD-related protein (sFRP) family of glycoproteins are antagonists of the Wnt pathway (Rattner *et al.,* 1997). They are silenced in several types of cancers including breast cancer and a study by Suzuki et al. (2008) demonstrated that overexpression of sFRP1, sFRP2, and sFRP5 decreases the proliferative ability of several breast cancer cell lines (Klarmann et al., 2008). In addition, Matsuda et al. (2009) reported that overexpression of sFRP1 in TNBC MDA-MB-231 cells blocks Wnt/β-catenin signalling, resulting in a decrease in cell proliferation and tumour growth and metastasis in xenograft mouse models. Renard *et al*. (2007) revealed that among other known β-

catenin gene targets such as the dynein light-chain genes, Tbx3 expression was significantly upregulated in the HCCs from the mice harbouring the mutant β-catenin. Similar results were observed in a number of hepatoblastomas and this suggested that Tbx3 is associated with Wnt/β-catenin signalling. A recent study by Aydoğdu et al. (2018) showed that canonical WNT signalling transcriptionally upregulates TBX3 in the ureteric mesenchyme to promote smooth muscle cell differentiation.

The protein kinase C (PKC) family is comprised of serine/threonine specific protein kinases that share a characteristic carboxyl-terminal kinase domain linked by a hinge segment to an amino-terminal region containing regulatory modules (Newton *et al*., 2003; Parker and Murray-Rust., 2004; Marengo *et al*., 2011). Each kinase has a distinct structure and co-factor association and consequently has unique substrate specificity (Takai *et al*., 1979). PKCs function in signal transduction pathways and regulate a wide range of biological functions including proliferation, apoptosis and differentiation and not surprisingly they have been associated with cellular transformation (Mochly-Rosen *et al*., 1991; Leitges *et al*., 2007; Marengo *et al*., 2011). For example, hyperactive expression of PKC has been linked with malignant central nervous tumour formation (Bredel et al., 1997; Shariff et al., 1999). Moreover, several PKCs are overexpressed in malignant breast tissue and breast cancer cell lines and this has been reported to lead to a more aggressive phenotype and to drug resistance (Tanaka et al., 2003; Ways et al., 1995; Frankel et al., 2007). A study by Mowla *et al*. (2011) demonstrated that the phorbol ester 12-O-tetradecanoylphorbol 13-acetate (TPA, also referred to as PMA), an intracellular activator of PKC enzymes, transcriptionally activates TBX3 in breast cancer cells. The authors showed that this was mediated by transcription factors c-Jun and JunB and that TBX3 is required for PMA-induced migration in MCF-7 breast cancer cells. This study suggests that the activation of TBX3 through PKC signalling is critical for metastasis in breast cancer. The PKC pathway has become an attractive therapeutic target in recent years and studies have investigated the use of several PKC inhibitors including small molecule kinase inhibitors and anti-sense oligonucleotides for the treatment of a number of cancers (Leskow et al., 2011).

The phosphatidylinositol 3-kinase/protein kinase B (PI3K/AKT) signalling pathway plays important roles in regulating cellular quiescence and proliferation (King et al.,

2015). Upon activation by growth factor signals, PI3K phosphorylates inositol lipids in the plasma membrane, leading to the recruitment of serine/threonine kinase Akt (also known as protein kinase B) which in turn conducts a series of downstream regulatory activities (Fry, 2001; Osaki *et al.*, 2004; Hemmings and Restuccia, 2012). The most common genomic abnormalities in cancer involve aberrations in the PI3K/AKT pathway. This pathway has been found to contribute to tumorigenesis through promoting cancer growth, survival, metastasis and adhesion, making it an attractive target for the treatment of certain cancers (Roymans and Sledgers., 2001; Courtney *et al*., 2010). Moreover, it has been reported to be activated in approximately 30–40% of breast cancer cases (Raphael et al., 2010). In addition, there is evidence to show that this pathway is upregulated by upstream regulators like EGFR in TNBC and it has been reported to lead to endocrine treatment resistance in breast cancer (Paplomata et al., 2013; Costa et al., 2018). More than 40 inhibitors of the PI3K/AKT signalling pathway have reached different stages of clinical development but only a few have been approved for clinical use due to problems of toxicity (Janku et al., 2018). A study by Niwa *et al*. (2009) showed that the cytokine leukaemia inhibitory factor (LIF) upregulates TBX3 expression through the PI3K/AKT pathway to maintain pluripotency of mESCs. Similarly, a more recent study by Minxia *et al*. (2018) showed that in marmoset iPSCs, LIF promotes TBX3 expression via PI3K/AKT, thus enhancing proliferation while having no effect on apoptosis. A study by Peres *et al*. (2014) showed that AKT3, the predominant AKT isoform in melanoma, phosphorylates TBX3 at S720, and this leads to an increase in TBX3 protein stability as well as its nuclear localization in melanoma. Furthermore, this enhanced the ability of TBX3 to transcriptionally repress the E-cadherin promoter, thus promoting melanoma cell migration and invasion.

c-Myc is a member of the Myc family of transcription factors which contain basic helix-loop-helix (bHLH) and leucine zipper (LZ) structural motifs (Adhikary et al., 2005; Pelengaris et al., 2002; Dang et al., 2010). It regulates transcription of its target genes by binding to the conserved E-box DNA sequence CACGTG. To do this, c-Myc binds to myc-associated factor X (Max) through the BR/HLH/LZ motif, thereby forming a heterodimer that recruits a chromatin modifying complex (TRRAP, GCN5, TIP60, and TIP48) (Adhikary et al., 2005; Pelengaris et al., 2002; Meyer et a., 2005). c-Myc is overexpressed in a number of human cancers and it has been considered a molecular hallmark and

feature of both the initiation and maintenance of cancer (Dang *et al*., 1995). It enforces progression through the cell cycle as well as cellular transformation through aberrant activation/repression of its target genes (Dang *et al*., 2006; Fernandez *et al*., 2003; Gartel *et al*., 2003). Studies in transgenic mouse models have reported that even transient silencing of Myc elicits pancreatic and lung tumour regression, suggesting that inhibiting oncogenic Myc could be a strategy to treat cancer patients (Schachaff et al., 2005; Soucek et al., 2008; Arvantis et al., 2011). However, attempts at developing drugs that directly target c-Myc have proven challenging as it lacks a specific active site for small molecule intervention, making it difficult to functionally inhibit its activities (Fletcher and Hamilton., 2007; Wells and McClendon., 2007; Meyer and Penn., 2008; Chen et al., 2018). Moreover, because c-Myc is localized in the nucleus, targeting it with monoclonal antibodies is a challenge (Samanarayake et al., 2009; Chen et al., 2018). To overcome these issues, a number of studies have investigated alternative ways of interfering with the oncogenic activity of c-Myc as treatment options for c-Myc-driven cancers. For example, JQ1, a powerful inhibitor of bromodomain-containing 4 (BRD4), the regulator of c-Myc transcription, has shown anti-cancer effects on c-Myc overexpressing cancers including hematopoietic cancers and pancreatic ductal adenocarcinoma (Dawson et al., 2011; Zuber et al., 2011; Mertz et al., 2011; Mazur et al., 2015). Other strategies have involved targeting the translation of c-Myc mRNA through inhibition of translation initiation factor 4E (eIF4E) binding protein 1 (4EBP1) (Wullschegger et al., 2006; Kim et al., 2002). The peptide mimetic, IIA6B17, a small-molecule inhibitor of Myc–Max dimerization has also been used (Berg et al., 2002; Adhikary et al., 2005). c-Myc stability is tightly controlled by the ubiquitin-proteasome system and an interesting strategy has involved deubiquitinases (Tavana et al., 2016; Adhikary et al., 2005). Important to the current study, Robanus-Mandaag et al. (2003) reported a correlation between c-Myc amplification and the progression from the in situ to the invasive stage of breast carcinomas. Another study by Sierra et al. (1999) reported co-operation of c-Myc with Bcl-2 in promoting lymph node metastasis in human breast carcinomas. Recent studies in the Prince laboratory identified TBX3 as a key downstream effector of c-Myc in chondrosarcoma (Willmer *et al*., 2015). The authors showed that during S-phase, c-Myc directly binds a region of the *TBX3* promoter containing the E-boxes located at -1210 and -701 bps and upregulates it transcriptionally. It would be interesting to determine if c-Myc upregulates TBX3 in breast cancer.

1.4.4.2. Co-factors that mediate the oncogenic activity of TBX3

As is the case with other T-box factors, it is thought that the functions of TBX3 will be governed by interaction with co-factors. To date, however, only histone deacetylases (HDACs) have been identified as TBX3 interactors in a cancer context. Indeed, TBX3 has been shown to interact with HDACs 1, 2, 3 and 5 in breast cancer to repress p14 (Yarosh *et al*., 2008). More recently a study by Dong et al. (2018) reported that Tbx3 directly interacts with the ^{585}LFSYPYT5^{91} and ^{604}HRH^{606} motifs of HDAC5 to suppress E-cadherin expression to promote HCC cell migration and metastasis. Moreover, the study showed that HDAC inhibition blocks Tbx3-mediated cell migration and thus highlights the importance of targeting the interaction between TBX3 and its interacting partners for anticancer drug development. Given the paucity of information regarding TBX3 protein co-factors in cancer, the current study performed immunoprecipitation analyses coupled with mass spectrometry to identify TBX3 interacting partners in breast cancer. Of the putative TBX3 co-factors identified, the heat shock cognate protein (Hsc70), heterogeneous nuclear ribonucleoprotein K (HnRNP K) and nucleolin were validated and characterized because of their overlapping oncogenic roles with TBX3 and therefore background information to only these three proteins will be provided below.

1.4.4.2.1. Heat shock cognate protein (Hsc70)

Hsc70 is a member of the heat shock protein (Hsp) 70 family of molecular chaperones that play essential roles in maintaining cellular homeostasis through translocating proteins across membranes, preventing protein aggregation under stress conditions, disassembly of clathrin coated vesicles and chaperone-mediated autophagy (Liao *et al*., 2014; Liu *et al*., 2012; Mayer *et al*., 2005). It is overexpressed in some cancers including glioma, breast, colon, oesophageal and non-small cell lung cancer (Murphy., 2013). Moreover, Hsc70 overexpression has been associated with numerous oncogenic processes including cell proliferation, survival, drug resistance and metastasis (Liu *et al*., 2012). In addition, heat shock proteins have been implicated in the maintenance of high levels of oncoproteins to permit cellular transformation (Calderwood *et al*., 2006). Studies have reported that Hsc70 is overexpressed chemoresistant cancer cells including

breast cancer cells (Nirde et al., 2010). Small molecule inhibitors that target Hsc70 have been designed and some are in early clinical trials (Evans et al., 2010). For example, rhodacyanine (MKT-077) binds near the ATP-binding site of the Hsc70 nucleotide binding domain (NBD) to inhibit proliferation of breast carcinoma cells (Wadhwa et al., 2000; Evans et al., 2010).

1.4.4.2.2. Heterogeneous nuclear ribonucleoprotein K (HnRNP K)

HnRNP K is a highly conserved RNA and DNA binding protein that belongs to the heterogeneous nuclear ribonucleoprotein (HnRNP) family. It is a multifunctional protein that is involved in many aspects of gene expression including transcription, chromatin remodelling, RNA splicing, RNA stability and translation and its expression is associated with actively proliferating cells (Bomsztyk et al., 2004; Pino, 2003). HnRNP K is overexpressed in a variety of cancers including breast, colorectal and pancreatic cancers, oesophageal and oral squamous cell carcinoma, head-and-neck carcinomas, lung adenocarcinoma, melanoma and chronic myeloid leukaemia, where it has been shown to correlate with tumour aggressiveness, poor prognosis and in some cases metastasis (Carpenter *et al*., 2006; Chen *et al*., 2008a; Hatakeyama *et al*., 2006; Matta *et al*., 2009; Pino, 2003; Wang *et al*., 2012). HnRNP K activates transcription of numerous oncogenes including c-Myc, EGR-1, VEGF and c-Src and plays direct roles in the oncogenic process (Lynch *et al*., 2005; Michelotti *et al*., 1996; Takimoto *et al*., 1993). For example, knockdown of HnRNP K in human lung carcinoma and pancreatic cancer cells inhibited proliferation and induced apoptosis and silencing it in non-epithelial lung cancer cells significantly decreased TGF-β-induced migration and EMT (Li *et al*., 2011; Tang *et al*., 2014; Zhou *et al*., 2010). Furthermore, HnRNP K can post-transcriptionally silence tumour suppressor genes, for example, it binds the 3'-UTR of *p21* mRNA and inhibits its translation (Yano *et al*., 2005). A few studies have investigated the efficacy of HnRNPK targeting agents as possible therapeutic treatments and a study by Zhang et al. (2016) showed that Nujiangexathon, a plant-based compound, accelerates the ubiquitin-proteasome-dependent degradation of hnRNPK and results in the cell cycle arrest of cervical cells and delayed tumour growth in a HeLa xenograft model.

1.4.4.2.3. Nucleolin

Nucleolin is a highly conserved, multifunctional phosphoprotein that is known for its roles in ribosome biogenesis (Tuteja *et al*., 1998). However, it is also involved in a number of other processes, including DNA metabolism, DNA replication and repair, telomere maintenance, chromatin remodelling, histone chaperoning and mRNA stability (reviewed in Abdelmohsen *et al*. 2012). Nucleolin is found at three main locations in cells: in the nucleolus where it controls many aspects of DNA and RNA metabolism; in the cytoplasm where it shuttles proteins into the nucleus and provides a posttranscriptional regulation of mRNAs; and on the cell surface it serves as an attachment protein for several ligands from growth factors to microorganisms (Storck et al., 2007; Fahling et al., 2005; Otake et al., 2007; Borer *et al*., 1989; Ginisty *et al*., 1999; Tuteja *et al*., 1998). Nucleolin expression has been reported to be a feature of actively dividing cells and its overexpression has been associated with a wide range of cancers including breast, gastric, cervical and colorectal cancers, chronic lymphocytic leukaemia, renal cell carcinoma and non-small cell lung carcinoma (Abdelmohsen *et al*., 2012; Bates *et al*., 2009; Fu *et al*., 2005; Grinstein *et al*., 2006; Hovanessian *et al*., 2010; Qiu *et al*., 2013; Tulchin *et al*., 2010; Zhao *et al*., 2013). Furthermore, nucleolin has been shown to influence several aspects of the cancer process such as cell survival, proliferation and invasion. Nucleolin has also been shown to be upregulated by c-Myc (Greasley, Bonnard and Amati, 2000). Cell surface nucleolin is continuously and abundantly expressed in cancer compared to normal cells and is associated with the proliferative capacity of cells (Hovanessian et al., 2000; Hovanessian et al., 2010). Moreover, it serves as a binding partner of several molecules and mediates their biological activities and in some cases, leads to their internalization. In light of these findings, nucleolin would appear to be a potentially good anti-cancer target and strategies aimed at targeting nucleolin have proven successful in multiple cancer types. For example, polyclonal anti-nucleolin antibodies which inhibit cell proliferation and migration, induce cell death of leukaemia and lymphoma cells (Huang et al., 2006; Krust et al., 2011). More recently, the nucleolin aptamer, AS1411, has been reported to have anti-proliferative activity in a number of cancer cell types tested (Bates et al., 2009). Moreover, results from Phase 1 and 2 clinical trials show that AS1411 has an excellent safety profile and indications of clinical activity (CREATE, NCT00881244, NCT00512083,

NCT00740441) (Bates et al., 2009; Laber et al., 2005; Rizzieri et al., 2010; Rosenberg et al., 2013).

1.5. Aims of this study

Breast cancer is the second most common malignancy worldwide and continues to be the leading cause of death in women globally. Despite enormous efforts to overcome this growing problem, there is still limited success with the existing therapeutic strategies due to poor therapy response, cancer cell drug resistance and side effects associated with most therapies. This therefore necessitates the need to understand the molecular mechanisms and oncogenic pathways involved in breast cancer in order to facilitate the development of novel and efficacious targeted therapies. The developmentally important transcription factor, TBX3 has been validated as a potential therapeutic target in several cancers including breast cancer.

To reveal versatile ways of interfering with the oncogenic activity of TBX3 in breast cancer, this project aims to identify (1) signalling molecules that upregulate TBX3 and (2) co-factors that mediate the oncogenic activity of TBX3. To achieve this, the following specific objectives of this study were:

1. To determine if c-Myc is, in part, responsible for upregulating TBX3 transcriptionally in MCF-7 breast cancer cells
2. To establish a MCF-7 breast cancer cell culture model in which TBX3 is overexpressed as a FLAG-tagged fusion protein and to confirm the effect of TBX3 overexpression on proliferation and migration of these cells
3. To use the cell culture model established above to identify and characterize TBX3 protein co-factors that (a) stabilize TBX3 protein levels and (b) regulate the oncogenic function of TBX3

CHAPTER 2

Materials and methods

2.1. Plasmids and constructs

All constructs used in this study were prepared according to standard techniques (Sambrook et al, 1989). The human pCMV-3XFLAG-TBX3 and the pCMV-3XFLAG-EMPTY expression constructs were kindly provided by our collaborator Professor Colin Goding (Ludwig Institute, University of Oxford, UK). The pcDNA FLAG-EMPTY and the pcDNA FLAG-tagged human c-Myc expression constructs were kindly provided by Professor Luscher from Institut für Biochemie, Germany. The pEGFP-C1 vector containing full length GFP-nucleolin was purchased from Addgene (plasmid # 28176) and was provided by Michael Kastan (Takagi et al., 2005). The pEGFP-C1 empty vector was previously constructed by Dr Emily Davis, a previous PhD student in the Prince laboratory. For vector maps see **appendix section 6.1**.

2.2. Cell culture

MCF-7 breast adenocarcinoma cells were cultured in Roswell Park Memorial Institute (RPMI) medium (Sigma Aldrich, USA) supplemented with 10% heat-inactivated foetal bovine serum (FBS), 100 μg/ml penicillin and 100 μg/ml streptomycin. The cells were maintained at 37°C in an atmosphere of 5% CO_2 and 65% humidity. Media was replaced every 48 to 72 hours and cells were routinely tested for mycoplasma infection. Mycoplasma-free cells were used in experiments.

2.2.1. Mycoplasma tests

To perform this test, cells were grown on sterile coverslips in antibiotic-free medium for 24 hours and fixed in fixing solution (25% glacial acetic acid; 75% methanol) for 10

seconds, washed with water and air-dried at room temperature (RT) for 5 minutes. DNA was then stained with Hoechst stain (0.5 µg/ml) for 30 seconds, washed with water and mounted on a slide with mounting fluid (**see appendix section 6.2**). The cells were viewed immediately by fluorescence microscopy using the DAPI filter. Mycoplasma negative cells stained positive with Hoechst only in the nucleus, while cells infected with mycoplasma showed staining in both the nucleus and the cytoplasm.

2.2.2. Transfections

Transfection is a process by which eukaryotic cells take up exogenous DNA or RNA. Prior to performing transfections, the concentration and quality of all DNA constructs were assessed using a NanoDrop ND-1000 spectrophotometer (Agilent Technologies, Boeblingen, Germany). The transfection reagents used in this study are lipid based and therefore allow the formation of micelles around the nucleic acids thus enabling them to fuse with the lipid soluble portion of the phospholipid bilayer of the cell membrane, resulting in the successful cellular uptake of exogenous nucleic acids into the cells. Two different transfection reagents were used as follows:

2.2.2.1. **FuGENE HD** (Roche, Germany):

Cells were plated at a density of 0.8 x 10^5 cells per well of a 12-well plate (1.4 x 10^5 cells per well of a 24-well plate) 48 hours before transfection. Cells were transfected at a 3:1 transfection reagent: DNA ratio according to the manufacturer's instructions. Three microliters (1.7 µl for 24-well plate) of Fugene HD was added to 97 µl (48 µl for 24-well plate) of serum free medium and incubated at room temperature (RT) for 5 minutes. The DNA was added to the above mixture, mixed and incubated at RT for another 5 minutes. The transfection reagent/DNA complex was added dropwise to the cells and incubated for 48 hours at 37°C.

Generation of FLAG-TBX3 and FLAG-EMPTY cell lines: MCF-7 cells were grown to 60% confluence in 35 mm dishes and subsequently transfected with 500 ng pCMV-3XFLAG-TBX3 or pCMV-3XFLAG-EMPTY expression constructs.

Transient c-Myc overexpression: MCF-7 cells were seeded at a density of 2.5 x 10^5 cells/well in 24 well plates and were subsequently transfected 48 hours later with 500 ng pcDNA-FLAG-c-Myc or pcDNA-FLAG-EMPTY expression constructs.
Transient nucleolin overexpression: MCF-7 cells were plated at a density of 1.4 x 10^5 cells/well in 24 well plates and were transfected with 150 ng of the pEGFP-nucleolin expression vector or pEGFP-Empty vector.

2.2.2.2. **Hiperfect®** (Qiagen, USA):

Transient knockdown of c-Myc, nucleolin or Hsc70 expression in MCF-7 cells was achieved by siRNA that specifically targets mRNA of c-Myc, nucleolin or Hsc70. MCF-7 cells were plated at 0.85 x 10^5 cells/well of a 24-well plate. The cells were transfected at 60% confluency with 10 nM si-c-Myc (Dharmacon, Lafayette, CO, USA and Qiagen, USA), 10 nM si-Nuc (SI02654925, Qiagen, USA), 50 nM si-Hsc70 (SI04236596, Qiagen, USA) or a control (non-silencing, siCtrl) siRNA (1027310; Qiagen, USA), according to manufacturer's instructions. Briefly, siRNAs were diluted in 100 µl serum-free medium after which 3 µl of HiPerFect® was added directly to the siRNA solution, incubated at RT for 5 minutes and added to cells. Cells were incubated for 6 hours at 37°C, after which 400 µl complete medium was added.

2.2.3. Generation of stable cell lines in which TBX3 is overexpressed

MCF-7 breast cancer cells were transfected with the pCMV-3XFLAG-TBX3 or pCMV-3XFLAG-EMPTY expression constructs as described in **section 2.2.2.1** and as depicted in **Figure 2.1.** Stably transfected clones were selected for with G-418 antibiotic (Promega, USA) 48 hours post transfection as described below.

2.2.4. G-418 selection

In order to ensure that only stable transfectants were selected, cells were treated with a previously established concentration (400 µg/ml) of G-418 (V7983, Promega, USA), a

neomycin analogue, as the pCMV-3XFLAG-TBX3 and pCMV-3XFLAG-EMPTY expression constructs carry a neomycin resistance gene. G-418 is an antibiotic that alters normal protein production through polypeptide synthesis inhibition both prokaryotic and eukaryotic cells, therefore ultimately resulting in cell death (Davies & Jimenez, 1980; Bar-Nun et al., 1983; Beck et al.,1982).

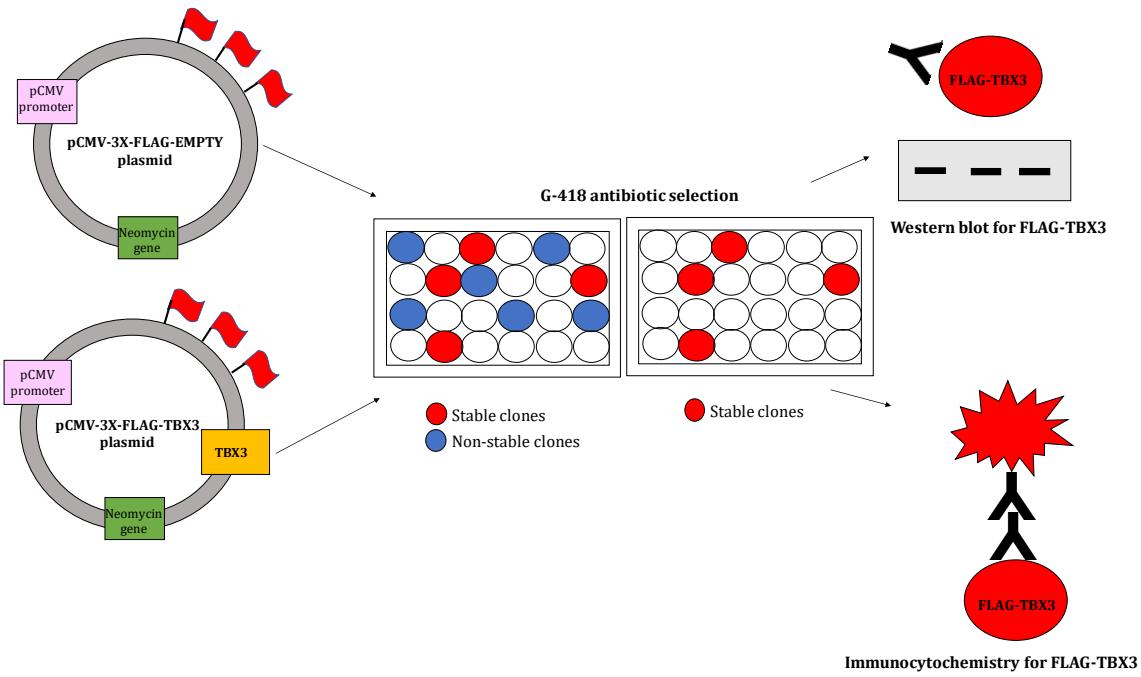

Figure 2.1: Generation of stable cell lines. MCF-7 breast cancer cells were transfected with the pCMV-3XFLAG-EMPTY or pCMV-3XFLAG-TBX3 expression constructs. Stably transfected clones were selected for using G-418 antibiotic selection. To determine whether the stable transfectants express pCMV-3XFLAG-TBX3 , the cells were subjected to western blotting using primary antibodies to FLAG. To determine whether the stable transfectants express pCMV-3XFLAG-TBX3 in the nucleus, the cells were subjected to immunocytochemistry using a primary antibody to FLAG and a fluorophore conjugated secondary antibody to the anti-FLAG primary antibody.

2.3. Cell treatments

2.3.1. MG132 treatment

In order to inhibit ubiquitin-mediated protein degradation, 48 hours after transfection with si-Hsc70 or siCtrl (as described in **section 2.2.2.2**), the medium was replaced with fresh medium containing a final concentration of 10 µM MG132 for 30 minutes. After

minutes, protein was harvested from the cells (as described in **section 2.10.1**) and analysed by western blotting with antibodies to TBX3 (1:1000) and Hsc70 (1:1000)

2.3.2. Actinomycin D treatment

In order to inhibit de novo transcription, 48 hours after transfection with pcDNA-FLAG-cMyc or pcDNA-FLAG-EMPTY (as described in **section 2.2.2.1**). The cells were treated with 5 µg/ml Actinomycin D (Sigma, USA) for 30 minutes. All incubations were done in the dark. RNA and protein were harvested from the cells (as described in **section 2.9.1** and **section 2.10.1** respectively) and analysed by (1) qRT-PCR with primers specific to TBX3 and c-Myc and (2) western blotting with antibodies to c-Myc and TBX3 respectively.

2.3.3. AS1411 and CRO aptamer treatment

To analyse the effect of inhibiting nucleolin, MCF-7 cells were treated with 10 µM AS1411 aptamer (5'-GGTGGTGGTGGTTGTGGTGGTGGTGG-3'; Intergrated DNA technologies) or an inactive control aptamer, CRO (5'-CCTCCTCCTCCTTCTCCTCCTCCTCC-3'; Intergrated DNA technologies) for 96 hours. For cell viability assays, MCF-7 cells were plated at a density of 1 X 10^3 cells/well in 96 well-plates and immediately treated with 10 µM AS1411 or CRO. Cells were subsequently processed as described in **section 2.4.1**. For migration assays, MCF-7 cells were plated at a density of 0.85 X 10^5 cells/ml in 24-well plates and immediately treated with 10 µM AS1411 or CRO. Cells were subsequently processed as described in **section 2.4.2**. For immunocytochemistry, MCF-7 cells were plated at a density of 0.25 X 10^5 cells/ml on glass coverslips in 35 mm dishes and immediately treated with 10 µM AS1411 or CRO. Cells were subsequently processed as described in **section 2.5**. For subcellular fractionation, MCF-7 cells were plated at a density of 5 X 10^5 cells/ml in 10 cm dishes and immediately treated with 10 µM AS1411 or CRO. Cells were subsequently processed as described in **section 2.6**.

2.4. Growth curve assays

Two methods were utilized to determine short term cell growth, namely: (1) cell viability as a measure of cell growth was determined using the 3-(4,5-dimethylthiazol-2-yl)-2,5-diphenyltetrazolium bromide (MTT) Cell Proliferation Kit (Roche, Germany) and (2) counting of cells at specific time points using a haemocytometer.

2.4.1. MTT (3-(4,5-dimethylthiazol-2-yl)-2,5-diphenyltetrazolium bromide) assay

To determine cell growth using the methylthiazol tetrazolium (MTT) Cell Proliferation Kit, cells were seeded in triplicate in a 96-well plate (1000 cells/well) and cell viability was determined according to the manufacturer's instructions. Briefly, 24 hours prior to harvesting 15 µl MTT labelling reagent was added to each well to a final concentration of 0.5 mg/ml and cells were incubated at 37°C in 9% CO_2 for 4 hours after which 100 µl of solubilisation solution was added and the cells incubated overnight. The spectrophotometric absorbance of the samples was determined at a wavelength of 595 nm using a 96-well plate reader, with the absorbance of the medium only control being subtracted from the samples. Cell proliferation was determined over 48-72 hours.

2.4.2. Counting using a haemocytometer

To determine the effect of overexpressing TBX3 on short term cell growth, cells were plated in triplicate in a 12-well plate at a density of 1 x 10^4 cells per well. Cells were collected by removing and keeping the media the cells had been growing in, washing the cells twice with 1XPBS, keeping the 1XPBS, and then by trypsinisation. Cells were counted using a haemocytometer at days 1, 4, 7 and 10.

2.5. In-vitro 2D cell scratch motility assays

To determine the effect of overexpressing TBX3 on cell migration a 2D scratch motility assay was performed in the following manner (as depicted in **Figure 2.2**): Cells were

seeded in a 24-well plate and grown to confluence. Thereafter a linear wound was made by making a scratching through the monolayer using a 10 µl pipette tip. To remove cell debris, the growth medium was removed, and the cells were washed with 1XPBS and thereafter the media replaced and to inhibit proliferation, Mitomycin C (Sigma, USA), was added at a final concentration of 10 µg/ml. Three markings were made along the scratch as reference points during the capturing of images, to ensure that the same area of the scratch was measured throughout the assay (As depicted in **Figure 2.2**). The wound area was measured at the time of making the scratch and at three-hour time intervals thereafter until the twenty-four-hour timepoint. Pictures were taken using a non-phase contrast lens at 20X magnification (Sony cyber shot, DSC-T20) using an Axiovert fluorescent microscope (Zeiss, Germany). The difference in area was measured using ImageJ software (National Institutes of Health, Bethesda, MD). Protein was harvested from the cells (as described in **section 2.10.1**) and analysed by western blotting using the relevant antibodies.

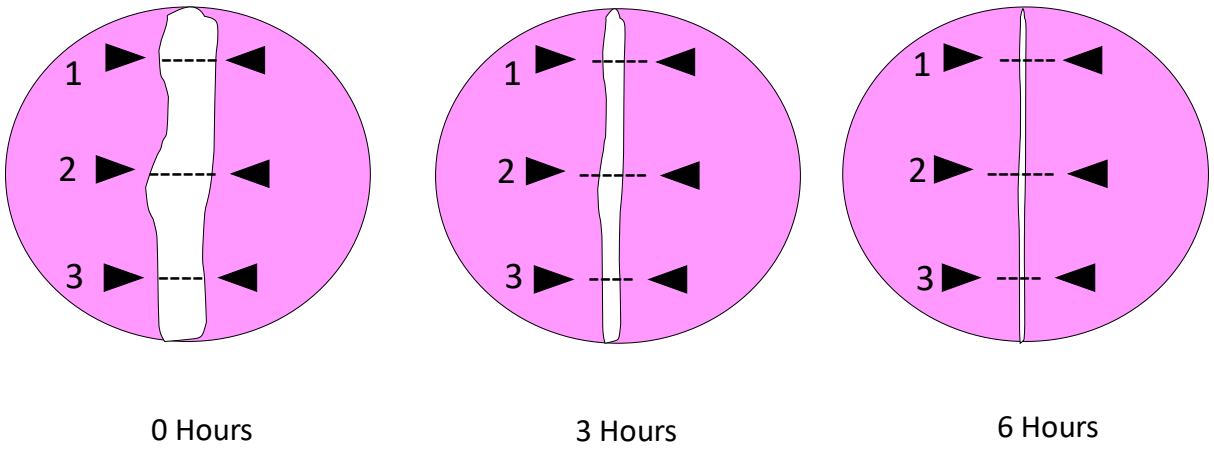

Figure 2.2: In vitro 2D scratch motility assay. Cell migration is monitored by making a scratch through a monolayer of cells and monitoring wound closure over time. Three markings were made along the scratch, at the bottom of the well to ensure that the gap/wound was measured at the same point for all time intervals.

2.6. Subcellular fractionation

Nuclear and cytoplasmic lysates were prepared from MCF-7 breast cancer cells. Briefly, sub-confluent cells from 10 cm cell culture dishes were washed three times in ice-cold

1XPBS, trypsinized, and pelleted at 5000 g for 3 minutes at 4°C. The cell pellet was then resuspended in 5 volumes of solution 1 (**See appendix section 6.3**) containing protease inhibitors and the cells allowed to swell on ice for 5 minutes, then 0.5% Triton X-100 was added to lyse the cell membranes and incubated for further 5 minutes. The cells were centrifuged at 900 g and the cytoplasmic fraction (supernatant) was transferred to fresh tubes and stored at -80°C. The pellet was washed in 5 volumes of solution 1 with protease inhibitors and centrifuged at 900 g. The supernatant was discarded and the cell pellet containing the nuclei of the cells was resuspended in 5 volumes of solution 2 (**see appendix section 6.3**) containing protease inhibitors and RNAse-free DNAse (100 µg/ml) and incubated for 45 minutes at 30°C. The lysate was centrifuged at 1500 g for 5 minutes at 4°C. The nuclear extract (supernatant) was transferred to fresh tubes and stored at -80°C. Protein concentration was assayed by BCA assay (Pierce, USA) with bovine serum albumin as the standard. For western blotting, GAPDH and p84 were used (1) as loading controls and (2) to confirm that the nuclear and cytoplasmic fractions were pure with GAPDH being a cytoplasmic protein marker and p84 being a nuclear protein marker.

2.7. Immunoprecipitation assays

Immunoprecipitation assays aim to reveal protein-protein interactions through pulling down one tagged protein, "Protein X", and then western blotting for its possible partner, "Y" using an antibody against "Protein Y" (as depicted in **Figure 2.3**).

2.7.1. FLAG affinity purification

FLAG-TBX3 or FLAG-EMPTY cells were grown in 15 cm dishes to 90% confluence and harvested in 700 µl of FLAG-lysis buffer (**see appendix section 6.4**). Cells were incubated for 30 minutes on a shaker at 4°C and cellular debris removed by centrifugation at 12 000 g for 10 minutes at 4°C. The supernatant was incubated with 30 µl of anti-FLAG antibody conjugated to agarose beads pre-equilibrated in 1XTris-buffered saline (1XTBS) (anti-FLAG M2 affinity gel, A2220, Sigma) with constant rotation overnight at 4°C. Following binding, protein-protein complexes were pelleted by centrifugation for 30 seconds at 6000 g and the supernatant removed with a syringe.

Beads were washed three times with 0.5 ml of 1XTBS. After the final wash, the immune complexes were resuspended in 20 µl of 2 X Laemmli buffer (**see appendix section 6.5**) and boiled for 3 minutes at 100°C. Protein samples were either analysed by SDS-PAGE and western blotting using antibodies to FLAG (1:1000) (F3165, Sigma, USA) or subjected to filter aided sample preparation and mass spectrometry analysi.

2.7.2. Co-immunoprecipitation assays

Following FLAG affinity purification as described in **section 2.7.1**, protein samples were either analysed by SDS-PAGE and western blotting using antibodies to nucleolin (1:1000) (sc-8031, Santa Cruz Biotechnology, Santa Cruz, CA), Hsc70 (1:1000) (SI04236596, Qiagen, USA) and HnRNP K (1:1000) (sc-28380) (Santa Cruz Biotechnology, Santa Cruz, CA).

2.8. Immunocytochemistry

Cells were grown to 60% confluence on glass coverslips in 35 mm dishes and subsequently washed three times with 1XPBS and fixed in ice cold absolute methanol for 10 minutes. Cells were permeabilised in 2% Triton X-100 in 1X PBS for 10 minutes at RT. Cells were blocked for 1 hour in 1% BSA in 1X PBS at RT and incubated with the mouse monoclonal anti-FLAG M2 antibody (1:500) (F1842) (Sigma, USA) for 2 hours at 37°C or with rabbit polyclonal anti-TBX3 antibody (1:100) (ab99302) (Abcam, USA), mouse polyclonal nucleolin (1:1000) (sc-8031, Santa Cruz Biotechnology, Santa Cruz, CA) , mouse polyclonal Hsc70 (1:1000) (SI04236596, Qiagen, USA) or mouse polyclonal HnRNP K (1:1000) (sc-28380) (Santa Cruz Biotechnology, Santa Cruz, CA) antibodies diluted in blocking buffer at 4^{0}C overnight in a humidifying chamber. Cells were washed three times with 1X PBS and incubated with the Cy3 goat anti-rabbit or Cy3 donkey anti mouse (1:1000; Molecular probes, USA) or Alexa 488 goat anti-mouse secondary antibody (1:1000; Molecular probes, USA) for 2 hours at RT in the dark. Cells were washed again with 1X PBS and the DNA was stained by incubating the cells with 1mg/ml Hoechst 33258 (Thermofischer Scientific, South Africa) for 10 minutes at RT in the dark. Cells were washed, then coverslips were mounted onto glass slides using Mowial mounting medium (Hoechst, Germany) containing n-Propyl gallate (anti-Fade) (Sigma,

USA) and the cells were visualised by confocal microscopy [(Zeiss LSM 510 Meta with NLO, Software: ZEN 2009 and lasers (Argon 488 green; solid state laser: 561 nm Red and MaiTai 2 photon laser: 750 nm for DAPI/ Hoechst, Germany)] (as depicted in **Figure 2.4**).

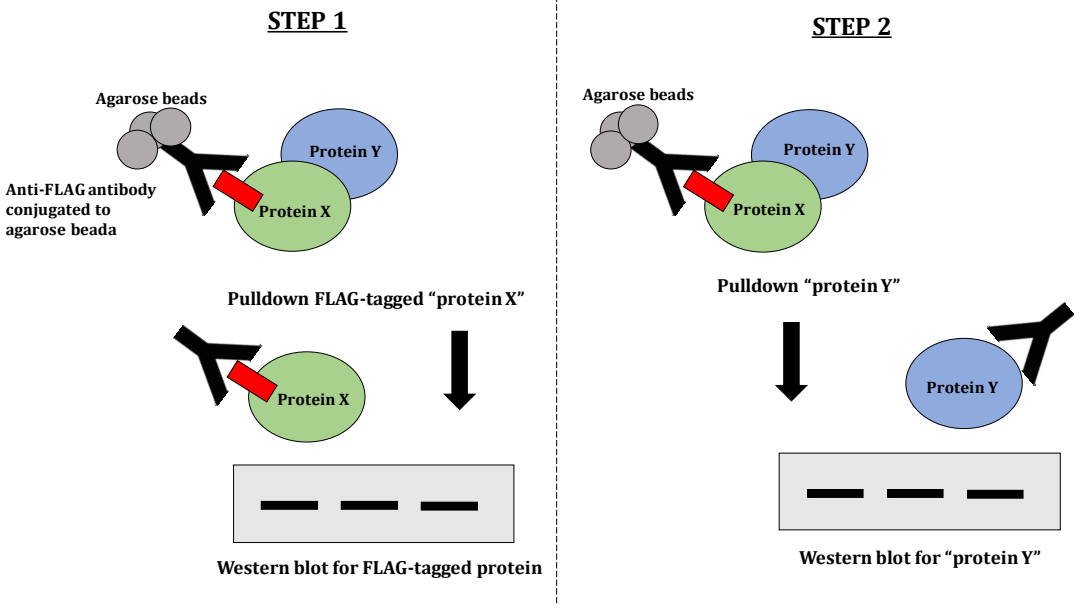

Figure 2.3: FLAG affinity purification and immunoprecipitation assays. Immunoprecipitation assays reveal protein-protein interactions through a two-step process. The first step involves pulling down and isolating one tagged protein, "Protein X" and confirming successful pulldown via western blotting using an antibody against the tag (in this case an anti-FLAG antibody; left panel). The second step involves determining whether another protein of interest "Protein Y" is bound to the FLAG tagged protein by subjecting the protein lysate obtained in step one to western blotting using an antibody against "Protein Y" (right panel).

Negative controls were appropriate to secondary antibodies only. Co-localisation analysis to obtain values for Mander's correlation coefficient (MCC), weighted correlation coefficient (WCC), and Pearson's correlation coefficient (PCC), in the whole cell, cytoplasmic and nuclear compartments was performed using Zeiss LSM 510 Meta Software. The PCC value defines the overall correlation between two channels as a value between -1 and 1, where a value of 1 represents perfect co-localisation and a value of -1 represents perfect exclusion. MCC values range between 0 and 1, where a value of 1 represents high co-localisation and 0 represents low co-localisation. WCC values range from 0 to 1 where a value of 0 indicates random staining and a value of 1 indicates dependent staining. The results of PCC, MCC and WCC were calculated from 20 random fields of view.

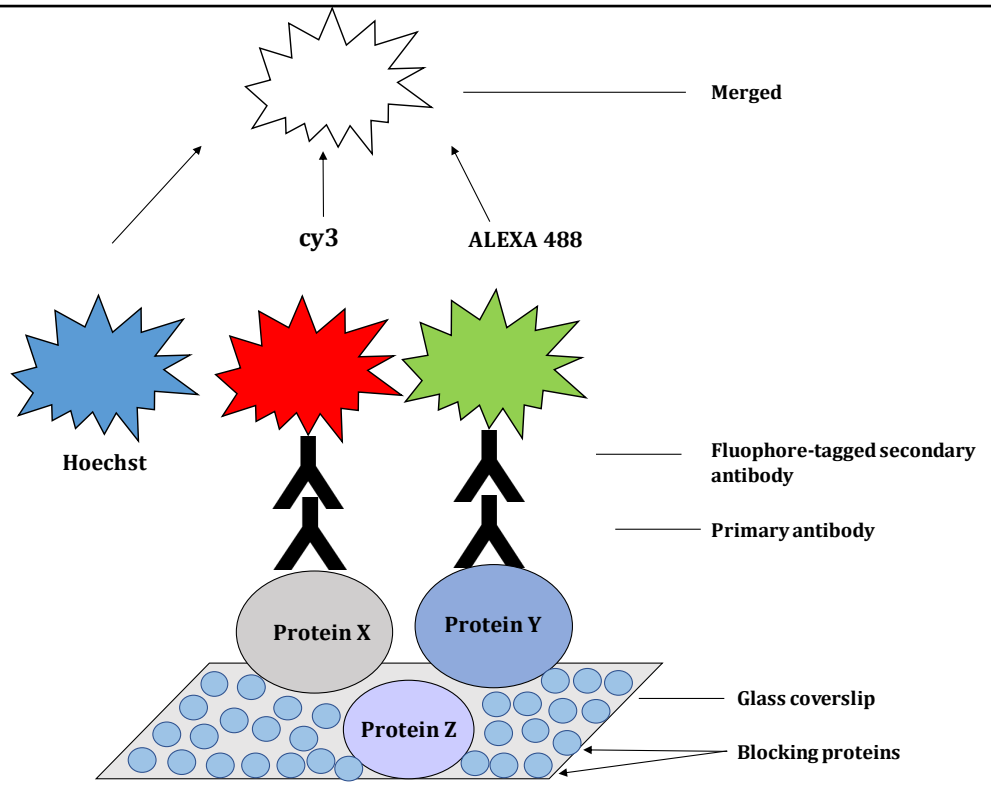

Figure 2.4: Immunocytochemistry. Immunofluorescence is used to visualize intracellular protein-protein interactions. Primary antibodies recognize and bind specific target proteins, and their complementary fluorophore-tagged secondary antibodies subsequently bind them. Protein interactions are then subsequently determined by measuring the fluorescence of single fluorophores and the degree of overlap between two or more fluorophores. (Image adapted from MSc thesis of Danica Smuts, University of Cape Town, 2016)

2.9. Quantitative real-time polymerase chain reaction (qRT-PCR)

To quantify the levels of TBX3, nucleolin and c-Myc mRNA, qRT-PCR was performed. Briefly, RNA was harvested and purified and subsequently converted to complementary DNA (cDNA) and cycles of PCR were performed. Forward and reverse primers specific to TBX3, nucleolin, c-Myc or GUSB mRNA sequences were added and PCR was performed in cycles. The crossover threshold (CT)/crossing point (CP) values obtained depend on the starting amount of the cDNA, and thus the starting amount of cDNA can be inferred from these values. For example, the lower the CT/CP value the larger the starting amount of mRNA in the sample and the higher the CT/CP value the smaller the starting amount of mRNA in the sample

2.9.1. RNA extraction

Total RNA was extracted from cells using the High Pure RNA Isolation Kit according to the manufacturer's instructions (Roche, Germany). Cells were grown in 6 cm dishes to 60% confluence and subsequently washed twice in 1XPBS washes (**see appendix section 6.5**). The cells were pelleted, resuspended in 200 µl 1XPBS and 400 µl of High Pure RNA Isolation Kit Lysis Buffer was added followed by brief vortexing. The lysis buffer contains Triton-X 100 detergent to permeabilize the cell membranes, Tris-HCl, to regulate pH and osmolarity of the lysate, and guanidine hydrochloride, to denature proteins, inactivate RNases and promote binding of the RNA to the membrane of the spin column. Genomic DNA was removed via addition of DNase and DNase incubation buffer followed by centrifugation at 6000 g. The phosphodiester backbone of the DNA was hydrolytically cleaved and the degraded DNA removed by washes and centrifugation, leaving behind the RNA. The RNA was eluted in nuclease free double distilled water. The wash buffers and centrifugation steps remove proteins, lipids, polysaccharides, salts and other cellular impurities from the RNA solution and, during the elution step, the polarity of the water disrupts the bonds between the RNA and membrane, enabling elution. The quality and concentration of RNA was determined by spectrophotometry using a NanoDropR ND-1000 spectrophotometer (Agilent Technologies, Boeblingen, Germany). The ratio of the absorbance maxima of nucleic acids (260 nm) to the absorbance at 280 nm was used as a measure of RNA purity. A 260/280 ratio of approximately 2.0 is generally accepted as "pure" for RNA. The resulting RNA produced was stored at -80°C or immediately converted to cDNA.

2.9.2. Reverse transcription

cDNA was produced from the extracted RNA samples by reverse transcription using the InProm-IITM reverse transcription system (Promega A3800) according to the manufacturer's instructions. Briefly, for each sample 1 µg of RNA was combined with 0.5 µg of Oligo (dT) primer in a 5 µl volume and denatured at 70˚C for 5 minutes, chilled on ice and combined with reverse transcription reaction mix (5X InProm-IITM reaction buffer, 25 mM $MgCl_2$, 10 mM dNTP mix, 20 units RNasinR ribonuclease inhibitor and 1 µl of ImProm-IITM reverse transcriptase) to a final volume of 20 µl. The annealing of the

primers to the template RNA occurred at 25°C for 5 minutes, the reactions were incubated at 25°C for 5 minutes, 42°C for 1 hour for the reverse transcription to occur, and 70°C for 15 minutes incubation to inactivate the reverse transcriptase prior to PCR. The resulting cDNA produced was stored at -20°C.

2.9.3. qRT-PCR experimental conditions

To quantify the relative levels of cDNA between samples, qRT-PCR was conducted in 96-well sealed plates on an Applied Biosystems StepOne Plus thermal cycler using 2X SYBR green master mix (Applied Biosystems, Carlsbad, CA, USA). PCR reactions contained 2X SYBR green master mix, sabax water and 0.4 µl of combined forward and reverse primers (10 µM) (Quantitect real-time PCR primers or Qiagen primers) per 8 µl reaction. The cDNA was added into the respective wells, followed by the addition of the master mix to give a final reaction volume of 20 µl. Primers specific to TBX3 (QT00022484, Qiagen, Germany) and nucleolin (Forward-5'-AACCTCTCCTACAGTGCAACA-3', Reverse-5'-CTGGCTTCTGGCATTAGGTG-3'; Integrated DNA technologies) were used. For internal normalisation to correct for sample-to-sample variations within a PCR run, Glucuronidase Beta (GUSB) (QT00046046, Qiagen, Germany) primers were used. The plate was centrifuged at 3000 rpm for 1 minute and placed in the Applied Biosystems StepOne Plus thermal cycler (Applied Biosystems, Carlsbad, CA, USA). PCR cycle parameters were: denaturation (15 minutes at 95°C), annealing and amplification for 35 cycles (5 seconds at 95°C; 3 seconds at 55°C; 5 seconds at 72°C), melting step (15 seconds at 65°C) and a cooling step (30 seconds at 40°C). Each sample was quantified in duplicate and a negative control without cDNA template was run with every assay to assess the overall specificity and monitor for contamination. Melting curve analyses was carried out to ensure product specificity and data was analysed using the 2-ΔΔCt method (Livak and Schmittgen, 2001). Relative mRNA expression levels were normalized to GUSB for each reaction with PCR efficiency correction calculated using the formula Ratio = (Etarget)CPtarget(control–sample)/(Eref)CPref(control–sample); E: real-time PCR efficiency, CP: crossing-point. The Microsoft Excel programme was used to calculate the statistically significant differences between samples using the Student t test. P values of <0.05 were considered statistically significant.

2.10. Western Blotting

Western blotting was performed to quantify protein expression levels. Briefly, protein was harvested and subjected to SDS-PAGE and western blotting analysis using primary antibodies specific to the protein of interest and secondary antibodies specific to the relevant primary antibody. Thereafter, proteins were detected (as depicted in **figure 2.5**).

2.10.1. Protein harvesting

Briefly cells were grown to 90% confluence in a 35 mm dish. Cells were subsequently harvested by trypsinisation and centrifuged at 2500 rpm for 3 minutes. The media was discarded, and the pellet resuspended in 70 µl of 2 X Laemmli lysis buffer (**see appendix section 6.5**). Alternatively, the cells were lysed in scaled volumes of 2 X Laemmli lysis buffer, according to the dish area and confluency. Cell lysates were collected into a microfuge tube, boiled for 10 minutes at 100°C and stored at -20°C.

2.10.2. Sodium-Dodecyl-Sulphate Polyacrylamide Gel Electrophoresis (SDS-PAGE)

Protein samples were separated by gel electrophoresis on 1.5 mm 8% resolving gels with a 5% stacking gel (**see appendix section 6.5**). Gels were assembled in Biorad Mini PROTEAN© casting apparatus, placed in the Biorad running tank and the tank was filled with 1X running buffer (**see appendix section 6.5**). In cases where protein concentration was determined using the BCA assay, equal amounts of sample were loaded and in cases where concentration was not determined, the housekeeping gene p38 was used and protein expression levels quantified relative to p38 to account for unequal protein volume loading. Six microlitres of PageRuler Prestained Protein Marker (Fermentas, USA) (**See appendix section 6.5**) was also loaded to determine the relative size of the proteins (**See appendix section 6.5**). The running apparatus was connected to the Biorad Powerpack 200 (South Africa) and electrophoresis occurred at 100 Volts for 2 hours.

2.10.3. Protein transfer onto a nitrocellulose membrane

Following electrophoresis proteins were transferred onto nitrocellulose membrane (Amersham, GE Healthcare, Life Sciences, Germany). Gels were placed in a transfer 'sandwich' cassette consisting of sponges, whatman filter paper, the gel and the nitrocellulose membrane pre-soaked in 1X transfer buffer (**See appendix section 6.5**) assembled into the correct order (As depicted in **Figure 2.5**). This assembly was then placed into the transfer unit of the Biorad Mini PROTEAN© 3 transfer tank in the correct orientation to ensure that the negatively charged proteins moved from the gel onto the membrane which is placed on the positive side of the transfer sandwich. An ice pack was placed in the tank to prevent overheating and the tank was filled with 1X transfer buffer. The transfer apparatus was connected to the Biorad Powerpack 200 and protein transfer took place at 100 Volts for 90 minutes.

2.10.4. Western blot detection

Following transfer, membranes were blocked for 1 hour in 5% PBS/T milk (**see appendix section 6.5**) and probed with appropriate primary antibodies overnight at 4˚C with continuous shaking. Primary antibodies were used as follows: Rabbit polyclonal anti-TBX3 (1:500) (Zymed 42– 4800, Zymed, San Francisco, CA) or (1:1000) (ab99302, Abcam, USA), rabbit polyclonal anti-p38 (1:5000) (M0800, Sigma, USA), mouse monoclonal anti-FLAG M2 (1:1000) (F1804, Sigma, USA), rabbit anti-c-Myc (1:1000) (sc-N262), mouse polyclonal anti-nucleolin (1:1000) (sc-8031), mouse polyclonal anti-Hsc70 (1:1000) (sc-7298), anti-HnRNP K (sc-28380) (Santa Cruz Biotechnology, Santa Cruz, CA), mouse monoclonal anti-p21 (1:200) (Santa Cruz, USA), mouse monoclonal anti-p53 (1:100) (Santa Cruz, USA), rabbit polyclonal anti-vimentin (1:1000) (Cell Signalling Technology, USA), mouse polyclonal anti-N-cadherin (1:1000) (Cell Signalling Technology, USA), mouse monoclonal anti-ß-catenin (1:500) (Thermo Fisher Scientific), mouse monoclonal anti-GAPDH (1:1000) and mouse monoclonal anti-p84 (1:1000) (Genetex, Irvine, CA, USA). p38 was selected as a loading control because it is ubiquitously expressed in the cells and its expression levels are not altered by experimental conditions.

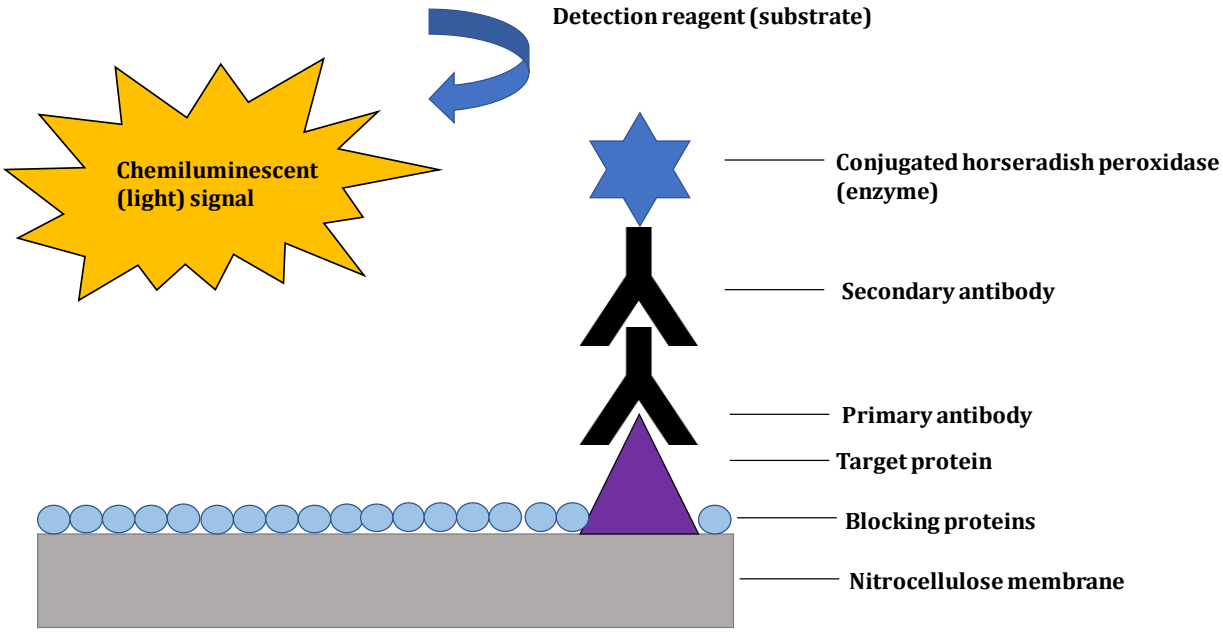

Figure 2.5: Western Blot detection by enhanced chemiluminescence. The primary antibody specific to the target protein will bind to it if present on the nitrocellulose membrane blot containing the transferred proteins. An enzyme conjugated secondary antibody against the primary antibody, binds to the primary antibody. Enzyme substrate is added directly onto the nitrocellulose membrane and a chemical reaction takes place. Through this reaction, a light signal that is detected via exposure to an autoradiography film in a dark room is emitted.

Membranes were washed for two five-minute and two ten-minute intervals and incubated with the appropriate secondary antibody: horseradish peroxidase conjugated anti-rabbit, anti-mouse (1:5000) (BioRad, Hercules, CA, USA) or A/G protein (1:5000) (20421, Thermo Fisher Scientific), for 1 hour at RT, then washed as previously described, before protein detection was performed and visualised by enhanced chemiluminescence (ECL) by addition of SuperSignal West Pico Chemilumninescent Substrate (Pierce, Rockford, IL, USA) or WesternBright (Advansta, USA). A 1:1 ratio of detection reagent A and detection reagent B was added per blot (total detection reagent volume = area of blot x 0.1 ml) and left to incubate for 3-5 minutes. When the detection reagent (containing the substrate) comes into contact with the enzyme-conjugated secondary antibody, the substrate is oxidised leading to the emission of a chemiluminescent signal (As depicted in **Figure 2.6**). Membranes were exposed to autoradiography film and the

chemiluminescent signal was captured by developing and fixing the autoradiography film. Densitometry analysis was carried out to quantify the protein bands using ImageJ software and the readings were normalized to the p38 loading control.

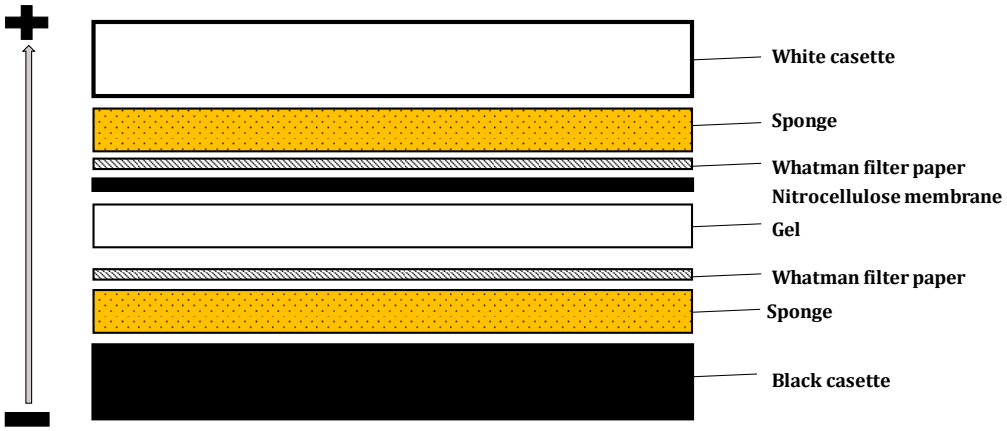

Figure 2.6: Western blot transfer sandwich. Once the SDS PAGE gel has run, the separated proteins are transferred from the gel to a nitrocellulose membrane. It is important that the layout of the transfer sandwich and orientation of the plastic cassette is as shown in the figure, to ensure that the proteins do indeed transfer from the gel onto the blot for later detection.

2.11. Mass spectrometry analysis

To identify putative TBX3 protein interaction partners, mass spectrometry analysis was performed. This was done in a three-step process which entailed (1) in-solution digestion of proteins, (2) desalting, and (3) liquid chromatography mass spectrometry analysis.

2.11.1. In-solution digestion

FLAG-Affinity purification was carried out as described in **section 2.7.1**. The washed agarose beads were incubated with denaturation buffer (6 M Urea, 2 M Thiourea, Tris pH 8.0) for 10 minutes at room temperature. The supernatant containing eluted interaction partners was transferred into a new Eppendorf tube. Proteins were reduced by incubation with 1 mM DTT for 1 hour at room temperature and further alkylated by incubation with 5.5 mM iodacetamide for 1 hour at room temperature in the dark. The samples were diluted by addition of 4 volumes of digestion buffer (20 mM ammonium bicarbonate, 20 mM $CaCl_2$, pH 8.0) and 1 µg of sequence-grade trypsin (New England

Biolabs) was added. Digestion was performed at room temperature overnight. The reaction was stopped the next morning by addition of 0.1% formic acid.

2.11.2. Desalting

Peptides obtained from in-solution digestion were desalted because - since mass spectrometry measures charged ions - salts, especially sodium and phosphate salts, should be removed prior to MS to minimize their detection as they can interfere with downstream processes. Desalting was conducted using a stage tip containing Empore Octadecyl C18 solid-phase extraction disk (Supelco) (Rappsilber et al., 2003). All activation, equilibration, peptide washes and elution steps were performed by centrifugation at 5000 g for 5 minutes. Activation and equilibration of the C18 disk was performed using three rinses with 80% acetonitrile (ACN) containing 0.1% formic acid (Sigma), followed by three rinses with 2% ACN containing 0.1% formic acid (Sigma). The peptide-rich solution was loaded onto the disk and centrifuged. Desalting was conducted using three washes of 2% ACN containing 0.1% formic acid (Sigma). The desalted peptides were then eluted into glass capillary tubes using three rounds of 50 µl of 60% ACN and 0.1% formic acid. Peptides were air dried in a vacuum after which they were resuspended in 2% ACN, 0.1% formic acid.

2.11.3. LC-MS/MS

Liquid chromatography separation was performed with a 100 µM ID × 20 mm precolumn connected to a 75 µM × 300 mm analytical column packed with C18 Aeris beads (5 µm diameter, 100 Å pore size; Phenomenex 04A-5452). Mass spectrometry was performed using LC-MS with a Dionex Ultimate3500 nano-LC coupled to a Q Exactive hybrid quadrupole-Orbitrap. Desalted peptides were loaded onto the column with starting mobile phase of 2% ACN and 0.1% formic acid. The injection volume was normalised to maximum TIC (total ion current). Peptides were eluted over a 40 minutes gradient from 6 – 40% solvent B (80% acetonitrile, 0.1% formic acid). The flow rate was constant at 300 µl/minute. Typical backpressure values during separation were <350 bar. Mass spectra were acquired with an Orbitrap Q Exactive mass spectrometer in a data-dependent manner, with automatic switching between MS and MS/MS scans using a top-10 method.

MS spectra were acquired at a resolution of 70 000 with a target value of 3×10^6 ions or a maximum integration time of 250 ms. The scan range was limited from 300 to 1750 m/z. Peptide fragmentation was performed via higher-energy collision dissociation (HCD) with the energy set at 25 NCE. Intensity threshold for ions selection was set at 1.7 e4 with charge exclusion of z = 1 and z > 5. The MS/MS spectra were acquired at a resolution of 17 500, with a target value of 2×10^5 ions or a maximum integration time of 120 ms and the isolation window was set at 4.0 m/z.

The obtained RAW data files were processed with Maxquant version 1.5.4.1 (http://www.biochem.mpg.de/5111795/maxquant) for protein and peptide identification using the Andromeda search engine and the Uniprot proteome for *Homo sapiens* (Proteome ID: UP000005640, 73101 proteins, 01/02/2018). The normal default parameter settings were used for the MS/MS database search, with carbamidomethylation of cysteine residues and acetylation of the protein N-terminus selected as fixed modifications. Trypsin/P was selected as protease and the 'match between runs' feature were enabled. Reverse hits and common contaminants were removed from the identified protein list. Likewise, only protein identifications with a q value < 0.01 were retained for the further analysis. Venny 2.1 software (http://bioinfogp.cnb.csic.es/tools/venny/) was used to visualize all possible peptide relations between replicate groups. The STRING database (https://string-db.org/) was used to generate a protein interaction network map to determine whether the interacting partners identified were involved in common networks and to carry out GO analysis.

2.12. Statistical analyses

All graphs were drawn using the Graphpad Prism 6 program. Statistical analysis of data was performed using the 2-sample t-test (Microsoft Excel software) and $p<0.05$ (*) was considered statistically significant, $p<0.001$ (**) very significant and $p<0.0001$ (***) extremely significant.

CHAPTER 3

Results

TBX3 is overexpressed in a plethora of cancers including a subset of breast cancer cell lines and tumours (Fan et al., 2004; Hansel et al., 2004; Lomnytska et al., 2006; Renard et al., 2007; Rodriguez et al., 2008; Yarosh et al., 2008; Fillmore et al., 2010; Fan *et al.*, 2004). This overexpression has been shown to be critical for the cancer phenotype and TBX3 has been identified and validated as a novel therapeutic target to treat breast cancer (Peres *et al.*, 2010). However, very little is known about the factors responsible for upregulating TBX3 and even less is known about the protein co-factors that it interacts with to promote its oncogenic roles. Thus, this study proposes to identify and characterize (1) c-Myc as a signalling molecule that upregulates TBX3 and (2) co-factors that interact with TBX3 to (a) stabilize the protein and (b) regulate its oncogenic functions.

3.1. The regulation of TBX3 expression in breast cancer by c-Myc

To date only the TGFβ pathway has been demonstrated to upregulate TBX3 in breast cancer but it is speculated that other oncogenic signalling pathways will also converge on TBX3 (Li *et al.*, 2013). In this regard, it was hypothesized that the basic helix-loop-helix oncogenic transcription factor c-Myc may be involved because like TBX3, c-Myc is overexpressed in some breast cancer subtypes and the Prince laboratory has previously shown that c-Myc directly binds and activates the TBX3 promoter in a number of sarcoma subtypes (Willmer *et al.*, 2015 and unpublished data).

3.1.1. c-Myc transcriptionally activates TBX3 in MCF-7 breast cancer cells

To investigate the possibility that c-Myc may be upstream of TBX3 in breast cancer cells where it is overexpressed, the impact of transiently knocking down c-Myc on TBX3 expression levels was assessed. Briefly, c-Myc was depleted in MCF-7 breast cancer cells using two different siRNA's (si-c-Myc#1 and si-c-Myc#2) and TBX3 mRNA and protein

levels were measured by qRT-PCR and western blotting respectively. The results show that the two different siRNAs were efficacious and resulted in a corresponding decrease in TBX3 mRNA (**Figure 3.1 A**) and protein levels (**Figure 3.1 B**). To determine whether this regulation is transcriptional, c-Myc was overexpressed by transiently transfecting MCF-7 breast cancer cells with a pcDNA expression vector containing FLAG-tagged c-Myc (FLAG c-Myc), with or without Actinomycin D, an inhibitor of de novo transcription, and TBX3 mRNA and protein levels were measured by qRT-PCR and western blotting respectively. The results show that in the presence of only ectopically expressed c-Myc there was a corresponding increase in TBX3 mRNA levels compared to FLAG-EMPTY cells (**Figure 3.1 C**). Importantly, when de novo transcription was inhibited in cells in which c-Myc is overexpressed, the c-Myc mediated activation of TBX3 mRNA was significantly abolished (twenty-fold reduction) (**Figure 3.1 C**). It is important to note that in the presence of Actinomycin D alone a two-fold reduction in TBX3 mRNA levels was observed, which suggests that the upregulation of basal levels of TBX3 mRNA is in part due to de novo transcription (**Figure 3.1 C**). The same trend for TBX3 mRNA levels was observed on a protein level (**Figure 3.1 D**). The western blot for endogenous c-Myc suggests that basal levels of c-Myc are also regulated by de novo transcription. In summary these results show that c-Myc transcriptionally upregulates TBX3 expression in MCF-7 breast cancer cells.

3.2. Identification and characterisation of TBX3 interaction partners in MCF-7 breast cancer cells

To identify TBX3 interaction partners in MCF-7 breast cancer cells, FLAG-tagged TBX3 was firstly stably overexpressed in MCF-7 breast cancer cells. The motivation for this was that transcription factors are expressed in relatively low abundance in the cell and the Prince laboratory has found that the commercially available TBX3 antibodies do not immunoprecipitate sufficient TBX3 protein for mass spectrometry analysis. Furthermore, since anti-FLAG antibodies have a strong affinity for FLAG-tagged fusion proteins, the FLAG co-immunoprecipitation system was chosen.

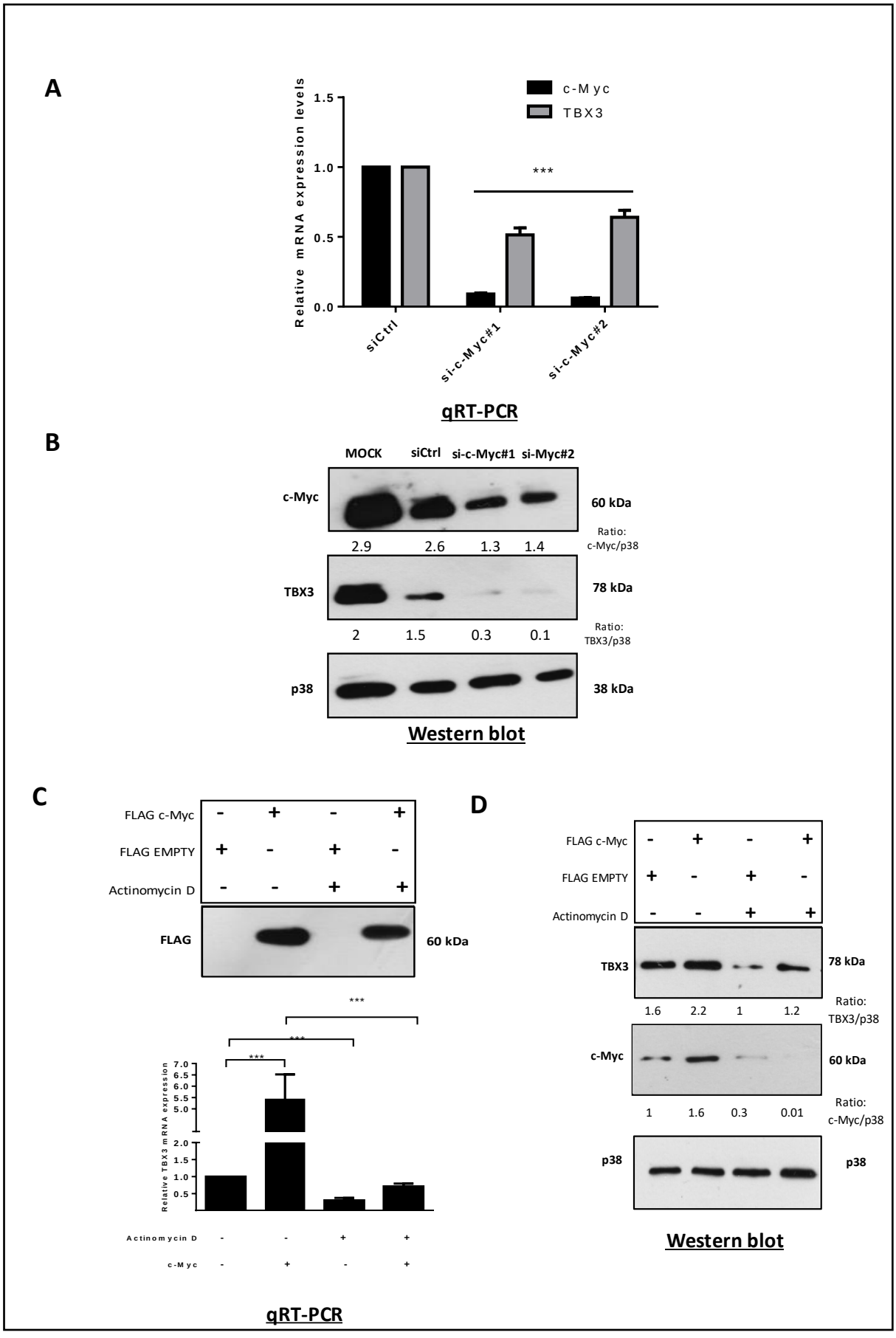
A
c-Myc
TBX3
Relative mRNA expression levels
1.5
1.0
0.5
0.0
***
siCtrl
si-c-Myc#1
si-c-Myc#2
qRT-PCR
B
MOCK
siCtrl
si-c-Myc#1
si-Myc#2
c-Myc
60 kDa
Ratio:
c-Myc/p38
2.9
2.6
1.3
1.4
TBX3
78 kDa
Ratio:
TBX3/p38
2
1.5
0.3
0.1
p38
38 kDa
Western blot
C
FLAG c-Myc
FLAG EMPTY
Actinomycin D
FLAG
60 kDa
***
***
***
Relative TBX3 mRNA expression
7.0
6.5
6.0
5.5
5.0
2.0
1.5
1.0
0.5
Actinomycin D
c-Myc
qRT-PCR
D
FLAG c-Myc
FLAG EMPTY
Actinomycin D
TBX3
78 kDa
Ratio:
TBX3/p38
1.6
2.2
1
1.2
c-Myc
60 kDa
Ratio:
c-Myc/p38
1
1.6
0.3
0.01
p38
p38
Western blot

Figure 3.1. c-Myc transcriptionally upregulates TBX3 in MCF-7 breast cancer cells. MCF-7 breast cancer cells were plated in triplicate in a 6-well plate at a density of 2.5 x 10^5 cells/well. The cells were transfected with either 10 nM si-c-Myc#1, si-c-Myc#2 or the equivalent concentration of control siRNA (siCtrl). **(A)** Quantitative real-time PCR (qRT-PCR) was performed on reverse transcribed RNA using primers to c-Myc and TBX3, mRNA levels were normalized to GUSB. Microsoft Excel student t-test was performed to calculate statistical significance, *p<0.05; **p<0.01; ***p<0.001; error bars represent standard error of the mean. **(B)** Protein was harvested from the cells, analysed by SDS-PAGE (8%) followed by western blotting with the following antibodies: rabbit polyclonal anti-TBX3 (1:1000), rabbit (1:1000) and a donkey anti-rabbit secondary antibody (1:5000). p38 was used as a loading control. Densitometric values represent the expression of each protein band quantified using Image J imaging software and normalized to p38 protein levels. **(C)** MCF-7 breast cancer cells were plated in a 6-well plate at a density of 2.5 x 10^5 cells/well and transfected forty-eight hours later with 500 ng pcDNA-FLAG-c-Myc or pcDNA-FLAG-EMPTY expression constructs. Forty-eight hours after transfection the cells were treated with 5 μg/ml Actinomycin D or the equivalent concentration of DMSO for 30 minutes. qRT-PCR was performed on reverse transcribed RNA using primers to TBX3 and mRNA levels were normalized to GUSB. Microsoft Excel student t-test was performed to calculate statistical significance, *p<0.05; **p<0.01; ***p<0.001; error bars represent standard error of the mean. **(D)** MCF-7 breast cancer cells were plated in a 24-well plate at a density of 0.85 x 10^5 cells/well and transfected forty-eight hours later with 500 ng pcDNA-FLAG-c-Myc or pcDNA-FLAG-EMPTY expression constructs. Forty-eight hours after transfection the cells were treated with 5 μg/ml Actinomycin D or the equivalent concentration of DMSO for 30 minutes. Protein was harvested from the cells, analysed by SDS-PAGE (8%) followed by western blotting to detect FLAG-tagged c-Myc, endogenous c-Myc and TBX3 using the following antibodies: mouse monoclonal FLAG M2 antibody (1:1000), rabbit anti-c-Myc (1:1000), rabbit polyclonal anti-TBX3 (1:500) and a donkey anti-rabbit secondary antibody (1:5000) or a goat anti-mouse secondary antibody (1:5000). p38 was used as a loading control. Densitometric values represent the expression of each protein band quantified using Image J imaging software and normalized to p38 protein levels.

3.2.1. Establishment of FLAG-TBX3 overexpressing MCF-7 breast cancer cell lines

The constructs used to establish the MCF-7 TBX3 overexpressing cell culture model included a pCMV expression vector containing FLAG tagged TBX3 (FLAG-TBX3) or the empty vector (FLAG-EMPTY). A key feature of these constructs is that they contain the mammalian neomycin gene that confers resistance to the antibiotic G-418, a neomycin

analogue, and this is critical for the selection of successfully transfected cells. To determine the lowest dose of G-418 required to kill untransfected MCF-7 cells, an antibiotic titration assay was first performed. The optimal dose of G-418 required is that which kills all untransfected cells by day 10 and based on the data obtained 400 μg/ml of G-418 was used for drug selection and clonal expansion of the positively transfected MCF-7 cells (data not shown). MCF-7 cells were subsequently transfected with FLAG-EMPTY or FLAG-TBX3 expression constructs and forty-eight hours later they were grown in the presence of G-418 (400 μg/ml) for a minimum of 10 days and twenty-four G-418 resistant clones were isolated and analysed for TBX3 overexpression using western blotting and immunocytochemistry with an antibody to FLAG. The western blotting results show that, as expected, no bands were detected in the protein from the FLAG-EMPTY cells (12 and 13), and bands of approximately 100 kDa were detected in the lanes containing protein extracts of eight of the FLAG-TBX3 clones 1, 6, 7, 8, 12, 18, 19, 22 (**Figure 3.2 A**). FLAG-TBX3 (1 and 22) and FLAG-EMPTY (12) were selected for further analysis and will hereafter be referred to as FLAG-TBX3 (1 and 2) and FLAG-EMPTY (12).

To confirm nuclear localization of TBX3 which is a critical feature for the functioning of transcription factors, immunocytochemistry was performed on the FLAG-TBX3 (1 and 2) cells and FLAG-EMPTY (12) clone. Briefly, the cells were seeded on coverslips and processed for immunocytochemistry using a primary mouse antibody to FLAG and a secondary anti-mouse antibody conjugated to a Cy3 fluorophore and viewed by confocal microscopy. The merged images show that the FLAG and DAPI signals overlap in the nuclei of FLAG-TBX3 positive clones which confirms that FLAG-TBX3 does indeed localize to the nucleus and, as expected, no FLAG expression was observed in the FLAG-EMPTY clone (**Figure 3.2 B**).

3.2.2. Confirming the impact of TBX3 overexpression on MCF-7 breast cancer cell proliferation and migration

TBX3 was previously reported to inhibit proliferation but promote migration of breast cancer cells (Peres *et al.*, 2010; Li *et al.*, 2013).

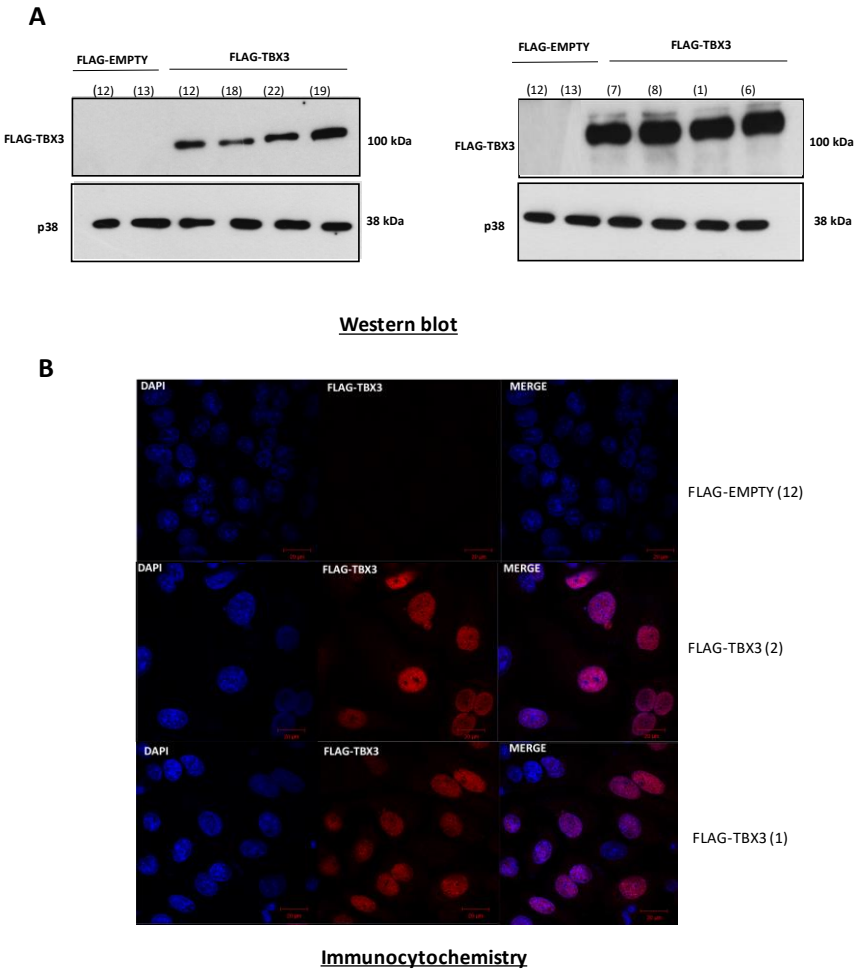

Figure 3.2. Establishment of MCF-7 breast cancer cell lines in which FLAG-TBX3 was stably overexpressed. MCF-7 breast cancer cells were stably transfected with the pCMV-3XFLAG-EMPTY (FLAG-EMPTY) or pCMV-3XFLAG-TBX3 (FLAG-TBX3) expression constructs. **(A)** Protein was harvested from the cells, analysed by SDS-PAGE (8%), followed by western blotting to detect FLAG-tagged TBX3 using a mouse monoclonal FLAG M2 antibody (1:1000) and a goat anti-mouse secondary antibody (1:5000). p38 was used as a loading control. **(B)** MCF-7 FLAG-EMPTY and FLAG-TBX3 cells were seeded on coverslips and processed for immunocytochemistry using mouse monoclonal FLAG M2 antibody (1:100) and a secondary anti-mouse antibody conjugated to a Cy3 fluorophore (1:1000). Cells were stained with Hoechst and viewed using the DAPI filter to determine the location of the nuclei using confocal microscopy. Representative images are shown (scale bars, 20 μm).

Therefore, before subjecting the newly established FLAG-TBX3 and FLAG-EMPTY cells to mass spectrometry, the next aim was to confirm that FLAG-TBX3 has the same effect as endogenous TBX3 on breast cancer cell proliferation and migration. It is important to

note that in all the experiments performed the parental MCF-7 cells were included in order to rule out the possibility that any effect seen could be due to the vector backbone.

3.2.2.1. FLAG-TBX3 overexpression alters the morphology of MCF-7 breast cancer cells

Microscopic images of parental MCF-7 cells, FLAG-EMPTY cells and FLAG-TBX3 cells were captured and a characteristic "cobble-stone" appearance was noted for both the parental MCF-7 cells and the FLAG-EMPTY cells. However, the FLAG-TBX3 (1) and FLAG-TBX3 (2) cells had poorly defined cell boundaries and adopted a more elongated appearance, reminiscent of cells undergoing epithelial-mesenchymal transition (EMT) (**Figure 3.3**).

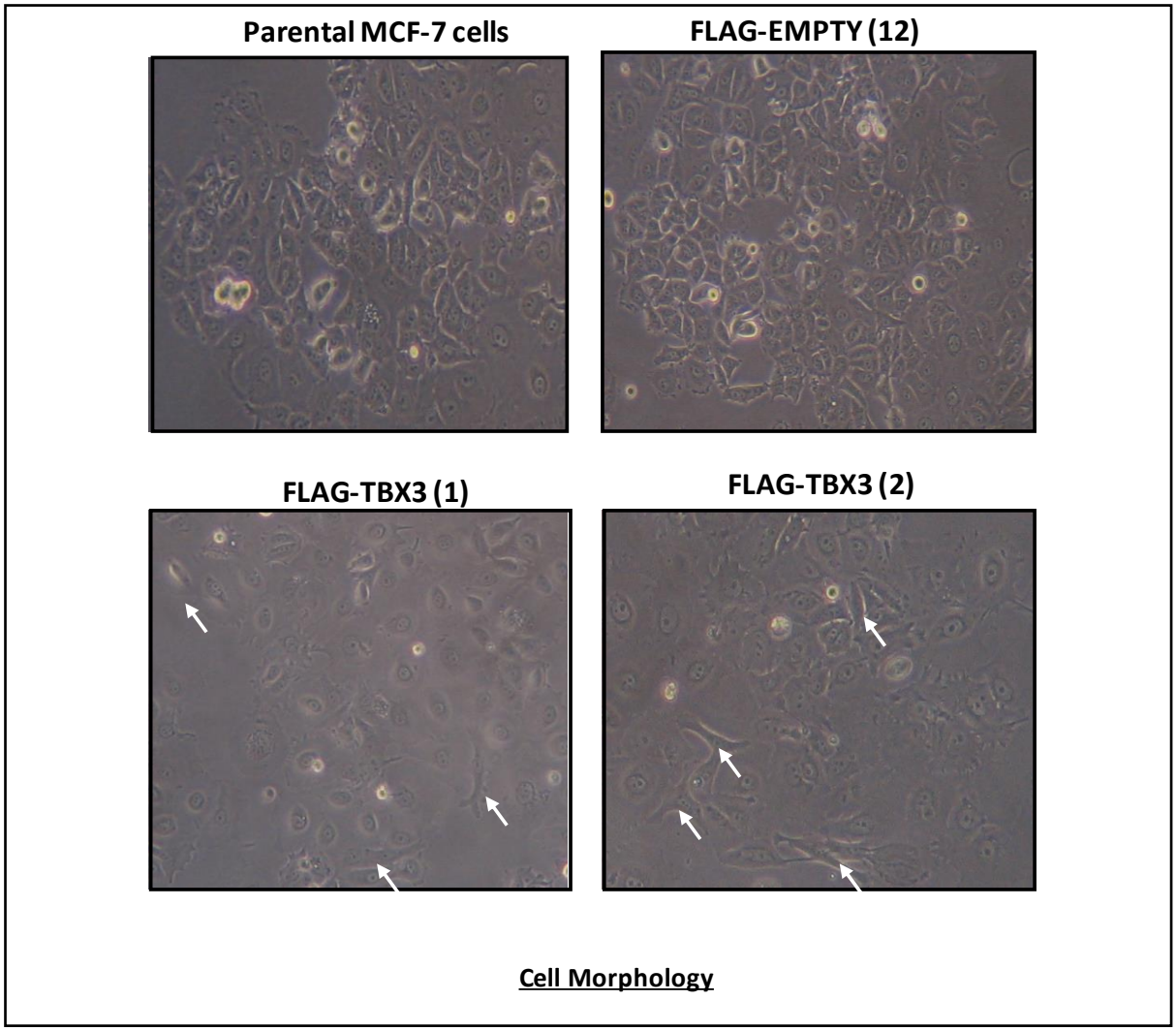

Figure 3.3. FLAG-TBX3 alters the morphology of MCF-7 breast cancer cells. Representative phase contrast light microscopic images of the indicated cell lines using a Canon camera (Powershot S50). Microscopic images of the cells at 400X magnification. The white arrows indicate elongated cells with poorly defined boundaries.

3.2.2.2. *FLAG-TBX3 overexpression inhibits proliferation of MCF-7 breast cancer cells*

To assess the impact of FLAG-TBX3 overexpression on cell proliferation, growth curves were performed by counting parental MCF-7, FLAG-EMPTY and FLAG-TBX3 cells grown under standard culture conditions over a period of 7 days. Results show that the parental MCF-7 and FLAG-EMPTY cells proliferated in a similar manner as there was no significant difference in proliferation between them (**Figure 3.4 A**). However, relative to the FLAG-EMPTY cells the FLAG-TBX3 cells proliferated significantly more slowly at day 7 (**Figure 3.4 A**). Previous studies in the Prince laboratory have shown that the mechanism by which TBX3 inhibits proliferation in breast cancer cells is through the repression of its homologue, TBX2, a powerful proliferative factor which normally represses key cell cycle regulators (Li et al., 2014). To confirm this mechanism in our cell culture model, western blotting was performed with antibodies to TBX2, p53 and p21. Results show that while TBX2 is downregulated, both p53 and p21 are upregulated in the FLAG-TBX3 overexpressing cells compared to the parental MCF-7 cells and the FLAG-EMPTY cells (**Figure 3.4 B**). These results confirm that FLAG-TBX3 has the same effect on breast cancer cell proliferation as endogenous TBX3.

3.2.2.3. FLAG-TBX3 overexpression promotes migration of MCF-7 breast cancer cells

To confirm previous results that TBX3 promotes migration of MCF-7 breast cancer cells a two-dimensional scratch motility assay was performed. Briefly, parental MCF-7, FLAG-EMPTY and FLAG-TBX3 cells were grown to confluence and then a linear scratch was made through the monolayer and mitomycin C was added to inhibit de novo cell proliferation.

A

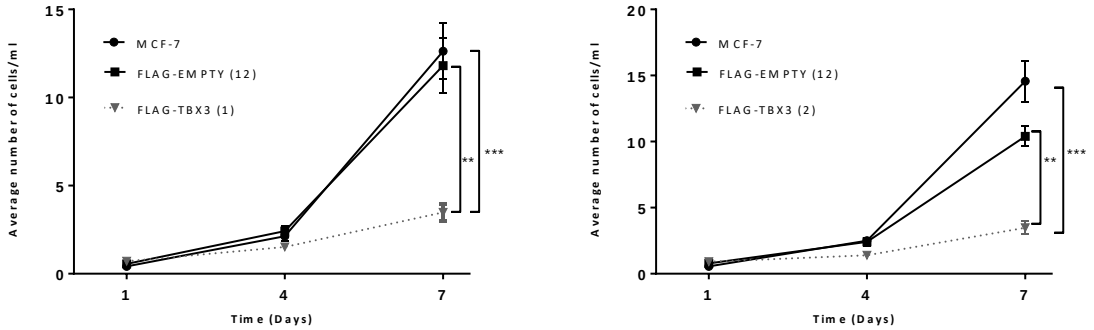

Growth curve assay

B

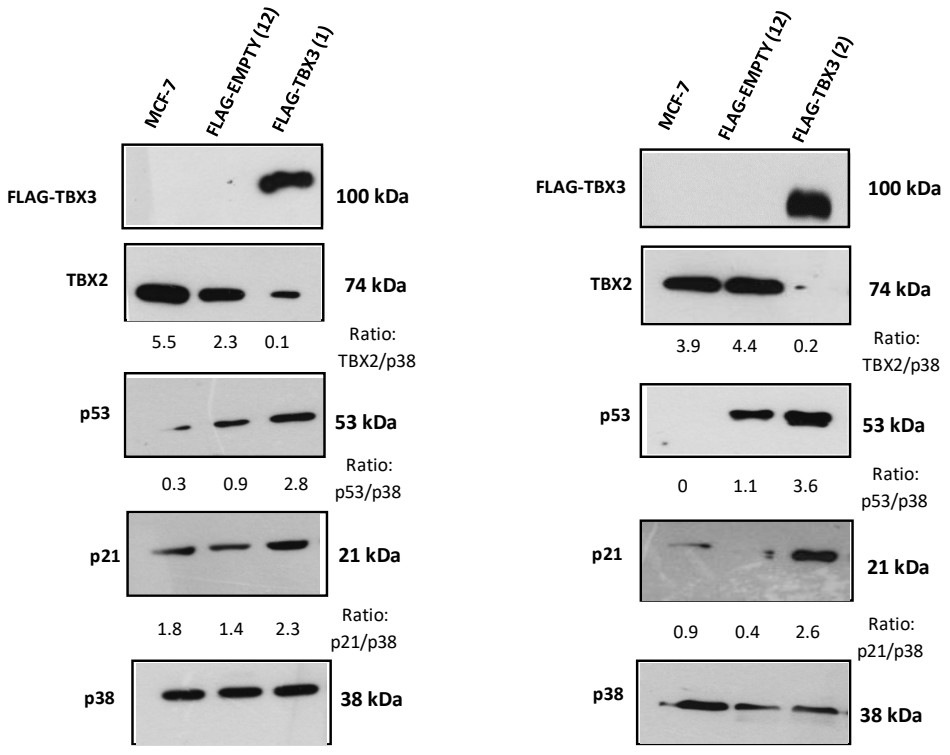

Western blot

Figure 3.4. TBX3 inhibits proliferation of MCF-7 breast cancer cells and represses its homologue, TBX2, resulting in the upregulation of key cell cycle regulators p53 and p21. MCF-7, MCF-7 FLAG-EMPTY and MCF-7 FLAG-TBX3 breast cancer cells were plated in triplicate in a 12-well plate at a density of 1 x 10^4 cells per well. **(A)** Cells were collected by removing and keeping the media the cells had been grown in, washing the cells twice with 1XPBS, keeping the 1XPBS, and then trypsinisation. Cells were counted using a haemocytometer at days 1, 4 and 10. *Left panel*: representative of MCF-7, MCF-7 FLAG-EMPTY and MCF-7 FLAG-TBX3 (1). *Right panel*: representative of MCF-7, MCF-7 FLAG-EMPTY and MCF-7 FLAG-TBX3 (2) cells. **(B)** Protein was harvested from the cells, analysed by SDS-PAGE (8%), followed by western blotting with antibodies to TBX2, p53 and p21 and p38 was used as a loading control. Densitometric values represent the expression of each protein band quantified using Image J imaging software and normalized to p38 protein levels. *Left panel*: representative of MCF-7, MCF-7 FLAG-EMPTY and MCF-7 FLAG-TBX3 (1). *Right panel*: representative of MCF-7, MCF-7 FLAG-EMPTY and MCF-7 FLAG-TBX3 (2) cells.

Light microscopy images of the scratch were captured at 3-hour intervals until the 24-hour timepoint. The area of the scratch was measured at each time point and the change in area over time was determined by calculating the decrease in scratch area at each timepoint. Results show that there was no significant difference in migration between the parental MCF-7 and FLAG-EMPTY cells (**Figure 3.5 A**). Compared to the FLAG-EMPTY cells, the FLAG-TBX3 cells migrated significantly faster at all timepoints (**Figure 3.5 A**).

To determine the molecular mechanism(s) by which TBX3 promotes migration, the expression levels of key EMT markers were investigated through western blotting with antibodies to E-cadherin (epithelial marker) and the mesenchymal markers N-cadherin, vimentin and β-catenin. The results revealed that compared to the parental MCF-7 and FLAG-EMPTY cells there was a decrease in E-cadherin levels but an increase in the levels of N-cadherin, vimentin and ß-catenin in the FLAG-TBX3 cells (**Figure 3.5 B**). These data confirm that, like endogenous TBX3, FLAG-TBX3 promotes migration and EMT of MCF-7 breast cancer cells.

A

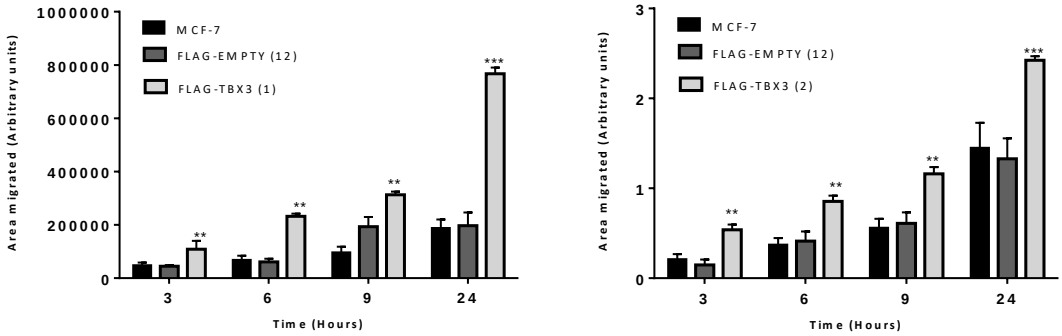

Scratch motility assay

B

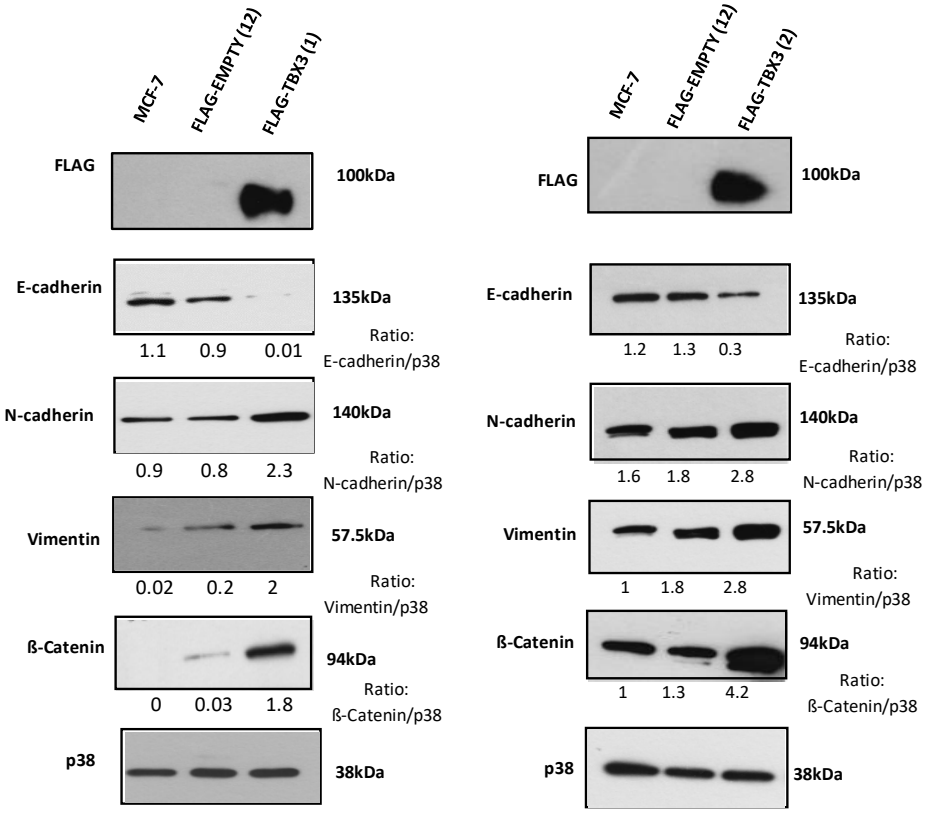

Western blot

Figure 3.5. TBX3 overexpression in MCF-7 breast cancer cells promotes migration and upregulates EMT marker expression. MCF-7 FLAG-EMPTY and FLAG-TBX3 breast cancer cells were plated in triplicate in a 24-well plate at a density of 1 x 10^4 cells per well and grown to 100% confluence. **(A)** Scratch motility assay. A linear wound was made by making a scratch through the cell monolayer. To inhibit proliferation, mitomycin C was added at a final concentration of 10 µg/ml and migration measured at 3-hour intervals. Results are plotted as the average area migrated over time. Each result is the mean of three independent experiments performed in triplicate. *Left panel*: representative of MCF-7**,** MCF-7 FLAG-EMPTY and MCF-7 FLAG-TBX3 (1). *Right panel*: representative of MCF-7**,** MCF-7 FLAG-EMPTY and MCF-7 FLAG-TBX3 (2) cells. **(B)** Western blotting. Protein was harvested from cells in (A), analysed by SDS-PAGE (8%) followed by western blotting with anti-FLAG (1:1000), anti-E-cadherin (1:1000), anti-N-cadherin (1:1000), anti-Vimentin (1:1000), and anti-ß-catenin (1:500) primary antibodies and either a goat anti-mouse secondary antibody (1:5000) or a donkey anti-rabbit secondary antibody (1:5000). p38 was used as a loading control. Densitometric values represent the expression of each protein band quantified using Image J imaging software and normalized to p38 protein levels. *Left panel*: representative of MCF-7**,** MCF-7 FLAG-EMPTY and MCF-7 FLAG-TBX3 (1). *Right panel*: representative of MCF-7**,** MCF-7 FLAG-EMPTY and MCF-7 FLAG-TBX3 (2) cells**.**

3.2.3. Affinity purification and identification of FLAG-TBX3 interaction complexes

To identify protein co-factors that stabilize the TBX3 protein and that mediate its oncogenic activity in MCF-7 breast cancer cells, affinity purification coupled with mass spectrometry analyses (AP-MS) was performed. To this end, immunoprecipitation assays were firstly carried out using anti-FLAG antibody conjugated to agarose beads. The immune complexes were then analysed by western blotting using an antibody to FLAG. As controls, cell extracts from the FLAG-EMPTY and FLAG-TBX3 (1 and 2) cells (referred to as "Input") were included. The results show that while no FLAG-TBX3 was detected in the Input of FLAG-EMPTY cells, it was detected in the Input of FLAG-TBX3 cells (**Figure 3.6 A and 3.6 B**). Importantly, results confirmed that in the immunoprecipitated lysate (referred to as "IP"), TBX3 was only immunoprecipitated from FLAG-TBX3 cells and not the FLAG-EMPTY cells (**Figure 3.6 A and 3.6 B**). It is important to note that two volumes of protein eluted from the agarose beads (2 µl and 7 µl) were used in order to demonstrate that the amount of FLAG-TBX3 detected is dependent on the amount of eluted protein lysate present.

Next, TBX3 was immunoprecipitated from FLAG-TBX3 (2) and FLAG-EMPTY cells, eluted by denaturation, digested with trypsin and subjected to LC-MS/MS using a Q Exactive hybrid quadrupole-Orbitrap. FLAG-TBX3 (2) was selected for no specific reason and the experiment was performed in biological quadruplicates. MS datasets were initially analysed using Microsoft Excel software. To exclude background binding contaminants from the analysis, any proteins that were identified in the FLAG-EMPTY control samples were excluded from further analysis. Collectively, a total of 197 unique proteins were identified in all four FLAG-TBX3 samples (hereafter referred to as PD1, PD2, PD3 and PD4) (**Figure 3.6 C**). Results show that PD1, PD2, PD3 and PD4 had 126, 64, 90 and 6 proteins respectively (**Figure 3.6 C**). Since PD4 had very few proteins it was subsequently excluded from the analysis as this indicated that it was an erroneous run. Thereafter, the proteins present in PD1, PD2 and PD3 were subjected to Venny 2.1.0 software analysis and results show that PD1, PD2 and PD3 had 47 interaction partners in common (**Figure 3.6 D**). **Table 3.1** shows the 47 possible interaction partners identified.

3.2.4. In silico characterisation of FLAG-TBX3 interacting complexes

To determine whether the interacting partners identified in **Figure 3.6 D** are involved in common networks, a protein interaction network map was generated using the STRING database (Search Tool for The Retrieval of Interacting Genes/proteins). The map revealed high confidence interactions (indicated by the bold connecting lines) between TBX3 interacting proteins within RNA splicing and mRNA metabolism networks suggesting that TBX3 may be a component of multi-protein complexes (**Figure 3.7 A**). This observation is consistent with a recent study that showed that TBX3 interacts with multiple splicing factors and regulates alternative splicing in vivo (Kumar et al., 2014). The interacting partners were subsequently subjected to Gene Ontology (GO) analysis and categorised by their biological function to determine whether they have common and/or overlapping biological functions (**Figure 3.7 B**).

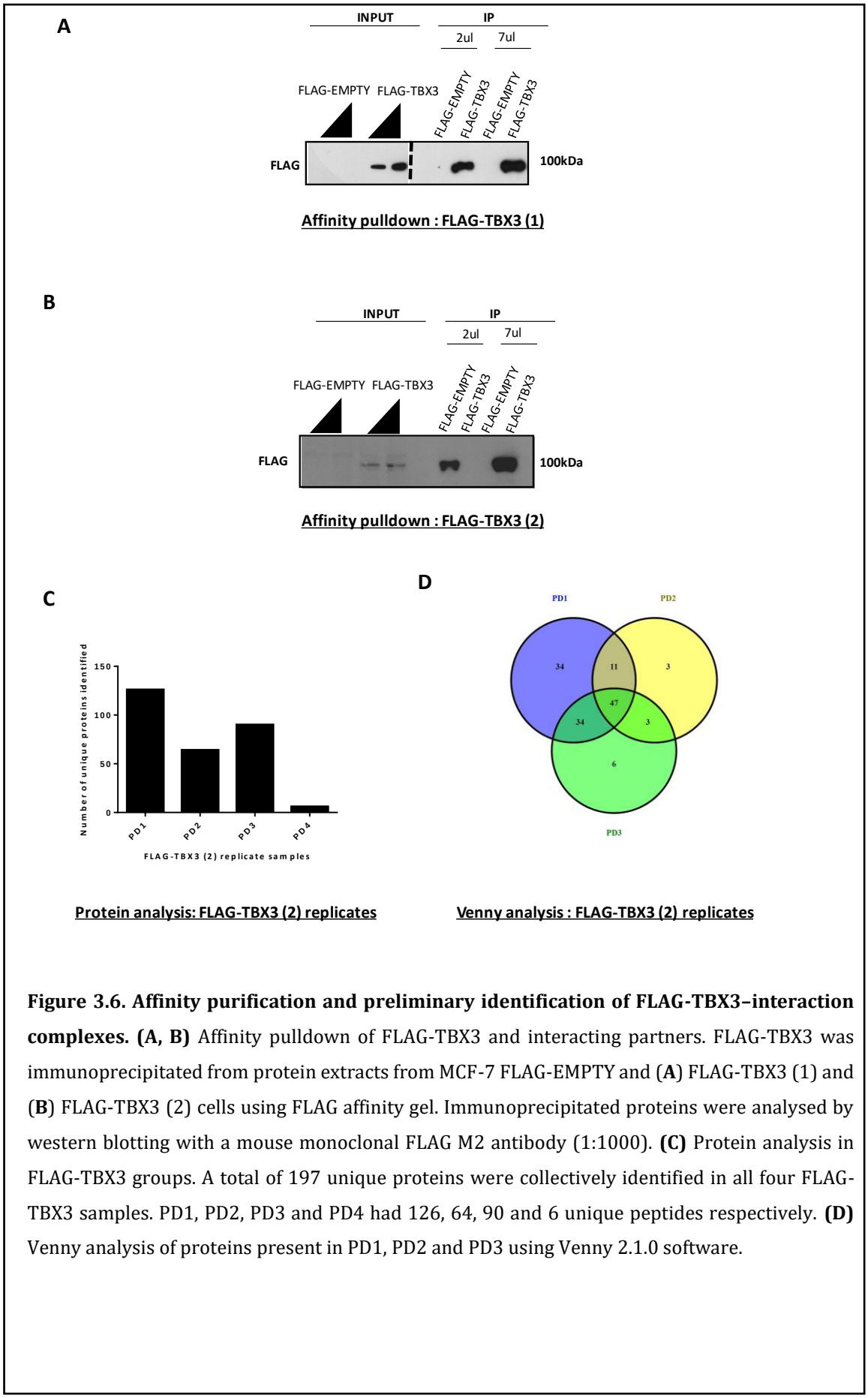

Figure 3.6. Affinity purification and preliminary identification of FLAG-TBX3–interaction complexes. (A, B) Affinity pulldown of FLAG-TBX3 and interacting partners. FLAG-TBX3 was immunoprecipitated from protein extracts from MCF-7 FLAG-EMPTY and (**A**) FLAG-TBX3 (1) and (**B**) FLAG-TBX3 (2) cells using FLAG affinity gel. Immunoprecipitated proteins were analysed by western blotting with a mouse monoclonal FLAG M2 antibody (1:1000). **(C)** Protein analysis in FLAG-TBX3 groups. A total of 197 unique proteins were collectively identified in all four FLAG-TBX3 samples. PD1, PD2, PD3 and PD4 had 126, 64, 90 and 6 unique peptides respectively. **(D)** Venny analysis of proteins present in PD1, PD2 and PD3 using Venny 2.1.0 software.

Table 3.1. Forty-seven possible TBX3 protein partners identified by mass spectrometry

Gene name	Protein name	Uniprot accession number
ATP5F1C	ATP synthase subunit gamma, mitochondrial (ATP synthase F1 subunit gamma)	P36542
CAPN1	Calpain-1 catalytic subunit	P07384
CLNS1A	Methylosome subunit pICln	E9PMI6
CSNK1A1	Casein kinase I isoform alpha	P48729
EMD	Emerin	P50402
EPPK1	Epiplakin (450 kDa epidermal antigen)	P58107
FARSA	Phenylalanine--tRNA ligase alpha subunit	K7ER16
FUS	RNA-binding protein FUS	P35637
HNRNPA1	Heterogeneous nuclear ribonucleoprotein A1	F8W6I7
HNRNPA3	Heterogeneous nuclear ribonucleoprotein A3	P51991
HNRNPAB	Heterogeneous nuclear ribonucleoprotein A/B	D6R9P3
HNRNPC	Heterogeneous nuclear ribonucleoproteins C1/C2 (Fragment)	G3V4W0
HNRNPH1	Heterogeneous nuclear ribonucleoprotein H	P31943
HNRNPK	Heterogeneous nuclear ribonucleoprotein K	P61978
HNRNPU	Heterogeneous nuclear ribonucleoprotein U	A0A1W2PPS1
HNRNPUL1	Heterogeneous nuclear ribonucleoprotein U-like protein 1	A0A0A0MRA5
HSP90AB1	Heat shock protein HSP 90-beta	P08238
HSPA8	Heat shock cognate 71k Da protein	P11142
IMMT	MICOS complex subunit MIC60 (Mitofilin)	H7C463
KHDRBS1	KH domain-containing, RNA-binding, signal transduction-associated protein 1	Q07666
KIF11	Kinesin-like protein	P52732
LMNB1	Lamin B1, isoform CRA_a	A0A0D9SFE5
NCL	Nucleolin	P19338
NPM1	Nucleophosmin	P06748
PCK2	Phosphoenolpyruvate carboxykinase [GTP]	Q16822
PRKDC	DNA-dependent protein kinase catalytic subunit	P78527
RBM10	RNA-binding protein 10	P98175
RCN2	Reticulocalbin-2	Q14257
RPL13	60S ribosomal protein L13	P26373
RPL13A	60S ribosomal protein L13a	P40429
RPL23A	60S ribosomal protein L23a (Large ribosomal subunit protein uL23)	P62750
RPL6	60S ribosomal protein L6	Q02878
RPL7	60S ribosomal protein L7	P18124
RPL7A	60S ribosomal protein L7a	Q5T8U3
RPLP2	60S acidic ribosomal protein P2	P05387
RPS18	40S ribosomal protein S18	P62269
RPS24	40S ribosomal protein S24	E7ETK0
RPS4X	40S ribosomal protein S4, X	P62701
RPS8	40S ribosomal protein S8	Q5JR95
RPS9	40S ribosomal protein S9	A0A024R4M0
SLC25A5	ADP/ATP translocase 2	P05141
SLC25A6	ADP/ATP translocase 3	P12236
SNRPD3	Small nuclear ribonucleoprotein Sm D3	P62318
SRSF1	Serine/arginine-rich splicing factor 1	Q07955
TMPO	Thymopoietin isoform alpha	P42166
TPM1	Tropomyosin 1 (Alpha)	H0YL52
TPM4	Tropomyosin alpha-4 chain	P67936

The results reveal a significant enrichment of proteins involved in mRNA metabolic processes, viral processes, intracellular transport, RNA processing, cytoplasmic transport, cellular component disassembly, mRNA processing, RNA splicing and establishment of protein localization to organelles (**Figure 3.7 C**). It is not surprising that many of the identified proteins are involved in gene expression regulatory mechanisms such as RNA splicing, RNA processing, translation initiation and elongation, considering that TBX3 has been well characterized as a transcription factor.

Heat shock cognate protein (Hsc70), Heterogeneous nuclear ribonucleoprotein K (HnRNP K) and nucleolin were selected for further analysis because they have overlapping roles with TBX3 in cancer and previous studies in the Prince laboratory have identified and characterized them as co-factors of TBX3 in chondrosarcoma and rhabdomyosarcoma cells (unpublished data).

3.2.5. Hsc70, HnRNP K and nucleolin interact with TBX3 in MCF-7 breast cancer cells

Hsc70, HnRNP K and nucleolin were identified as "high confidence" putative co-factors of TBX3 as they all had (1) high peptide numbers in the FLAG-TBX3 samples compared to the FLAG-EMPTY control samples (**Figure 3.8 A, B, C**) and (2) very low Q-values (not shown). This indicated that there was a good match between the measured MS/MS spectra in the experiments and the predicted spectra for the respective identified peptides (**Figure 3.9 A, B, C**). It is important to note that TBX3 was not identified in the FLAG-TBX3 samples. A possible explanation for this is that since a high-affinity monoclonal antibody against a linear tag (FLAG-tag) was used to elute the interaction partners, the denaturation buffer used after immunoprecipitation might not have weakened the bond between the antibody and the FLAG-tag enough. If this were the case, TBX3 would not be released but the bound interaction partners, such as Hsc70, nucleolin and HnRNP K, may be eluted. Since our laboratory had previously validated Hsc70, nucleolin and HnRNP K as TBX3 co-factors in chondrosarcoma and rhabdomyosarcoma, the data from the current study were regarded as reliable and these three proteins were further validated and characterised.

3.2.5.1. Identification and characterization of Hsc70 as a TBX3 co-factor

Hsc70 has been reported to contribute to numerous oncogenic processes including cell proliferation, survival, drug resistance and metastasis, in part, through its ability to facilitate the accumulation and aggregation of mutated and incorrectly folded oncoproteins (Luo *et al*., 2009; Liu *et al*., 2012).

A

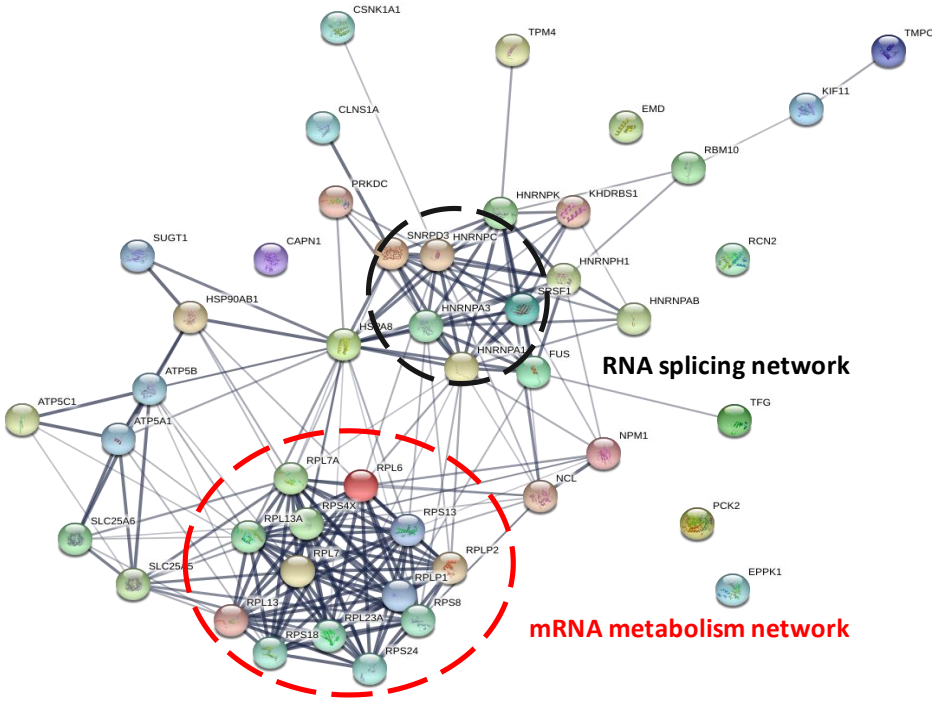

STRING interaction map

B

Table 3.2. Gene ontology functional classification of the TBX3 interactome by biological processes

Biological process	Count in gene set	False discovery rate
mRNA metabolic process	16	9.01E-13
Viral process	13	1.03E-07
Viral life cycle	9	3.14E-07
SRP-dependent cotranslational protein targeting to membrane	7	7.83E-07
Viral transcription	7	8.01E-07
Nuclear-transcribed mRNA catabolic process, nonsense-mediated decay	7	8.55E-07
Viral gene expression	7	1.00E-06
Cellular protein complex disassembly	8	1.00E-06
Cellular component disassembly	10	2.87E-06
mRNA processing	9	5.86E-06
Translational termination	7	6.72E-06
Translational elongation	7	1.11E-05
mRNA splicing, via spliceosome	7	2.13E-05
RNA splicing	8	2.13E-05
Establishment of protein localization to organelle	8	2.78E-05
Translational initiation	7	2.83E-05
RNA processing	10	3.23E-05
Cytoplasmic transport	10	3.23E-05
Protein targeting	7	8.07E-05
Intracellular transport	12	9.36E-05
Single-organism intracellular transport	11	0.000208
Intracellular protein transport	9	0.000384
Protein localization to organelle	8	0.00042

Figure 3.7: STRING and Gene Ontology (GO) analyses of TBX3 interacting partners. **(A)** A network integrating physical interactions of identified TBX3 protein partners was generated using STRING. Nodes represent proteins, whereas edges represent interactions. "Bold" edges represent high confidence interactions while "Non-bold" edges represent medium confidence interactions. Clusters of interacting partners involved in RNA splicing and mRNA processing are circled in black and red respectively **(B)** Functional classification of the TBX3 interactome. TBX3 interactors were categorised according to their biological function using GO analysis. The count in gene set represents the number of proteins in the interactome that are enriched for the function, while the false discovery rate is the type I statistical error rate.

Importantly, recent studies in the Prince laboratory have demonstrated that TBX3 interacts with Hsc70 and that Hsc70 is required for TBX3 stability in chondrosarcoma and rhabdomyosarcoma cells. This together with the mass spectrometry data from the current study begged the questions as to whether TBX3 and Hsc70 also interact with one another in breast cancer cells and whether this interaction is important to stabilize TBX3.

Hsc70 binds and co-localises with TBX3 in vitro

To validate the interaction between Hsc70 and TBX3, co-immunoprecipitation assays were performed using FLAG-EMPTY and FLAG-TBX3 overexpressing cells (1 and 2) and anti-FLAG agarose beads and complexes were analysed by western blotting with antibodies against FLAG and Hsc70. Results show that the FLAG agarose beads did indeed immunoprecipitate the FLAG-TBX3 protein and that Hsc70 is in complex with TBX3 in both FLAG-TBX3 clones (**Figure 3.10 A and 3.11 A**). Immunocytochemistry and confocal microscopy analyses were performed to determine if TBX3 and Hsc70 co-localise. Briefly, FLAG-TBX3 overexpressing cells (1 and 2) were processed for immunocytochemistry with primary antibodies to Hsc70 and FLAG while the FLAG-EMPTY and parental MCF-7 cells were processed for immunocytochemistry with primary antibodies to Hsc70 and endogenous TBX3. Fluorophore-conjugated ALEXA 488 and Cy3 secondary antibodies were used for Hsc70 and FLAG or TBX3 respectively. Hoechst staining was performed to visualize nuclei (blue channel) and, as negative controls, the primary antibodies were excluded, and cells were incubated with only the secondary antibodies used to detect FLAG, TBX3 and Hsc70 (data not shown).

A

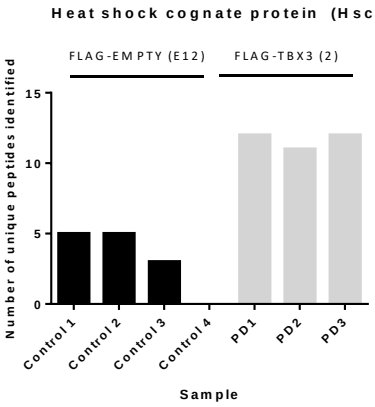

B

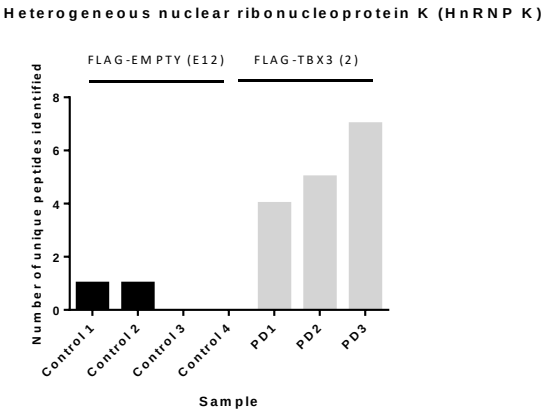

C

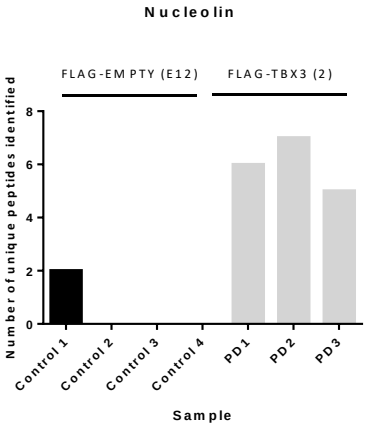

Figure 3.8. Hsc70, HnRNP K and nucleolin are putative co-factors of TBX3 in MCF-7 breast cancer cells: Co-factors were sorted based on peptide number in FLAG-TBX3 samples ad Q-values. Q-value is the posterior error probability and is indicative of the significance of the peptides identified. **(A)** Hsc70, **(B)** HnRNP K and **(C)** Nucleolin were identified as "high confidence" putative co-factors of TBX3 as they had high peptide numbers in the FLAG-TBX3 samples compared to the FLAG-EMPTY control samples.

A

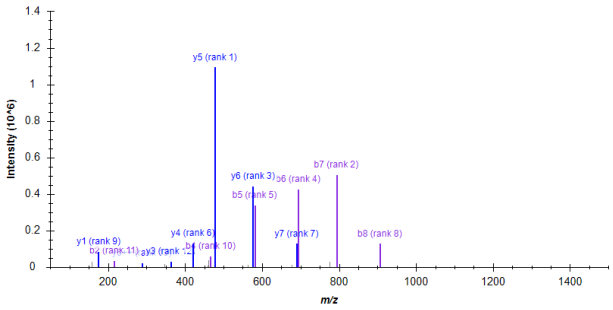

Mass spectrum: Hsc70

B

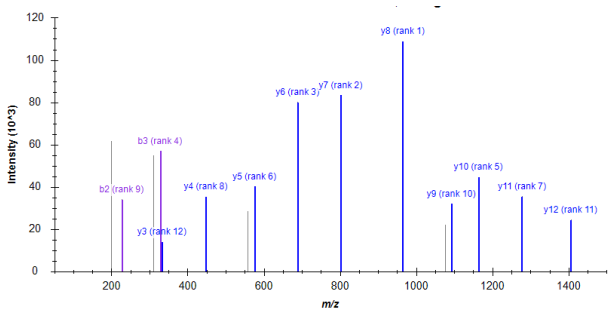

Mass spectrum: HnRNP K

C

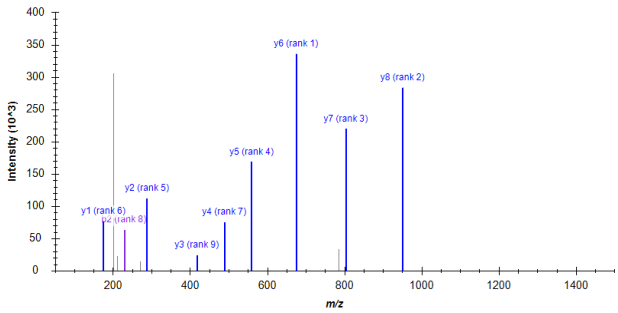

Mass spectrum: nucelolin

Figure 3.9. Hsc70, HnRNP K and nucleolin mass spectra. Representative fragmentation spectra identified by mass spectrometry of **(A)** one of the Hsc70 peptides with the sequence SQIHDIVLLGGSTR; (**B**) one of the HnRNP K peptides with the sequence IITITGTQDQIQNAQYLLQNSVK; and (**C**) one of the nucleolin peptides with the sequence EVFEDAAEIR.

The cells were visualized by confocal microscopy and the results show that in the FLAG-TBX3 overexpressing cells (1 and 2), there is partial interaction between TBX3 and Hsc70 in the cytoplasm and in the nucleus as seen by the overlapping DAPI, Cy3 and ALEXA 488 signals (**Figure 3.10 B, Figure 3.11 B**). Similar results were observed in FLAG-EMPTY cells as well as parental MCF-7 cells (**Figure 3.12 A top panel, 3.12 B top panel**) suggesting that endogenous TBX3 interacts with endogenous Hsc70 in MCF-7 cells.

It is important to note that since the staining indicated that TBX3 and Hsc70 occur in the nucleus and the cytoplasm, co-localisation was further measured in both compartments to determine whether there are any differences in co-localisation between them. The co-localisation between TBX3 and Hsc70 in the FLAG-TBX3 overexpressing cells (1 and 2) was quantified using Zen (Carl Zeiss) imaging software. **Figure 3.10 C and 3.11 C** (Top left panel) shows a different visualization of the co-localisation observed in the "merge" image of **Figure 3.10 B and 3.11 B** whereby the overlap of Hsc70 (green channel) and TBX3 (red channel) is indicated by yellow or white pixels. **Figure 3.10 C and 3.11 C** (Top right panel) shows a representative two-dimensional scatter plot of the intensities of Hsc70 (quadrant 1, bottom right), TBX3 (quadrant 2, top left) and the overlap between the TBX3 and Hsc70 (quadrant 3, top right). Pearson's correlation coefficient (PCC), Manders correlation coefficient (MCC) and weighted correlation coefficient (WCC) were used to measure the proportion of TBX3 co-localising with Hsc70 and vice versa. The PCC value defines the overall correlation between two channels as a value between -1 and 1, where a value of 1 represents perfect co-localisation and a value of -1 represents perfect exclusion. MCC values range between 0 and 1, where a value of 1 represents high co-localisation and 0 represents low co-localisation. WCC values range from 0 to 1 where a value of 0 indicates random staining and a value of 1 indicates dependent staining. The results of PCC, MCC and WCC were calculated from 20 random fields of view. As determined by the PCC, MCC and WCC values (**Figure 3.10 C, Figure 13.11 C**) there is partial co-localisation between TBX3 and Hsc70 proteins in the nucleus and the cytoplasm. Moreover, MCC and PCC values show that in the nucleus, there is a larger proportion of TBX3 that co-localises with a smaller proportion of Hsc70 as expected as there is more TBX3 in the nucleus than in the cytoplasm (**Figure 3.10** and **Figure 3.11**). In the cytoplasm, a larger proportion of TBX3 co-localises with a smaller proportion of Hsc70 as well even though there appears to be more Hsc70 and less TBX3 present in the

cytoplasm (**Figure 3.10 C and Figure 3.11 C**). A possible explanation for this could be that, in the cytoplasm, all the TBX3 interacts with Hsc70 but not all the Hsc70 interacts with TBX3 as it may also be interacting with other protein cargo. Similar results were observed in the FLAG-EMPTY cells as well as parental MCF-7 cells (**Figure 3.12 A bottom panel, 3.12 B bottom panel**)

It is also worth noting that the immunofluorescence was performed using a primary antibody that recognises all heat shock protein 70 members and therefore the low co-localisation values obtained may be due to TBX3 interacting with only Hsc70 and not the other members. Overall there appears to be no difference in the co-localisation pattern between the whole cell or the nuclear and cytoplasmic compartments. Taken together, this data shows that TBX3 interacts with Hsc70 in MCF-7 breast cancer cells.

Hsc70 is required for TBX3 stability

Having established that Hsc70 co-localises with TBX3 in MCF-7 cells, the next step was to investigate the functional significance of this interaction. To explore this, the effect of knocking down Hsc70 on TBX3 protein levels was firstly assessed. Briefly, MCF-7 cells were either Mock transfected (using DMSO) or transfected with a control si-RNA (si-Ctrl) or a si-RNA to Hsc70 (si-Hsc70) and the effect on Hsc70 and TBX3 protein levels was examined through western blotting. **Figure 13.13 A** shows that compared to Mock transfected cells and cells transfected with si-Ctrl, Hsc70 levels were knocked down in the cells transfected with si-Hsc70. Importantly, depleting Hsc70 results in a substantial reduction of TBX3 levels. To determine whether Hsc70 stabilizes TBX3 by preventing its degradation via the proteasome, MCF-7 cells were either Mock transfected, transfected with si-Ctrl or si-Hsc70 in the absence or presence of MG132, an inhibitor of the 26S proteasome. The results show that treatment of cells with MG132 rescued the levels of TBX3 protein in si-Hsc70 transfected cells (**Figure 3.13 B**). Together these results show that Hsc70 is required for TBX3 stability and provide an additional mechanism that may be responsible for TBX3 upregulation in MCF-7 breast cancer cells.

A

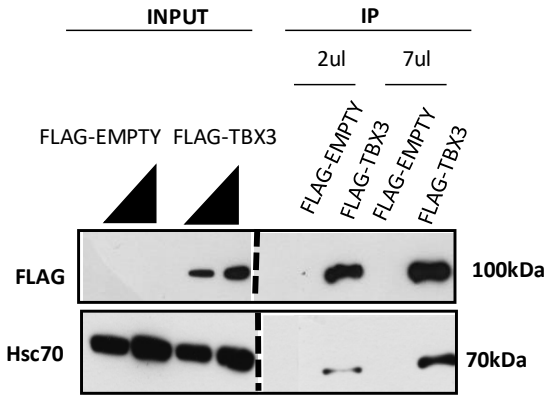

Immunoprecipitation: Hsc70

B

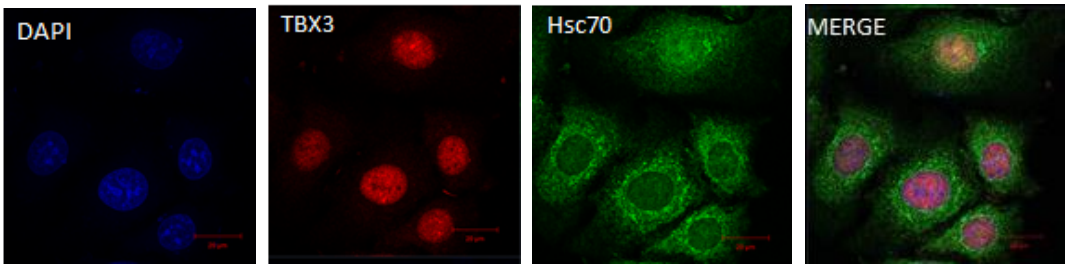

Immunocytochemistry : FLAG-TBX3 (1)

C

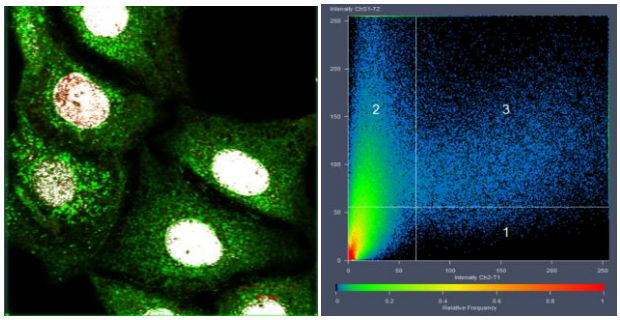

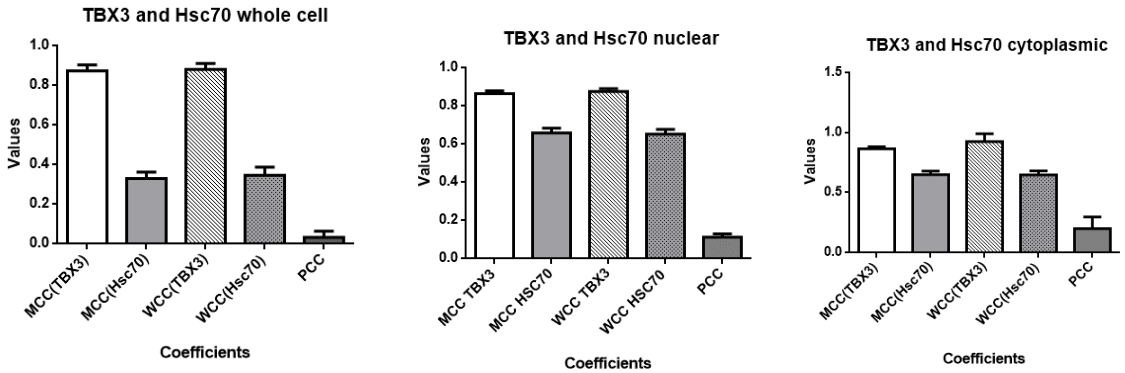

Co-localisation analysis : FLAG-TBX3 (1)

Figure 3.10. (A) Hsc70 directly interacts with TBX3. Protein extracts from FLAG-EMPTY and FLAG-TBX3 MCF-7 cells were immunoprecipitated using an anti-FLAG antibody. Purified complexes were subjected to western blot analysis using antibodies to mouse monoclonal FLAG M2 antibody (1:1000) or mouse polyclonal Hsc70 (1:1000). **(B)** Hsc70 co-localises with TBX3. FLAG-TBX3 overexpressing MCF-7 cells were seeded at a density of 0.85 X 10^5 on coverslips in 35 mm dishes and 48 hours later were processed for immunofluorescence with antibodies specific to TBX3 (Cy3; red channel) and Hsc70 (Alexa 488; green channel) and visualized by confocal microscopy. Representative images are shown at 400X magnification. All cells were co-stained with Hoechst to determine the location of the nuclei. **(C)** *Top panel (left):* Merged image from co-localisation analysis with white pixels indicating TBX3 and Hsc70 co-localisation in FLAG-TBX3 overexpressing MCF-7 cells. *Top panel (right):* Representative scatter plot of TBX3 and Hsc70 co-localisation in FLAG-TBX3 overexpressing MCF7 cells. Images were analysed by Zeiss software where the signal intensity of each channel is shown on a 2D graph. *Bottom panel:* Co-localisation of TBX3 and Hsc70 was quantified by Manders, Weighted and Pearson's correlation coefficients using Zeiss software. Data is represented as ± SEM of 20 fields of view.

3.2.5.2. Identification of HnRNP K as a TBX3 co-factor

HnRNP K activates transcription of numerous oncogenes including c-Myc, EGR-1, VEGF and c-Src and can post-transcriptionally silence tumour suppressor genes (Lynch et al., 2005; Michelotti et al., 1996; Takimoto et al., 1993; Yano et al., 2005). Importantly, our laboratory has shown that TBX3 interacts with HnRNP K in chondrosarcoma cells (unpublished data) and a study by Kumar et al. (2014) identified HnRNP K as a TBX3 interaction partner in HEK293 cells and mouse embryos. It was of interest to this study to determine whether TBX3 also interacts and co-localises with HnRNP K in breast cancer cells and therefore preliminary experiments were carried out as described below.

HnRNP K binds and co-localises with TBX3 in vitro

To validate the interaction between HnRNP K and TBX3, co-immunoprecipitation assays and western blotting were performed as previously described in **section 3.2.5.1**.

A

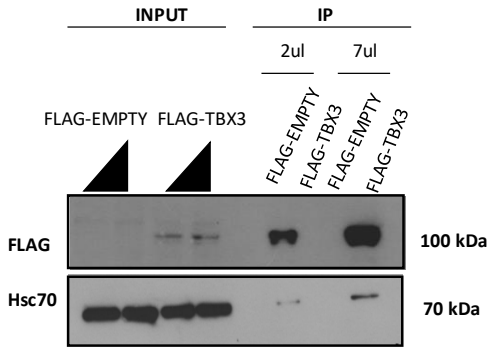

Immunoprecipitation: Hsc70

B

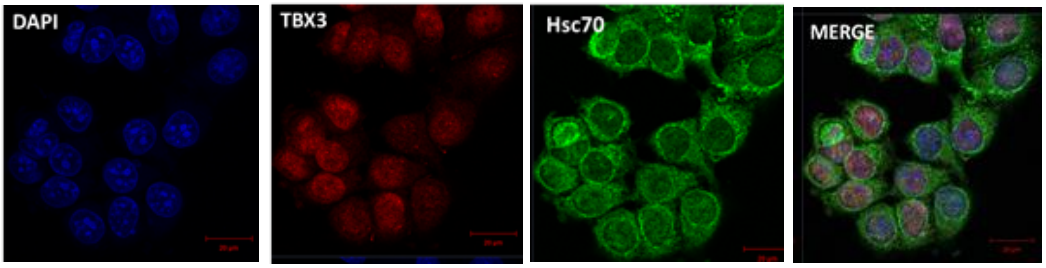

Immunocytochemistry : FLAG-TBX3 (2)

C

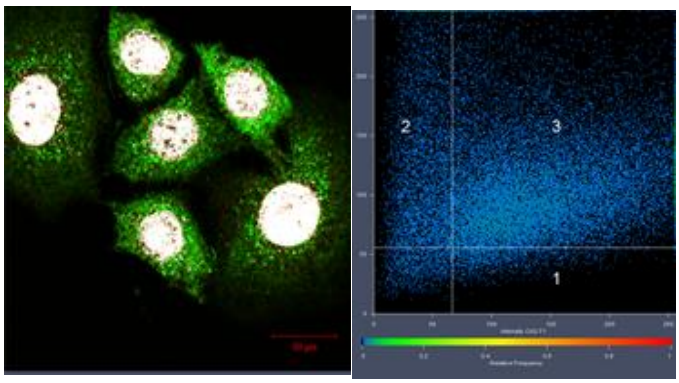

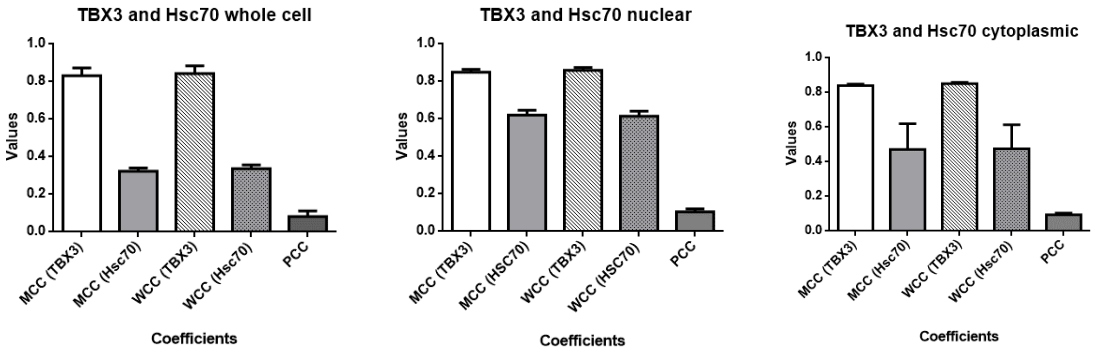

Co-localisation analysis : FLAG-TBX3 (2)

Figure 3.11. Hsc70 binds and colocalises with TBX3 in FLAG-TBX3 (2) overexpressing MCF-7 cells in vivo. **(A)** Hsc70 directly interacts with TBX3. Protein extracts from FLAG-EMPTY and FLAG-TBX3 MCF-7 cells were immunoprecipitated using an anti-FLAG antibody. Purified complexes were subjected to western blot analysis using antibodies to mouse monoclonal FLAG M2 antibody (1:1000) or mouse polyclonal Hsc70 (1:1000). **(B)** Hsc70 co-localises with TBX3. FLAG-TBX3 overexpressing MCF-7 cells were seeded at a density of 0.85 X 10^5 on coverslips in 35 mm dishes and 48 hours later were processed for immunofluorescence with antibodies specific to TBX3 (Cy3; red channel) and Hsc70 (Alexa 488; green channel) and visualized by confocal microscopy. Representative images are shown at 400X magnification. All cells were co-stained with Hoechst to determine the location of the nuclei. **(C)** *Top panel (left):* Merged image from co-localisation analysis with white pixels indicating TBX3 and Hsc70 co-localisation in FLAG-TBX3 overexpressing MCF-7 cells. *Top panel (right):* Representative scatter plot of TBX3 and Hsc70 co-localisation in FLAG-TBX3 overexpressing MCF7 cells. Images were analysed by Zeiss software where the signal intensity of each channel is shown on a 2D graph. *Bottom panel:* Co-localisation of TBX3 and Hsc70 was quantified by Manders, Weighted and Pearson's correlation coefficients using Zeiss software. Data is represented as ± SEM of 20 fields of view.

Results show that the FLAG agarose beads did indeed immunoprecipitate the FLAG-TBX3 protein and that HnRNP K is in complex with TBX3 (**Figure 3.14 A**).

Immunocytochemistry and confocal microscopy analyses were performed to determine if TBX3 and HnRNP K co-localise as described in **section 3.2.5.1**. Results show that in the FLAG-TBX3 overexpressing cells, there is partial interaction between TBX3 and HnRNP K as seen by the overlapping DAPI, Cy3 (TBX3) and ALEXA 488 (HnRNP K) signals in **Figure 3.14 B**. Similar results were observed in FLAG-EMPTY cells as well as parental MCF-7 cells (**Figure 3.15 A and B top panels**) suggesting that endogenous TBX3 interacts with endogenous HnRNP K in MCF-7 cells. The co-localisation between TBX3 and HnRNP K in the nuclear and cytoplasmic compartments of the FLAG-TBX3 overexpressing cells was next measured as described for Hsc70 in **section 3.2.5.1**. **Figure 3.14 C** (Top left panel) shows a different visualization of the co-localization observed in the "merge" image of **Figure 3.14 B** where the overlap of HnRNP K (green channel) and TBX3 (red channel) is indicated by yellow or white pixels.

A

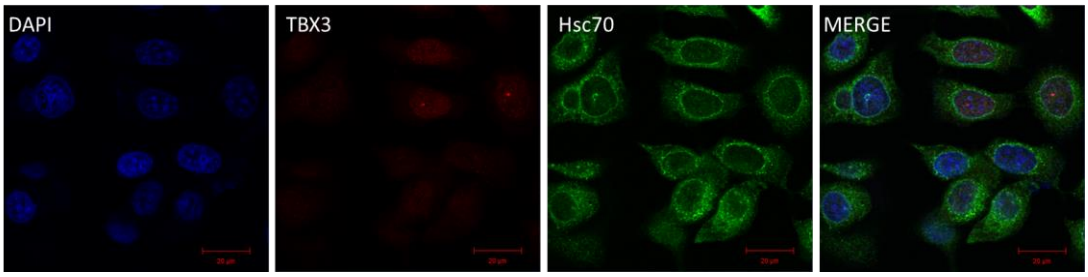

Immunocytochemistry : Parental MCF-7

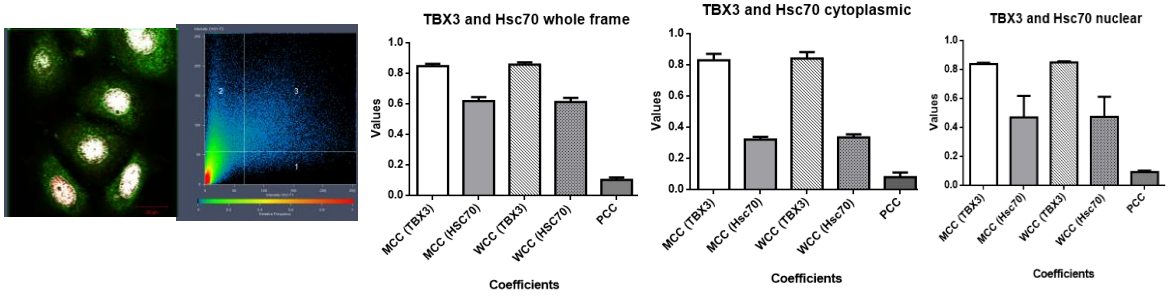

Co-localisation analysis : Parental MCF-7

B

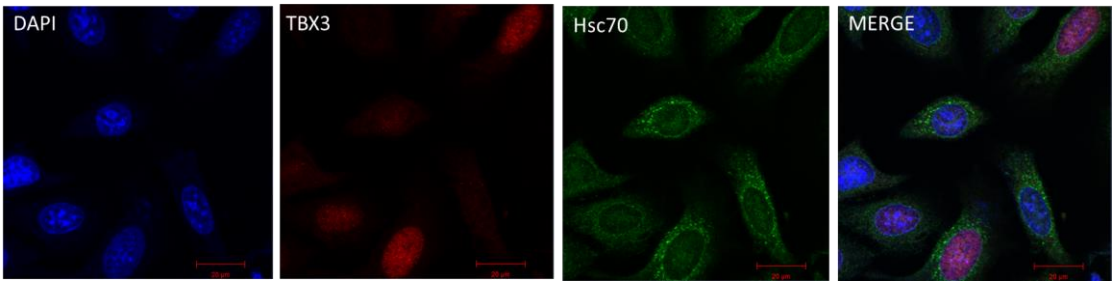

Immunocytochemistry : FLAG EMPTY (E12)

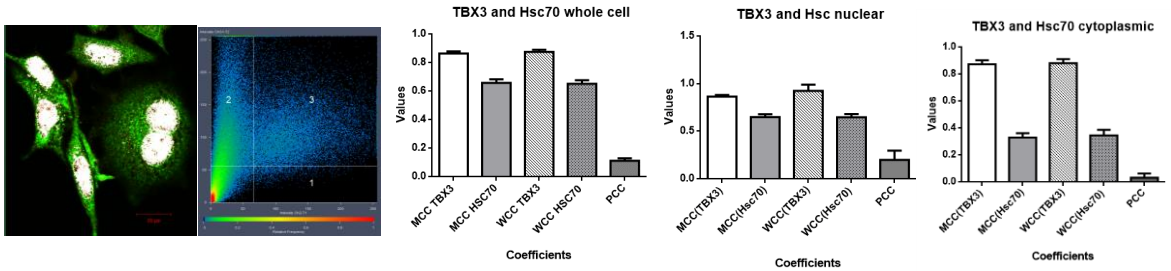

Co-loccalisation analysis : FLAG EMPTY (E12)

Figure 3.12. Endogenous Hsc70 and TBX3 co-localise in parental MCF-7 and FLAG-EMPTY MCF-7 cells. (A) Hsc70 co-localises with TBX3 in parental MCF-7 cells. *Top panel:* cells were seeded at a density of 0.85 X 10^5 on coverslips in 35 mm dishes and 48 hours later were processed for immunofluorescence with antibodies specific to TBX3 (Cy3; red channel) and Hsc70 (Alexa 488; green channel) and visualized by confocal microscopy. Representative images are shown at 400X magnification. All cells were co-stained with Hoechst to determine the location of the nuclei. *Bottom panel (left):* Merged image from co-localisation analysis with white pixels indicating TBX3 and Hsc70 co-localisation. *Bottom panel (right):* Representative scatter plot of TBX3 and Hsc70 co-localisation. Images were analysed by Zeiss software where the signal intensity of each channel is shown on a 2D graph. *Bottom panel:* Co-localisation of TBX3 and Hsc70 was quantified by Manders, Weighted and Pearson's correlation coefficients using Zeiss software. Data is represented as ± SEM of 20 fields of view. **(B)** Hsc70 co-localises with TBX3 in FLAG-EMPTY MCF-7 cells. *Top panel:* cells were seeded and processed for immunofluorescence as described in (**A**). *Bottom panel (left)*: Merged image from co-localisation analysis with white pixels indicating TBX3 and Hsc70 co-localisation. *Bottom panel (right)*: Representative scatter plot of TBX3 and Hsc70 co-localisation. Images were analysed by Zeiss software where the signal intensity of each channel is shown on a 2D graph. *Bottom panel:* Co-localisation of TBX3 and Hsc70 was quantified by Manders, Weighted and Pearson's correlation coefficients using Zeiss software. Data is represented as ± SEM of 20 fields of view.

Figure 3.14 C (Top right panel) shows a representative two-dimensional scatter plot of the intensities of HnRNP K (quadrant 1, bottom right), TBX3 (quadrant 2, top left) and the overlap between the TBX3 and HnRNP K (quadrant 3, top right). The PCC, MCC and WCC coefficients were determined as described in **section 3.2.5.1**. Results show that there is partial co-localisation between TBX3 and HnRNP K proteins in the nucleus and the cytoplasm (**Figure 3.14 C,** lower panel). Moreover, MCC and PCC values show that, in the nucleus, there is a larger proportion of TBX3 that co-localises with a smaller proportion of HnRNP K as expected as there is more TBX3 in the nucleus than in the cytoplasm (**Figure 3.14 C**). In the cytoplasm, a larger proportion of TBX3 co-localises with a smaller proportion of HnRNP K as well even though there appears to be more HnRNP K and less TBX3 present in the cytoplasm (**Figure 3.14 C**). This indicates that while all the TBX3 in the cytoplasm interacts with the HnRNP K, not all the HnRNP K interacts with TBX3 which can be expected because it also interacts with other proteins. Overall, no notable difference in the co-localisation pattern was observed between the whole cell, nuclear

and cytoplasmic compartments in the cells. Similar results were observed in the parental MCF-7 and FLAG-EMPTY cells (**Figure 3.15**).

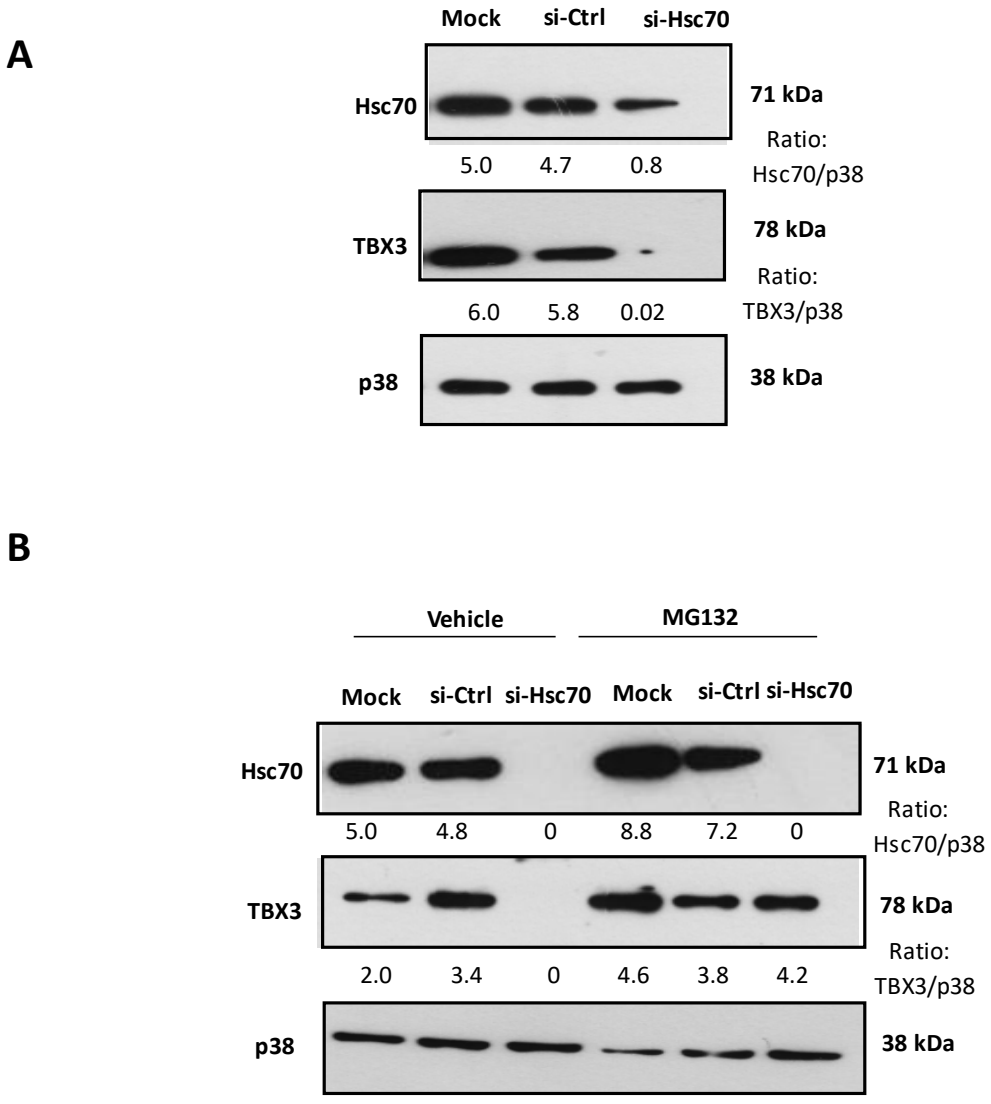

Figure 3.13. Hsc70 is required for TBX3 stability. ***(*****A)** Knockdown of Hsc70 led to a decrease in TBX3 levels. MCF-7 cells transiently transfected with 50 nM si-Hsc70 or the equivalent concentration of control si-Ctrl for 48 hours were analysed by SDS-PAGE (8%) and western blotting with antibodies to Hsc70 and TBX3. p38 was used as a loading control. **(B)** MG132 rescued TBX3 protein levels in MCF-7 cells after Hsc70 knockdown. MCF-7 cells were transiently transfected with 50 nM si-Hsc70 or the equivalent concentration of control si-Ctrl and treated with 10 μM MG132 (proteasome inhibitor) or vehicle (DMSO) 8 hours before harvesting. Protein extracts were analysed by SDS-PAGE (8%) and western blotting using antibodies to Hsc70 and TBX3. p38 was used as loading control.

A

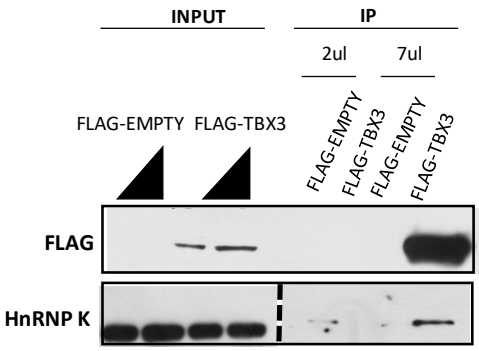

Immunoprecipitation: HnRNP K

B

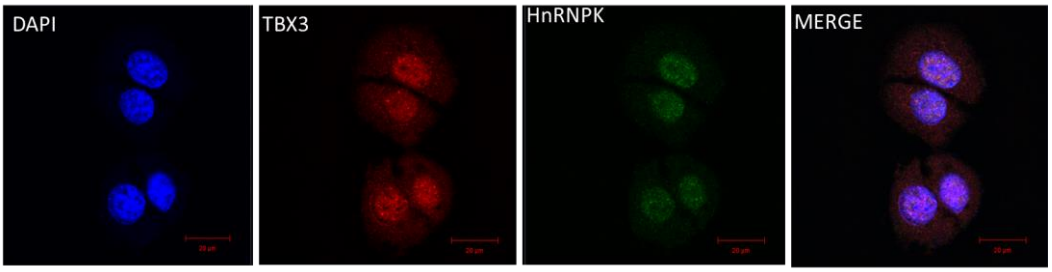

Immunocytochemistry: : FLAG-TBX3 (2)

C

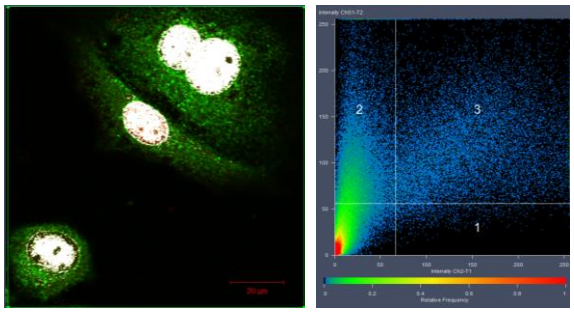

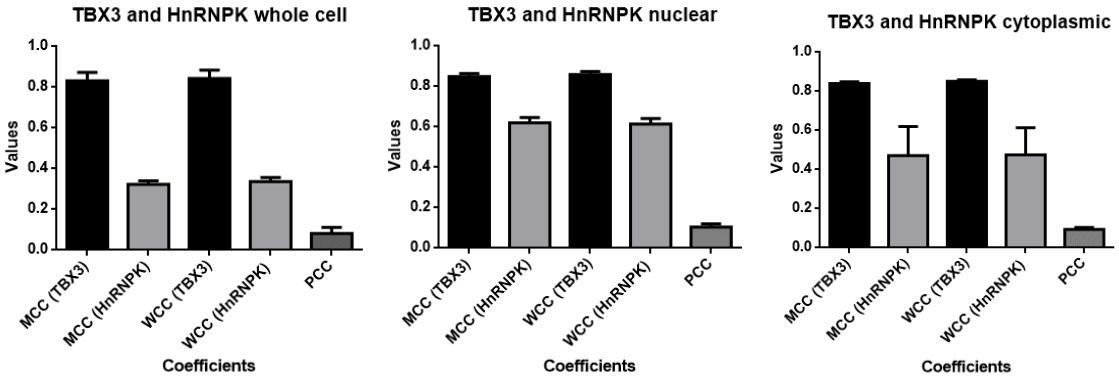

Co-localisation analysis : FLAG-TBX3 (2)

Figure 3.14. HnRNP K binds and co-localises with TBX3 in FLAG-TBX3 overexpressing MCF-7 cells in vivo. **(A)** HnRNP K directly interacts with TBX3. Protein extracts from FLAG-EMPTY and FLAG-TBX3 (2) MCF-7 cells were immunoprecipitated using an anti-FLAG antibody and purified complexes were subjected to western blot analysis with antibodies to mouse monoclonal FLAG M2 antibody (1:1000) or mouse polyclonal HnRNP K (1:1000) (Santa Cruz, USA). **(B)** HnRNP K co-localises with TBX3. FLAG-TBX3 (2) overexpressing MCF-7 cells were seeded at a density of 0.85 X 10^5 on coverslips in 35 mm dishes and 48 hours later were processed for immunofluorescence with antibodies specific to TBX3 (Cy3; red channel) and HnRNP K (Alexa 488; green channel) and visualized by confocal microscopy. Representative images are shown at 400X magnification. All cells were co-stained with DAPI to determine the location of the nuclei. **(C)** Representative scatter plot of HnRNP K and TBX3 co-localisation in MCF-7 cells. *Top panel (left):* Merged image from co-localisation analysis with white pixels indicating TBX3 and HnRNP K co-localisation in FLAG-TBX3 overexpressing MCF-7 cells. *Top panel (right):* Images shown in top panel were analysed by Zeiss software where the signal intensity of each channel is shown in the 2D graph. *Bottom panel:* Co-localisation of TBX3 and HnRNP K was quantified by Manders, Weighted and Pearson's correlation coefficients using Zeiss software. Data are represented as ± SEM of 20 fields of view.

3.2.5.3. Identification and characterisation of nucleolin as a TBX3 co-factor

Nucleolin has been shown to (1) have overlapping oncogenic roles with TBX3 such as promoting migration and (2) like TBX3, be upregulated by c-Myc. Together this suggests that c-Myc/TBX3/nucleolin may form an important oncogenic signalling axis in breast cancer. This is investigated in the following section of the thesis.

Nucleolin binds and co-localises with TBX3 in vitro

To validate that nucleolin is a bona fide co-factor of TBX3, co-immunoprecipitation assays were firstly performed as described previously. Results show that the FLAG agarose beads did indeed immunoprecipitate the FLAG-TBX3 protein and that nucleolin is in complex with TBX3 in both FLAG-TBX3 clones (**Figure 3.16 A and 3.17 A**). To determine if TBX3 and nucleolin co-localise, immunocytochemistry and confocal microscopy analyses were performed as described previously.

A

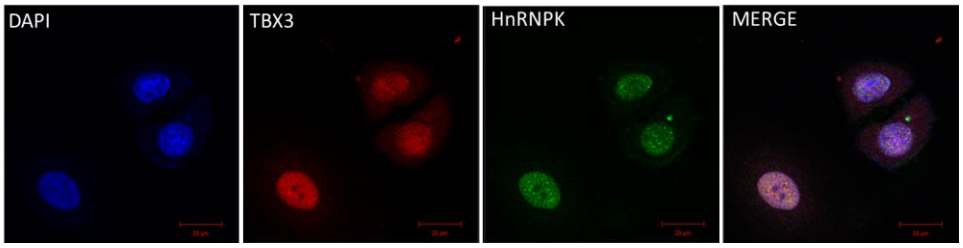

Immunocytochemistry : Parental MCF-7

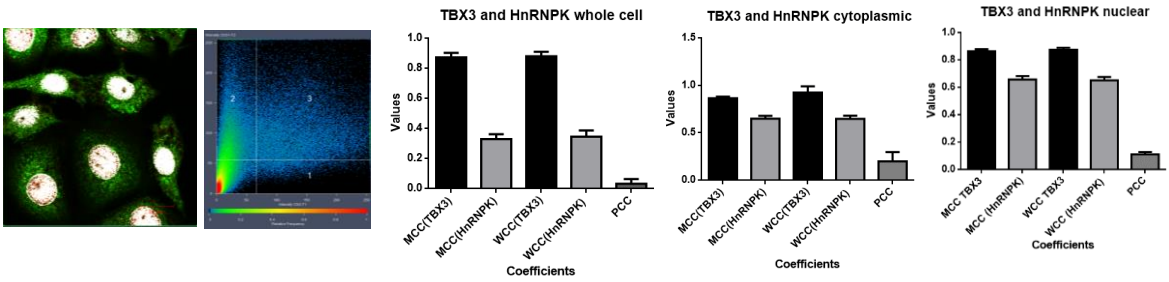

Co-localisation analysis : Parental MCF-7

B

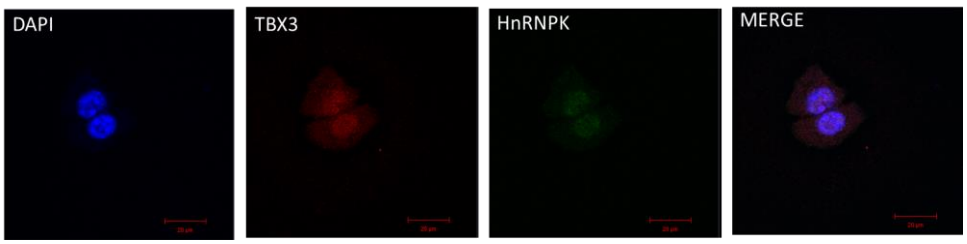

Immunocytochemistry : FLAG EMPTY (E12)

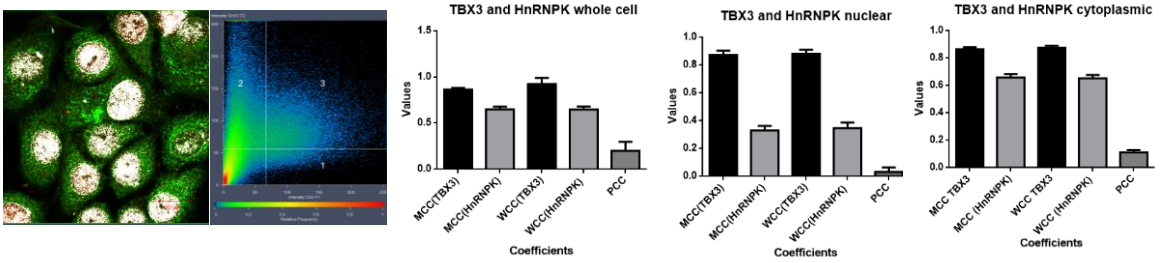

Co-localisation analysis : FLAG EMPTY (E12)

Figure 3.15. Endogenous HnRNP K co-localises with endogenous TBX3 in parental and FLAG-EMPTY MCF-7 cells. (A) HnRNP K co-localises with TBX3. *Top panel:* Parental MCF-7 cells were seeded at a density of 0.85 X 10^5 on coverslips in 35 mm dishes and 48 hours later were processed for immunofluorescence with antibodies specific to TBX3 (Cy3; red channel) and HnRNP K (Alexa 488; green channel) and visualized by confocal microscopy. Representative images are shown at 400X magnification. All cells were co-stained with DAPI to determine the location of the nuclei. *Bottom panel (left):* Merged image from co-localisation analysis with white pixels indicating TBX3 and HnRNP K co-localisation in parental MCF-7 cells. *Bottom panel (right):* Representative scatter plot of TBX3 and HnRNP K co-localisation in parental MCF-7 cells. Images were analysed by Zeiss software where the signal intensity of each channel is shown in the 2D graph. *Bottom panel:* Co-localisation of TBX3 and HnRNP K was quantified by Manders, Weighted and Pearson's correlation coefficients using Zeiss software. Data is represented as ± SEM of 20 fields of view. **(B)** *Top panel:* FLAG-EMPTY MCF-7 cells processed for immunofluorescence as described in **(A)**. Bottom panel (left): Merged images from co-localisation analysis with white pixels indicating TBX3 and HnRNP K co-localisation in FLAG-EMPTY MCF-7 cells. *Bottom panel* (right): Representative scatter plot of TBX3 and HnRNP K co-localisation in FLAG-EMPTY MCF-7 cells. Images were analysed by Zeiss software where the signal intensity of each channel is shown in the 2D graph. *Bottom panel*: Co-localisation of TBX3 and HnRNP K was quantified by Manders, Weighted and Pearson's correlation coefficients using Zeiss software. Data are represented as ± SEM of 20 fields of view.

FLAG-TBX3 overexpressing cells (1 and 2) were processed for immunocytochemistry with primary antibodies to FLAG and nucleolin while the FLAG-EMPTY and parental MCF-7 cells were processed for immunocytochemistry with primary antibodies to endogenous TBX3 and nucleolin. Results show that in the FLAG-TBX3 overexpressing cells (1 and 2), there is partial interaction between TBX3 and nucleolin as seen by the overlapping DAPI, Cy3 (TBX3) and ALEXA 488 (nucleolin) signals in **Figure 3.16 B** and **Figure 3.17 B**. Similar results were observed in parental and FLAG-EMPTY MCF-7cells (**Figure 3.18 A** and **B, top panels**)

Co-localisation of TBX3 and nucleolin was further measured in nuclear and cytoplasmic compartments of the FLAG-TBX3 overexpressing cells as described for Hsc70. **Figures 3.16 C** and **3.17 C** (top left panels) show a different visualization of the co-localisation observed in the "merge" image of **Figures 3.16 B** and **3.17 B** where the overlap of nucleolin (green channel) and TBX3 (red channel) is indicated by yellow or white pixels. **Figures 3.16 C** and **3.17 C** (Top right panel) shows a representative two-dimensional

scatter plot of the intensities of nucleolin (quadrant 1, bottom right), TBX3 (quadrant 2, top left) and the overlap between the TBX3 and nucleolin (quadrant 3, top right). The PCC, MCC and WCC coefficients were used to measure the proportion of TBX3 co-localising with nucleolin and vice versa as described for Hsc70 and HnRNP K above. As determined by the PCC, MCC and WCC values there is partial co-localisation between TBX3 and nucleolin proteins in the nucleus and the cytoplasm (**Figure 3.16 C, Figure 3.17 C**). Moreover, MCC and PCC values show that, in the nucleus, there is larger proportion of nucleolin that co-localises with a smaller proportion of TBX3 (**Figure 3.16 C, Figure 3.17 C**). This is not unexpected as nucleolin appears to be exclusively nuclear whereas, while predominantly nuclear, TBX3 is also present in the cytoplasm. Consistent with this, there is a larger proportion of TBX3 that co-localises with a smaller portion of nucleolin in the cytoplasm (**Figure 3.16 C, Figure 3.17 C**). Similar results were observed in the parental and FLAG-EMPTY MCF-7 cells (**Figure 3.18 A bottom panel, 3.18 B bottom panel**)
Taken together, this data shows that endogenous TBX3 interacts with endogenous nucleolin in MCF-7 breast cancer cells.

Nucleolin cooperates with TBX3 to promote migration

The next set of experiments were performed to determine whether TBX3 and nucleolin cooperate to promote migration. To this end, nucleolin was transiently silenced in FLAG-EMPTY and FLAG-TBX3 cells (1 and 2) using an siRNA against nucleolin (si-Nucleolin) and the effect on cell migration was measured using a scratch motility assay. The overexpression of TBX3 and the efficacy of the si-Nucleolin was confirmed by western blotting using antibodies to FLAG and nucleolin respectively (**Figure 3.19 A and B**, **left hand side**). Results show that compared to the FLAG-EMPTY MCF-7 cells transfected with si-Ctrl, silencing nucleolin in these cells inhibits their migratory ability (**Figure 3.19 A and B, right hand side**). Similar results have been reported for silencing TBX3 in MCF-7 cells (Peres et al., 2010). Importantly, as was shown earlier in this thesis, overexpressing FLAG-TBX3 enhanced the migratory ability of the cells (**Figure 3.5**), however the results shown here demonstrate that this effect is abrogated when nucleolin was depleted in these cells (**Figure 3.19 A and B, right hand side**).

A

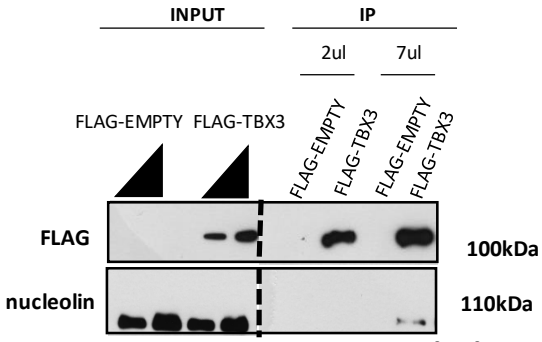

Immunoprecipitation: Nucleolin

B

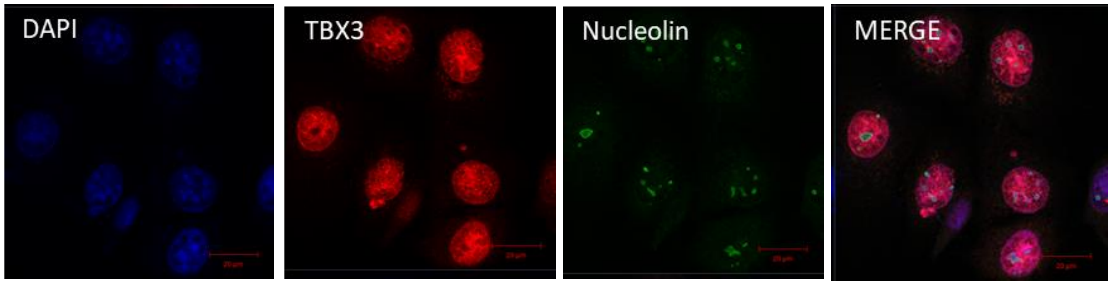

Immunocytochemistry : FLAG-TBX3 (1)

C

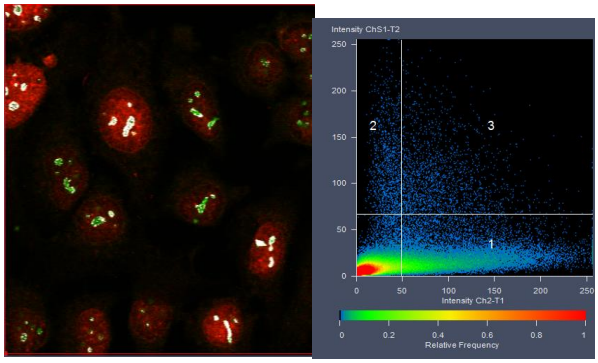

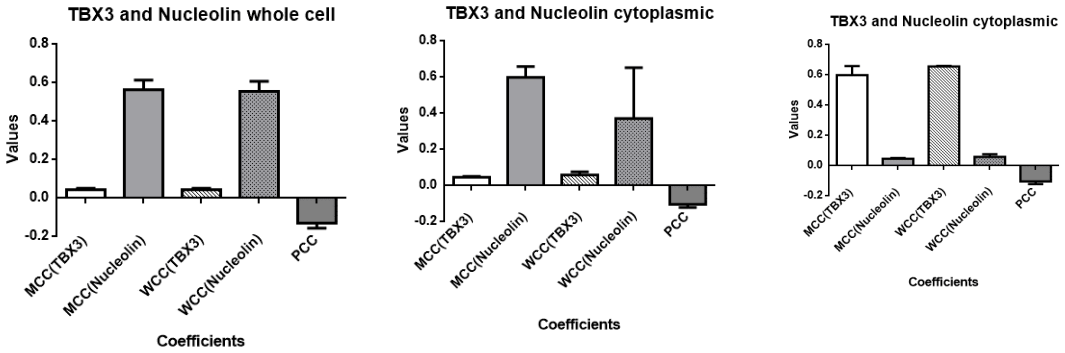

Co-localisation analysis : FLAG-TBX3 (1)

Figure 3.16. Nucleolin binds and colocalises with TBX3 in FLAG-TBX3 (1) overexpressing MCF-7 cells in vivo. **(A)** Protein extracts from FLAG-EMPTY (12) and FLAG-TBX3 (1) MCF-7 cells were immunoprecipitated using an anti-FLAG antibody, pulling down FLAG-tagged TBX3 and protein partners bound to it. Purified immune complexes were subjected to western blot analysis using antibodies to mouse monoclonal FLAG M2 antibody (1:1000), mouse polyclonal nucleolin (1:1000) and secondary A/G protein (1:5000). **(B)** FLAG-TBX3 (1) overexpressing MCF-7 cells were seeded at a density of 0.85 X 10^5 on coverslips in 35mm dishes and 48 hours later were processed for immunofluorescence with antibodies specific to TBX3 (Cy3; red channel) and nucleolin (Alexa 488; green channel) and visualized by confocal microscopy. Representative images are shown at 400X magnification. All cells were co-stained with Hoechst to determine the location of the nuclei. **(C)** *Top panel (left):* Merged image from colocalisation analysis with white pixels indicating TBX3 and nucleolin co-localisation in FLAG-TBX3 (1) overexpressing MCF-7 cells. *Top panel (right):* Representative scatter plot of TBX3 and nucleolin colocalisation in MCF7 cells. Images were analysed by Zeiss software where the signal intensity of each channel is shown on a 2D graph. *Bottom panel:* Colocalisation of TBX3 and nucleolin was quantified by Manders,Weighted and Pearson's correlation coefficients using Zeiss software. Data is represented as ± SEM of 20 fields of view

These results suggest that TBX3 requires nucleolin for its pro-migratory function in these MCF-7 breast cancer cells. If this was the case, then overexpressing nucleolin should not rescue the effect of knocking down TBX3 in the MCF-7 cells. To test this, nucleolin was ectopically overexpressed in shCtrl and shTBX3 MCF-7 cells and migration assays were performed. The overexpression of nucleolin (GFP-Nucleolin) and the knock down of TBX3 (shTBX3) was confirmed through western blotting with antibodies to nucleolin and TBX3 (**Figure 3.19 C**, left panel). Results show that, compared to shCtrl-untransfected and shCtrl-Empty cells, overexpressing nucleolin in shCtrl cells promotes their migratory ability after 3 hours (**Figure 3.19 C, right panel**). As expected, compared to shCtrl-untransfected and shCtrl-empty cells, knocking down TBX3 (shTBX3-Empty) inhibits the migratory ability of the cells (**Figure 3.19 B, right panel**). Importantly, results show that overexpressing nucleolin (shTBX3-nucleolin) cannot rescue the effect of silencing TBX3 on cell migration, thereby suggesting that nucleolin too, requires TBX3 to promote migration (**Figure 3.19 B, right panel,**). This set of data confirms that nucleolin and TBX3 require each other to promote migration of MCF-7 breast cancer cells.

A

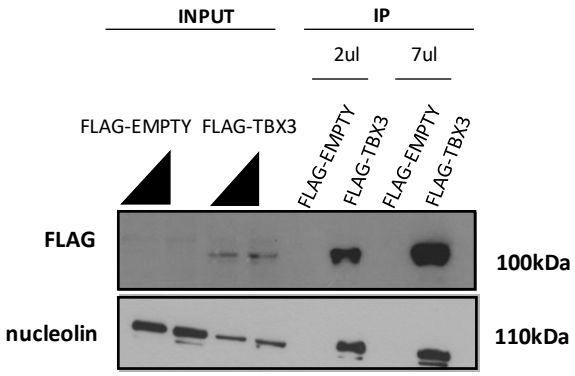

Immunoprecipitation: Nucleolin

B

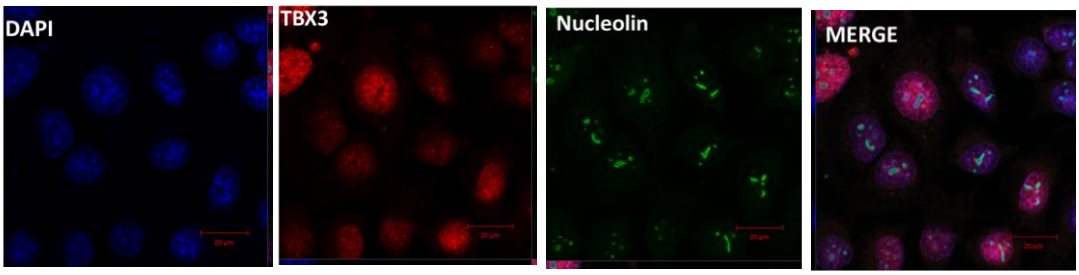

Immunocytochemistry : FLAG-TBX3 (2)

C

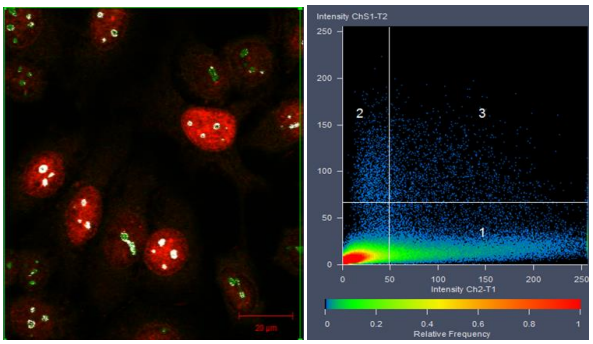

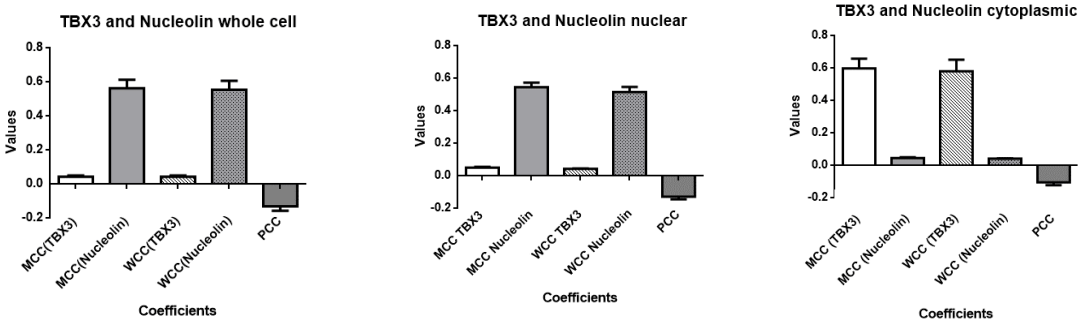

Co-localisation analysis : FLAG-TBX3 (2)

Figure 3.17. Nucleolin binds and colocalises with TBX3 in FLAG-TBX3 (2) overexpressing MCF-7 cells in vivo. (A) Protein extracts from FLAG-EMPTY and FLAG-TBX3 (2) MCF-7 cells were immunoprecipitated using an anti-FLAG antibody, pulling down FLAG-tagged TBX3 and protein partners bound to it. Purified immune complexes were subjected to western blot analysis using antibodies to mouse monoclonal FLAG M2 antibody (1:1000), mouse polyclonal nucleolin (1:1000) and secondary A/G protein (1:5000). **(B)** FLAG-TBX3 (2) overexpressing MCF-7 cells were seeded at a density of 0.85 X 10^5 on coverslips in 35mm dishes and 48 hours later were processed for immunofluorescence with antibodies specific to TBX3 (Cy3; red channel) and nucleolin (Alexa 488; green channel) and visualized by confocal microscopy. Representative images are shown at 400X magnification. All cells were co-stained with Hoechst to determine the location of the nuclei. **(C)** *Top panel (left):* Merged image from colocalisation analysis with white pixels indicating TBX3 and nucleolin colocalisation in FLAG-TBX3 (2) overexpressing MCF-7 cells. *Top panel (right):* Representative scatter plot of TBX3 and nucleolin colocalisation in FLAG-TBX3 (1) overexpressing MCF-7 cells. Images were analysed by Zeiss software where the signal intensity of each channel is shown on a 2D graph. *Bottom panel:* Colocalisation of TBX3 and nucleolin was quantified by Manders,Weighted and Pearson's correlation coefficients using Zeiss software. Data is represented as ± SEM of 20 fields of view.

c-Myc transcriptionally activates nucleolin in MCF-7 breast cancer cells

The current study revealed that c-Myc upregulates TBX3 expression and that TBX3 and nucleolin interact and co-localise in MCF-7 breast cancer cells to promote their migration. Interestingly, a study using site-directed mutagenesis and reporter assays has shown that nucleolin is also transcriptionally activated by c-Myc in human embryonic kidney cells (Greasley, Bonnard and Amati, 2000). Together this raised the interesting possibility that c-Myc may also upregulate nucleolin in MCF-7 breast cancer cells and together c-Myc/TBX3/nucleolin form an important oncogenic signalling axis in these cells. To investigate this, the impact of transiently knocking down c-Myc on nucleolin mRNA and protein levels was determined in MCF-7 cells. Briefly, MCF-7 cells were transiently transfected with two different siRNAs to c-Myc (si-c-Myc#1 and si-c-Myc#2) and c-Myc and nucleolin mRNA and protein levels were assessed by qRT-PCR and western blotting respectively. The results show that c-Myc mRNA and protein were successfully depleted by si- c-Myc#1 and si-c-Myc#2 (**Figure 3.20 A** and **B**).

A

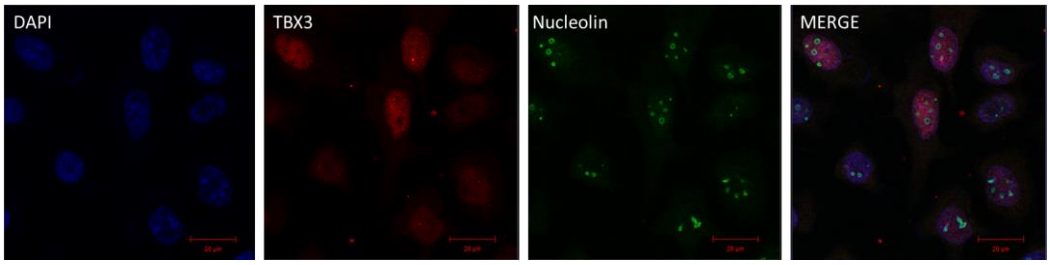

Immunocytochemistry : Parental MCF-7

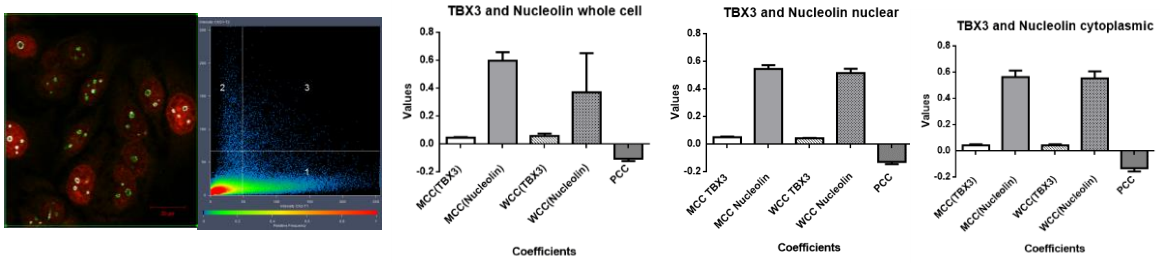

Colocalisation analysis : Parental MCF-7

B

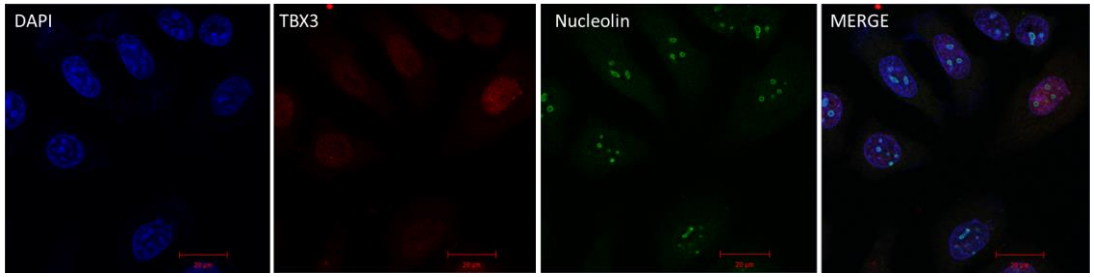

Immunocytochemistry : FLAG-EMPTY (12)

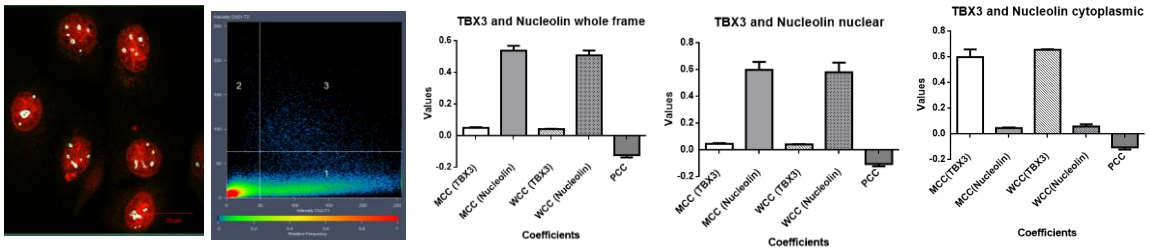

Colocalisation analysis : FLAG-EMPTY (12)

Figure 3.18. Nucleolin binds and colocalises with TBX3 in parental MCF-7 and FLAG-EMPTY (12) MCF-7 cells. (A) *Top panel:* Parental MCF-7 cells were seeded at a density of 0.85 X 10^5 on coverslips in 35mm dishes and 48 hours later were processed for immunofluorescence with antibodies specific to TBX3 (Cy3; red channel) and nucleolin (Alexa 488; green channel) and visualized by confocal microscopy. Representative images are shown at 400X magnification. All cells were co-stained with Hoechst to determine the location of the nuclei. *Bottom panel (left):* Merged image from co-localisation analysis with white pixels indicating TBX3 and nucleolin colocalisation in parental MCF-7 cells. *Bottom panel (right):* Representative scatter plot of TBX3 and nucleolin colocalisation in parental MCF-7 cells. Images were analysed by Zeiss software where the signal intensity of each channel is shown on a 2D graph. *Bottom panel:* Colocalisation of TBX3 and nucleolin was quantified by Manders, Weighted and Pearson's correlation coefficients using Zeiss software. Data is represented as ± SEM of 20 fields of view. **(B)** *Top panel:* FLAG-EMPTY (12) MCF-7 cells were processed for immunofluorescence as described in (A). *Bottom panel (left):* Merged image from co-localisation analysis with white pixels indicating TBX3 and nucleolin colocalisation in FLAG-EMPTY (12) MCF-7 cells. *Bottom panel (right):* Representative scatter plot of TBX3 and nucleolin colocalisation in FLAG-EMPTY (12) MCF-7 cells. Images were analysed by Zeiss software where the signal intensity of each channel is shown on a 2D graph. *Bottom panel:* Colocalisation of TBX3 and nucleolin was quantified by Manders, Weighted and Pearson's correlation coefficients using Zeiss software. Data is represented as ± SEM of 20 fields of view.

Importantly, when c-Myc was depleted there was a corresponding decrease in nucleolin mRNA (**Figure 3.20 A**) and protein (**Figure 3.20 B**). These results suggested that c-Myc acts upstream of nucleolin. To determine whether this regulation is transcriptional, c-Myc was overexpressed in MCF-7 breast cancer cells in the presence or absence of Actinomycin D, an inhibitor of de novo transcription, and nucleolin mRNA and protein levels were measured by qRT-PCR and western blotting respectively. The results show that in the presence of ectopically expressed c-Myc there is a corresponding increase in nucleolin mRNA levels (**Figure 3.20 C**). When FLAG EMPTY cells were treated with Actinomycin D there was a two-fold decrease in nucleolin mRNA levels, which suggests that basal levels of nucleolin is, in part, due to de novo transcription (**Figure 3.20 C**). When de novo transcription was, however, inhibited in FLAG c-Myc cells, the c-Myc mediated activation of nucleolin mRNA was reduced by approximately 19-fold (**Figure 3.20 C**). The same trend was observed for nucleolin protein levels (**Figure 3.20 D**).

A

Nucleolin knockdown

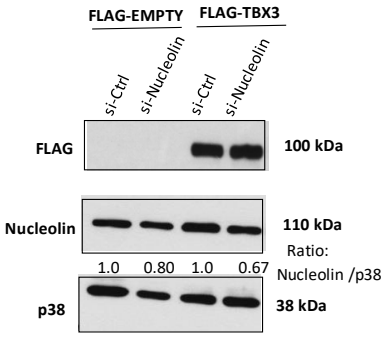

Western blot

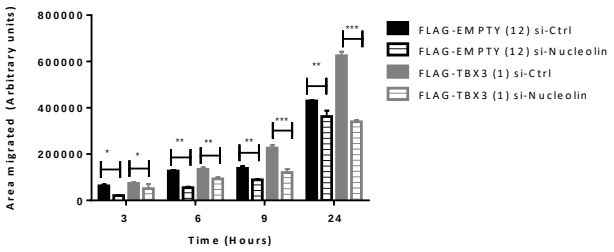

Scratch motility assay

B

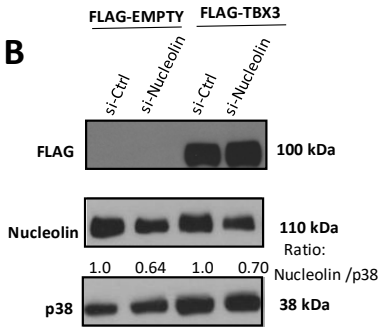

Western blot

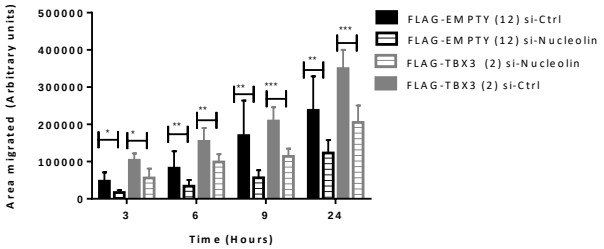

Scratch motility assay

Nucleolin overexpression

C

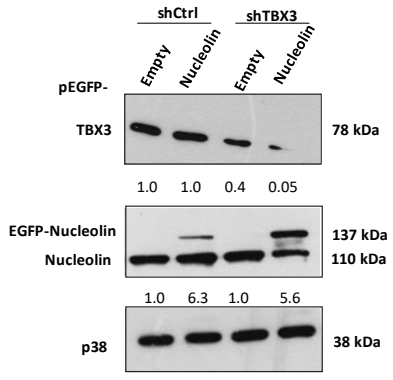

Western blot

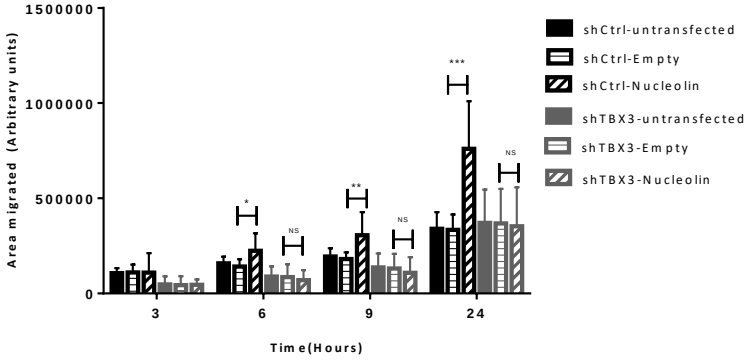

Scratch motility assay

Figure 3.19. Nucleolin and TBX3 cooperate to promote MCF-7 breast cancer cell migration. **(A, B)** Knockdown of nucleolin inhibits TBX3 induced cell migration. Migration was measured using a two-dimensional in vitro scratch motility assay. MCF-7 FLAG-Empty and FLAG-TBX3 cells were seeded in triplicate in 24 well plates and left to adhere for 48 hours. Cells were transiently transfected with 100 nM siNucleolin or siControl (siCtrl) and 48 hours later a linear wound was made by scratching through the monolayer using a sterile 10 µl pipette tip. Mitomycin C (10 µg/ml) was added to prevent cell proliferation and migration measured over a 24-hour period. *Left panels*: Western blots with antibodies to FLAG and nucleolin show the effective overexpression of FLAG-TBX3 and knockdown of nucleolin respectively. p38 was used as a loading control. *Right panel:* Scratch motility assays. **(C)** Ectopic overexpression of nucleolin cannot rescue the effect of silencing TBX3 on MCF-7 cell migration. MCF-7 shTBX3 and shCtrl cells were seeded in triplicate in 24 well plates and left to adhere for 48 hours. Cells were transiently transfected with either pEGFP-EMPTY (Empty) or pEGFP-Nucleolin (Nucleolin) and the scratch motility assay was performed as for (A, B) above. *Left panel*: Western blot analysis with antibodies to TBX3, nucleolin and p38 (loading control) shows the efficacy of TBX3 knockdown and nucleolin overexpression. *Right panel*: Scratch motility assays. For **A, B and C** results are representative of three independent experiments. Microsoft Excel student t-test was performed to calculate statistical significance, *p<0.05; **p<0.01; ***p<0.001; error bars represent standard error of the mean.

Interestingly, the western blot for endogenous c-Myc suggests that endogenous c-Myc is also upregulated by de novo transcription. In summary these results show that c-Myc transcriptionally upregulates nucleolin expression in MCF-7 breast cancer cells.

The effect of the nucleolin targeting aptamer, AS1411, on MCF-7 cell viability and migration

In this study, TBX3 and nucleolin were shown to interact and co-operate with one another to drive migration of MCF-7 breast cancer cells. It was therefore postulated that disrupting the interaction between TBX3 and nucleolin could inhibit MCF-7 cell migration which has important implications for treating TBX3-driven advanced breast cancer. To investigate this, the nucleolin targeting aptamer AS1411 was employed in this study because it has been found to interfere with nucleolin protein-protein interactions (Teng et al., 2007). AS1411 is a 26-base guanine rich oligodeoxynucleotide that specifically recognizes the shape of nucleolin and binds to it with high affinity and specificity (Reyes-Reyes *et al.*, 2015).

A

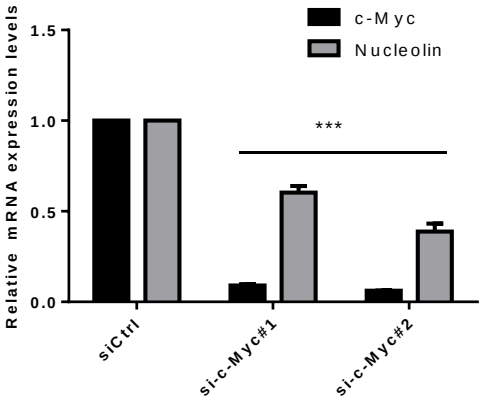

qRT-PCR

B

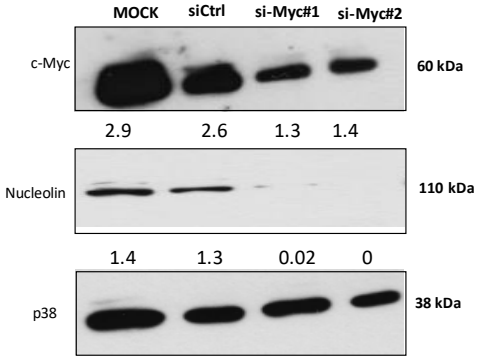

Western blot

C

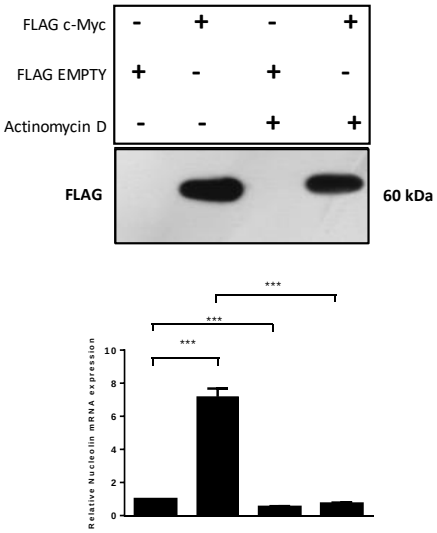

qRT-PCR

D

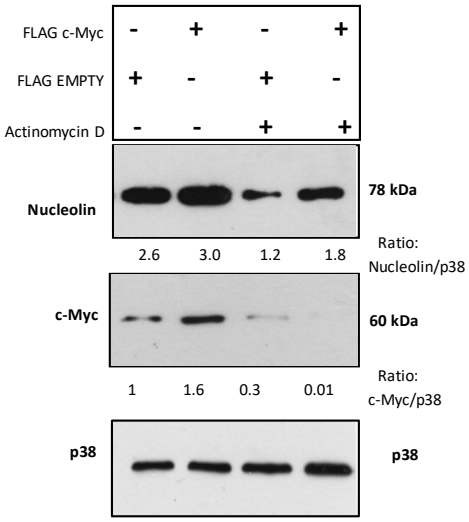

Western blot

Figure 3.20. c-Myc transcriptionally upregulates nucleolin in MCF-7 breast cancer cells.

(A, B) MCF-7 breast cancer cells were plated in triplicate in a 6-well plate at a density of 2.5 x 10^5 cells/well. The cells were transfected with either 10 nM si-cMyc#1, si-cMyc#2 or the equivalent concentration of control siRNA (siCtrl). **(A)** RNA was extracted from the cells and quantitative real-time PCR was performed on reverse transcribed RNA using primers to c-Myc and nucleolin, mRNA levels were normalized to GUSB. Microsoft Excel student t-test was performed to calculate statistical significance, *p<0.05; **p<0.01; ***p<0.001; error bars represent standard error of the mean. **(B)** Western blotting was performed with protein harvested from the cells and the following antibodies to c-Myc and nucleolin: rabbit polyclonal anti-TBX3 (1:500) or mouse anti-nucleolin (1:1000). p38 was used as a loading control. Densitometric values represent the expression of each protein band quantified using Image J imaging software and normalized to p38 protein levels. **(C, D)** MCF-7 breast cancer cells were plated as for **(A, B)** and transfected with 500 ng pcDNA-FLAG-c-Myc or pcDNA-FLAG-EMPTY expression constructs. Forty-eight hours after transfection the cells were treated with 5 μg/ml Actinomycin D or the equivalent concentration of vehicle (DMSO) for 30 minutes. **(C)** RNA was extracted from the cells and quantitative real-time PCR was performed on reverse transcribed RNA using primers to TBX3 and mRNA levels were normalized to GUSB. Microsoft Excel student t-test was performed to calculate statistical significance, *p<0.05; **p<0.01; ***p<0.001; error bars represent standard error of the mean. **(D)** Western blotting was performed with protein harvested from the cells and FLAG-tagged c-Myc, endogenous c-Myc and nucleolin were detected using the following antibodies: mouse monoclonal FLAG M2 antibody (1:1000), mouse anti-nucleolin (1:1000) or rabbit polyclonal anti-TBX3 (1:500) and p38 was used as a loading control. Densitometric values represent the expression of each protein band quantified using Image J imaging software and normalized to p38 protein levels.

Furthermore, AS1411 is currently in Phase II clinical trials for acute myeloid leukaemia and renal carcinoma and has been shown to inhibit HT1080 fibrosarcoma cell viability (Bates et al., 2009).

To determine the anti-cancer activity of AS1411 in MCF-7 breast cancer cells, cell viability and scratch motility assays were carried out after treatment with AS1411 or a non-targeting control aptamer, CRO. The results show that AS1411 treatment caused a significant reduction in MCF-7 cell viability compared to CRO treatment for all tested concentrations (**Figure 3.21 A**). Moreover, AS1411 treatment had no significant effect on the viability of the DMB and FG0 "normal" human fibroblast cell lines (**Figure 3.21 A**). Results from the scratch motility assays show that, compared to untreated and CRO

treated cells, the AS1411 treated cells had a significantly decreased migratory ability at all time points tested (**Figure 3.21 B**). To determine if this effect was due to alterations in EMT markers, protein was harvested from the cells subjected to the migration assay and was subjected to western blotting using antibodies to E-cadherin, N-cadherin, vimentin and ß-catenin (**Figure 3.21 C**). Indeed, the AS1411 treated cells had an increase in expression of the epithelial marker E-cadherin and a decrease in the mesenchymal markers, N-cadherin, vimentin and ß-catenin (**Figure 3.21 C**). Together the above observations suggest that AS1411 may be an effective anti-breast cancer treatment strategy and that its mechanism of action may, in part, involve the disruption of the interaction between TBX3 and nucleolin.

AS1411 treatment of MCF-7 cells mislocalizes TBX3 and nucleolin to the cytoplasm

It was hypothesised that the inhibitory effect of AS1411 on MCF-7 cell migration may be due to its ability to disrupt the interaction between nucleolin and TBX3. To begin to investigate this, immunocytochemistry with antibodies to nucleolin and TBX3 was performed on untreated, CRO treated and AS1411 treated MCF-7 cells. The results show that while nucleolin is almost exclusively present in the nuclei of untreated and CRO treated cells, after AS1411 treatment there is a significant decrease in nuclear nucleolin and a significant increase in cytoplasmic nucleolin (**Figure 3.22 A and 3.22 B**). Moreover, there is a significant decrease in nuclear TBX3 expression and a significant increase in cytoplasmic TBX3 after AS1411 treatment (**Figure 3.22 A and 3.22 B**). To confirm these findings, cells were left untreated or treated with either CRO or AS1411 for 48 hours after which the nuclear and cytoplasmic components of the cells were separated and subjected to western blotting using antibodies against TBX3 and nucleolin. To exclude the possibility of contamination of the cytoplasmic and nuclear fractions used in the above experiments, western blots were probed for GAPDH (a cytoplasmic marker) and p84 (a nuclear marker). The results show that after AS1411 treatment there is a marked decrease in nuclear TBX3 and nucleolin and a marked increase of the two proteins in the cytoplasm (**Figure 3.22 C**). Taken together, this data suggests that AS1411 may reduce MCF-7 cell migration by mislocalizing TBX3 and nucleolin from the nucleus into the cytoplasm.

A

MCF-7 breast cancer cells

Primary skin fibroblasts

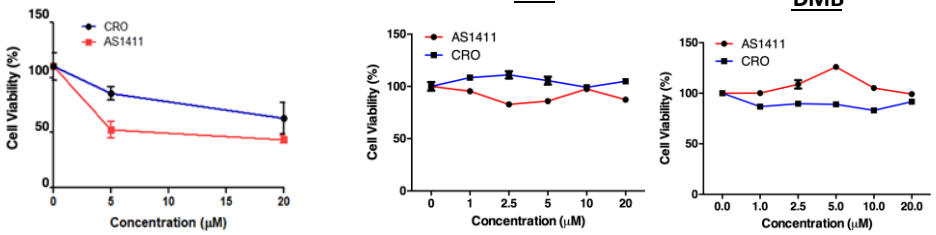

Cell viability assay

B

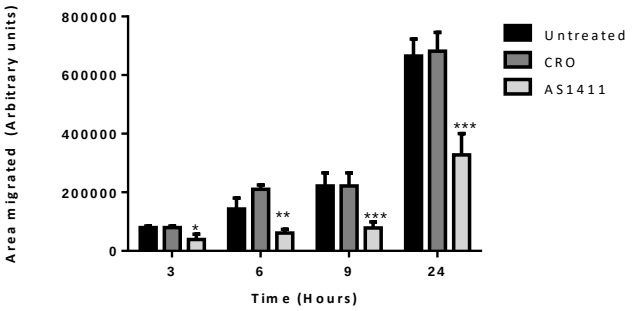

Scratch motility assay

C

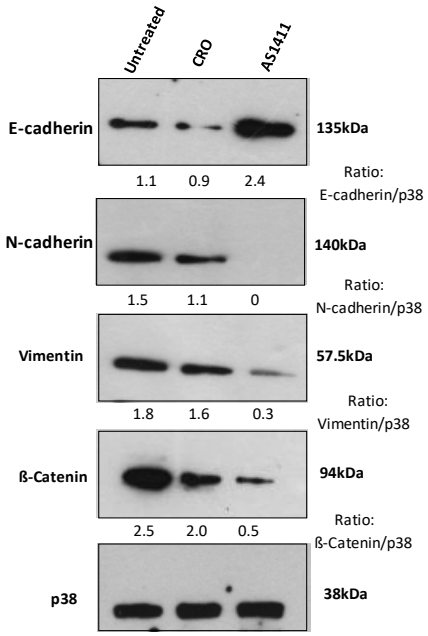

Western blot

Figure 3.21. The nucleolin targeting aptamer, AS1411, inhibits MCF-7 breast cancer cell viability and migration. (A) AS1411 inhibits short-term MCF-7 cell viability. The methylthiazol tetrazolium (MTT) assay was performed on MCF-7 cells plated in quadruplicate at a density of 1 X 10^3 cells/well in 96 well-plates and treated immediately with 10 μM AS1411 or CRO for 96 hours. After addition of the MTT solution and solubilization buffer, absorbance (595 nm) was determined by spectrophotometry. Two-way ANOVA was used to measure statistical significance, data are the mean±sem of three independent experiments performed in quadruplicate, *p<0.05; **p<0.01; ***p<0.001. Error bars represent the standard error of the mean. **(B)** AS1411 inhibits MCF-7 cell migration. MCF-7 cells were plated at a density of 0.85 X 10^5 cells/ml in 24-well plates and immediately treated with 10 μM AS1411 or CRO for 96 hours. Scratch motility assays were performed over a 24-hour period. Results are representative of three independent experiments. Microsoft Excel student t-test was performed to calculate statistical significance, *p<0.05; **p<0.01; ***p<0.001; error bars represent standard error of the mean. **(C)** AS1411 inhibits EMT markers in MCF-7 cells. Western blotting with protein harvested from cells after the migration assay and probed with the following antibodies: mouse monoclonal anti-E-cadherin (1:1000), mouse polyclonal anti-N-cadherin (1:1000), rabbit polyclonal anti-vimentin (1:1000) and mouse monoclonal anti-ß-catenin (1:500). p38 was used as a loading control. Densitometric values represent the expression of each protein band quantified using Image J imaging software and normalized to p38 protein levels.

A

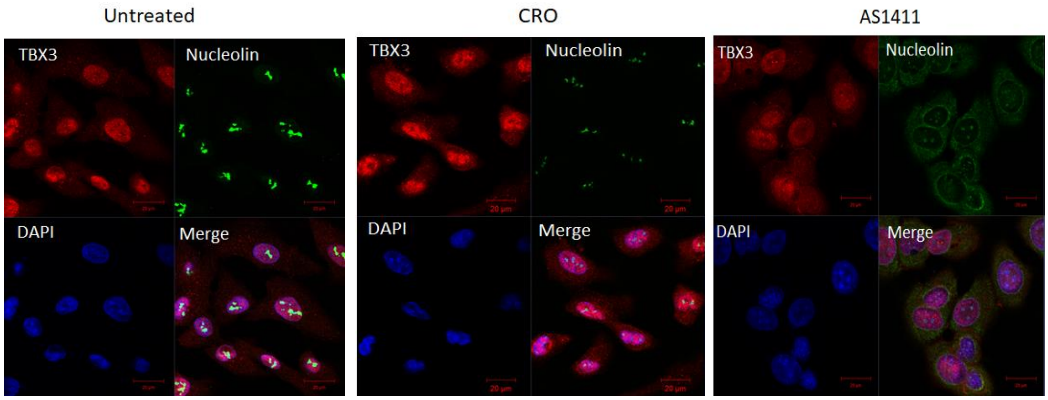

Immunocytochemistry

B

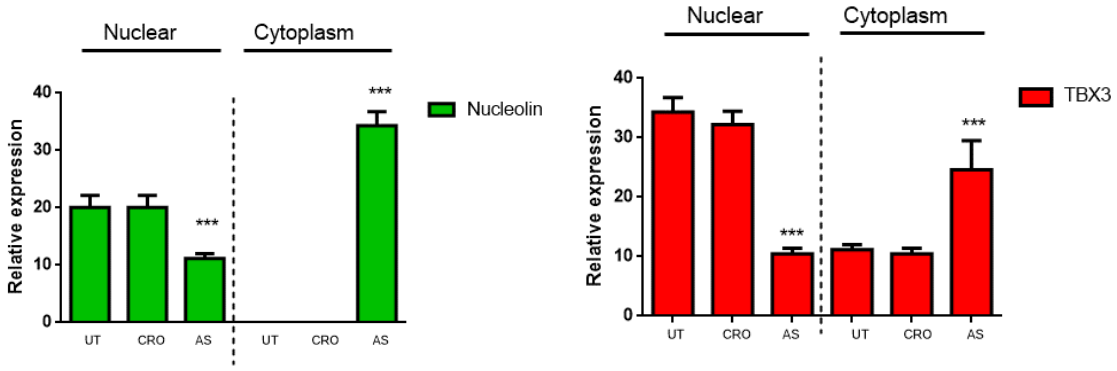

C

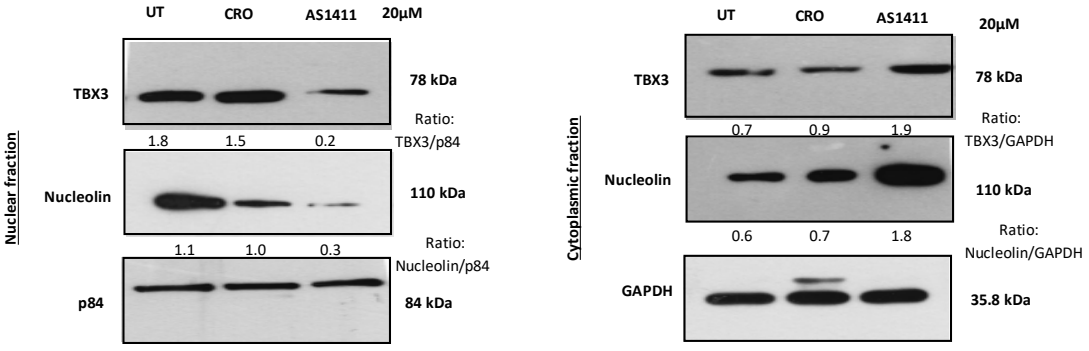

Subcellular fractionation

Figure 3.22. AS1411 mislocalises TBX3 and nucleolin to the cytoplasm. (A) MCF-7 cells were plated at a density of 0.25 X 10^5 cells/ml on glass coverslips in 35 mm dishes and immediately treated with 10 μM AS1411 or CRO and 48 hours later were processed for immunofluorescence with antibodies specific to TBX3 (Cy3; red channel) and nucleolin (Alexa 488; green channel) and visualized by confocal microscopy. Representative images are shown at 400X magnification. All cells were co-stained with DAPI to determine the location of the nuclei. **(B)** Images were analysed by Zeiss software where the signal intensity of each channel was quantified in the nucleus and cytoplasm. Data is represented as ± SEM of 20 fields of view. **(C)** MCF-7 cells were plated at a density of 5 X 10^5 cells/ml in 10 cm dishes and immediately treated with 10 μM AS1411 or CRO for 48 hours. Nuclear and cytoplasmic proteins were separated and subjected to western blot analysis using primary antibodies to rabbit polyclonal anti-TBX3 (1:1000), mouse polyclonal anti-nucleolin (1:1000), mouse monoclonal anti-GAPDH (1: 1000) and mouse monoclonal anti-p84 (1:1000). Densitometric values represent the expression of each protein band quantified using Image J imaging software and normalized to GAPDH (cytoplasmic fraction marker) and p84 (nuclear fraction marker) protein levels.

CHAPTER 4

Discussion and conclusion

Breast cancer is the second most common cancer in the world and the leading cause of cancer mortality in women (Cheng *et al*.,1998; Ferlay *et al*., 2012). Due to a number of factors including drug resistance and poor therapy response, this cancer remains a global burden. This has therefore necessitated a deeper understanding of the molecular mechanisms underpinning this disease in order to design more effective treatment modalities. The T-box transcription factor, TBX3, has been identified as an attractive therapeutic target to treat breast cancer. It is overexpressed in breast cancer where it plays an important role in several aspects of the cancer process. Transcription factors are however notoriously challenging to target and therefore more effective treatment options may be through interfering with (1) signalling molecules responsible for upregulating TBX3, (2) protein co-factors that bind to TBX3 to stabilize the protein and (3) protein co-factors that co-operate with TBX3 to drive its oncogenic activity in breast cancer cells. The current study addresses this in the MCF-7 breast cancer cells and provides novel evidence that (1) TBX3 is transcriptionally upregulated by c-Myc; (2) TBX3 interacts with heat shock cognate protein (Hsc70) which results in an increase in its protein stability and (3) nucleolin is a bona fide TBX3 co-factor that co-operates with TBX3 to promote breast cancer cell migration.

The transcriptional upregulation of TBX3 by c-Myc in MCF-7 breast cancer cells

Although TBX3 is upregulated in a number of cancers including a subset of breast cancer, very little is known about the signalling molecules upstream of TBX3. Indeed, to date only the TGFβ and FGF pathways have been demonstrated to upregulate TBX3 in breast cancer and breast cancer stem cells respectively (Li *et al.*, 2013; Fillmore et al., 2010). It is anticipated that other oncogenic signalling factors will also be involved, and this study speculated that the basic helix-loop-helix oncogenic transcription factor c-Myc may be

one such factor. The rationale for this was that similar to TBX3, c-Myc is overexpressed in some breast cancer subtypes and the Prince laboratory has previously shown that it directly binds and activates the TBX3 promoter in a number of sarcoma subtypes (Barrios et al.,1994; Barrios et al., 1993; Castresana et al., 1992; Demir et al., 2014; Sollazzo et al., 1999; Fallah et al., 2017; Willmer *et al.*, 2015 and unpublished data). Indeed, using qRT-PCR and western blotting this study shows that when c-Myc was effectively knocked down by two different siRNAs there was a corresponding decrease in TBX3 mRNA and protein levels, suggesting that c-Myc acts upstream of TBX3. Moreover, when de novo transcription was inhibited in cells in which c-Myc was overexpressed, the c-Myc mediated activation of TBX3 mRNA was significantly abolished. This shows that c-Myc directly activates TBX3 transcriptionally in MCF-7 breast cancer cells. This is an important finding as it provides insight to the mechanism of upregulation of TBX3 in breast cancer. Moreover, while there is a wealth of information on the role of c-Myc in cellular transformation, only a few target genes that mediate its oncogenic functions have been validated to date. Thus, this study adds to our understanding of the molecular mechanism by which c-Myc contributes to breast cancer.

Identification and characterisation of TBX3 co-factors that mediate its oncogenic activity in breast cancer

TBX3 has many diverse roles in cancer but the molecular mechanisms underpinning these remain largely unknown. There is however general consensus in the T-box field that these functions are regulated by protein co-factor interactions. To date, very few TBX3 co-factors have however been identified. This study therefore performed liquid chromatography coupled with mass spectrometry analyses (LC-MS/MS) to identify TBX3 interaction partners that may mediate its oncogenic roles in MCF-7 breast cancer cells. A total of 47 candidate interaction partners were identified and three proteins with previously established oncogenic roles were validated as *bona fide* TBX3 co-factors, namely Hsc70, HnRNP K and nucleolin.

Hsc70 was of particular interest to this study because it has been speculated to contribute to proliferation, drug resistance and metastasis in part, through its ability to facilitate the accumulation and aggregation of mutated and incorrectly folded oncoproteins (Luo et al., 2009). Moreover, studies in the Prince laboratory have validated Hsc70 as a *bona fide*

TBX3 co-factor in chondrosarcoma, rhabdomyosarcoma and liposarcoma cells (unpublished data). This study was therefore interested to determine if Hsc70 also interacts with TBX3 in MCF-7 breast cancer cells. Indeed, using immunoprecipitation assays and co-localisation experiments, this study shows that Hsc70 interacts and colocalizes with endogenous TBX3. Moreover, this study shows that TBX3 requires Hsc70 for its protein stability. This is consistent with findings from previous studies that have reported the function of Hsc70 in oncogenesis to be to bind and stabilize oncoproteins and thus sustain abundant levels of the protein thereby permitting cellular transformation (Finlay *et al.*, 1989; Calderwood et al., 2006; Shiota *et al.*, 2009; Koren *et al.*, 2009; Ding *et al.*, 2012; Tanaka *et al.*, 2014; Prince laboratory, unpublished data). It is therefore tempting to speculate that in MCF-7 breast cancer cells, TBX3 it is especially dependent on Hsc70 for optimal protein folding to prevent its degradation, thus promoting cellular transformation and cancer progression. Moreover, it is possible that after TBX3 is transcriptionally activated by c-Myc, Hsc70 assists in TBX3 protein folding and stability. This provides an interesting mechanism by which TBX3 levels are elevated in breast cancer cells.

This study also identified HnRNP K as a direct binding partner of TBX3 through immunoprecipitation and co-localisation analyses. This is consistent with previous data that also identified HnRNP K as a TBX3 interaction partner during development and in chondrosarcoma (Kumar et al., 2014; Uribe et al., 2011; Prince laboratory, unpublished data). Importantly, HnRNP K has also been identified as a nucleolin co-factor and it has overlapping oncogenic roles with TBX3 and nucleolin such as promotion of proliferation and migration (Inoue et al., 2007; Lynch et al., 2005). Moreover, since HnRNP K has been shown to promote the expression of certain oncogenes through promoter binding and recruitment of transcription machinery, it was speculated that it may regulate TBX3 in this manner (Bomsztyk et al., 2004). Due to time constraints, the functional consequences of the interaction between TBX3 and HnRNP K in MCF-7 breast cancer cells could not be determined. In future, this could be investigated through the following experiments: (1) qRT-PCR, western blotting and luciferase reporter assays to determine whether like TBX3, HnRNP K can also upregulate the mesenchymal markers N-cadherin, vimentin and β-catenin to promote migration, (2) luciferase reporter assays to determine whether TBX3 and HnRNP K synergistically repress the N-cadherin, vimentin and β-catenin

promoters, (3) ChIP assays to determine whether TBX3 and HnRNP K occupy the N-cadherin, vimentin and β-catenin promoters and (4) knockdown and overexpression experiments to determine whether TBX3 and HnRNP K cooperate to promote migration. It would also be interesting to determine whether HnRNP K forms part of the TBX3/nucleolin complex to promote migration.

This study uses immunoprecipitation assays and confocal immunofluorescence microscopy to validate nucleolin as a direct binding partner of TBX3 in MCF-7 breast cancer cells. The rationale for investigating this interaction was two-fold. Firstly, a spate of therapies aimed at targeting nucleolin have proven successful in multiple cancer types including leukaemia and lymphoma (Huang et al., 2006; Watanabe et al., 2010; Krust et al., 2011; Mosafer et al., 2018). Secondly, nucleolin has overlapping oncogenic roles with TBX3 such as promoting migration and there is evidence that like TBX3 it is also upregulated by c-Myc suggesting that c-Myc/TBX3/nucleolin may form an important signalling axis in breast cancer (Greasley et al., 2000; Bhatt et al., 2012; Takagi et al., 2005; Wu et al., 2014). This study hypothesised that nucleolin and TBX3 may co-operate to promote migration of MCF-7 breast cancer cells. Indeed, knocking down nucleolin in TBX3 overexpressing cells abrogated the ability of TBX3 to promote migration and overexpressing nucleolin in TBX3 knockdown cells could not rescue the effect of knocking down TBX3 on migration. This data revealed that nucleolin and TBX3 require each other to promote migration. In addition to this, this study showed that c-Myc also transcriptionally upregulates nucleolin expression in MCF-7 breast cancer cells. This is a critical finding as it suggests that c-Myc, TBX3 and nucleolin may indeed form an important signalling axis in breast cancer. Moreover, this study showed that the overexpression of TBX3 correlated with increased expression of the mesenchymal markers N-cadherin, vimentin and β-catenin and it would be interesting to know whether c-Myc, nucleolin and TBX3 cooperate to promote this upregulation. Furthermore, it would be interesting to determine whether TBX3, nucleolin and HnRNP K together cooperate to promote migration through regulation of common downstream target genes. For example, since nucleolin has been shown to regulate multiple genes involved in tumorigenesis including *gastrin, AKT1, CCN1* (*cyclin I*) and *Sp1* by binding their mRNAs and either enhancing their translation or protein stability this begs the question as to whether TBX3 and HnRNP K also impact on the regulation of these mRNAs and whether

they cooperate with nucleolin to post-transcriptionally regulate these genes (Abdelmohsen et al., 2011; Hers et al., 2011; Hung et al., 2014; Lee et al., 2007).

The well-investigated nucleolin aptamer, AS1411, a quadruplex-forming DNA strand that specifically binds to the cell surface nucleolin receptor, has sparked great interest as it has been shown to exhibit anti-cancer activities in a number of cancers. The 28 base pair guanine-rich oligonucleotide has shown anti-proliferative activity in a number of cancer cell types tested and is currently in phase I clinical trials for advanced solid tumours and phase II clinical trials for acute myeloid leukaemia and renal cell carcinoma (CREATE, NCT00881244, NCT00512083, NCT00740441) (Bates et al., 2009). Important to this study, AS1411 disrupts nucleolin protein-protein interactions and consequently their oncogenic functions (Teng et al., 2007; Schokoroy et al., 2013; Prince laboratory, unpublished data). This raised the exciting possibility that disrupting the TBX3-nucleolin interaction with this aptamer could potentially lead to a possible treatment strategy for TBX3 driven cancers such as breast cancer. This study confirmed that AS1411 inhibits cell viability of MCF-7 breast cancer cells while having no effect on primary skin fibroblasts. Moreover, migration assays and western blot analysis revealed that AS1411 inhibits the migratory ability of MCF-7 cells through decreased expression of the mesenchymal markers, N-cadherin, vimentin and β-catenin and increased expression of E-cadherin. Interestingly, following AS1411 treatment, western blotting and immunocytochemistry revealed that while nuclear levels of TBX3 and nucleolin decrease, cytoplasmic levels of these proteins increase. This is consistent with a previous study that showed that AS1411 treatment disrupted the interaction of nucleolin with its binding partner PRMT5 and led to the mislocalisation of PRMT5 to the cytoplasm (Teng et al., 2007). These findings are important as they suggest that AS1411 disrupts the TBX3-nucleolin interaction and consequently their oncogenic functions and hence it holds promise in the treatment of TBX3 driven cancers. Moreover, this provides a mechanistic insight of the mode of action of AS1411 in cancer cells. In future, it would be interesting to identify and characterize the domains of the TBX3 and nucleolin proteins required for their interaction as this could reveal additional ways of disrupting the oncogenic functions of TBX3 and nucleolin. This can be done using GST-pull-down experiments. Preliminary unpublished studies in the Prince laboratory have shown that in chondrosarcoma, AS1411 disrupts the TBX3-nucleolin interaction which prevents them

from regulating their downstream targets. It would therefore be interesting to determine if the same is true in breast cancer.

It is important to note that while the experiments in the current study were carried out in a single breast cancer cell line, this project forms part of a larger study in the Prince laboratory and future investigations will include additional breast cancer cell lines as well as patient tumour tissues.

Concluding remarks

Based on the results generated in this study and the current literature the following model is proposed for the c-Myc/TBX3/Nucleolin/Hsc70 signalling axis in MCF-7 breast cancer cells (see **Figure 4**). Briefly, c-Myc transcriptionally upregulates both TBX3 and nucleolin. Interaction with Hsc70 leads to correct protein folding and further stabilization of the TBX3 and nucleolin proteins and facilitate their translocation into the nucleus. When it reaches the nucleus, TBX3 then interacts and cooperates with nucleolin and HnRNP K to retain its nuclear localisation and to regulate target genes that encode EMT markers, thereby promoting migration in MCF-7 breast cancer cells.

In conclusion, this study shows that the c-Myc/TBX3/Nucleolin/Hsc70 interaction forms an important signalling axis in breast cancer and disrupting this signalling axis presents a potentially viable treatment strategy for breast cancer.

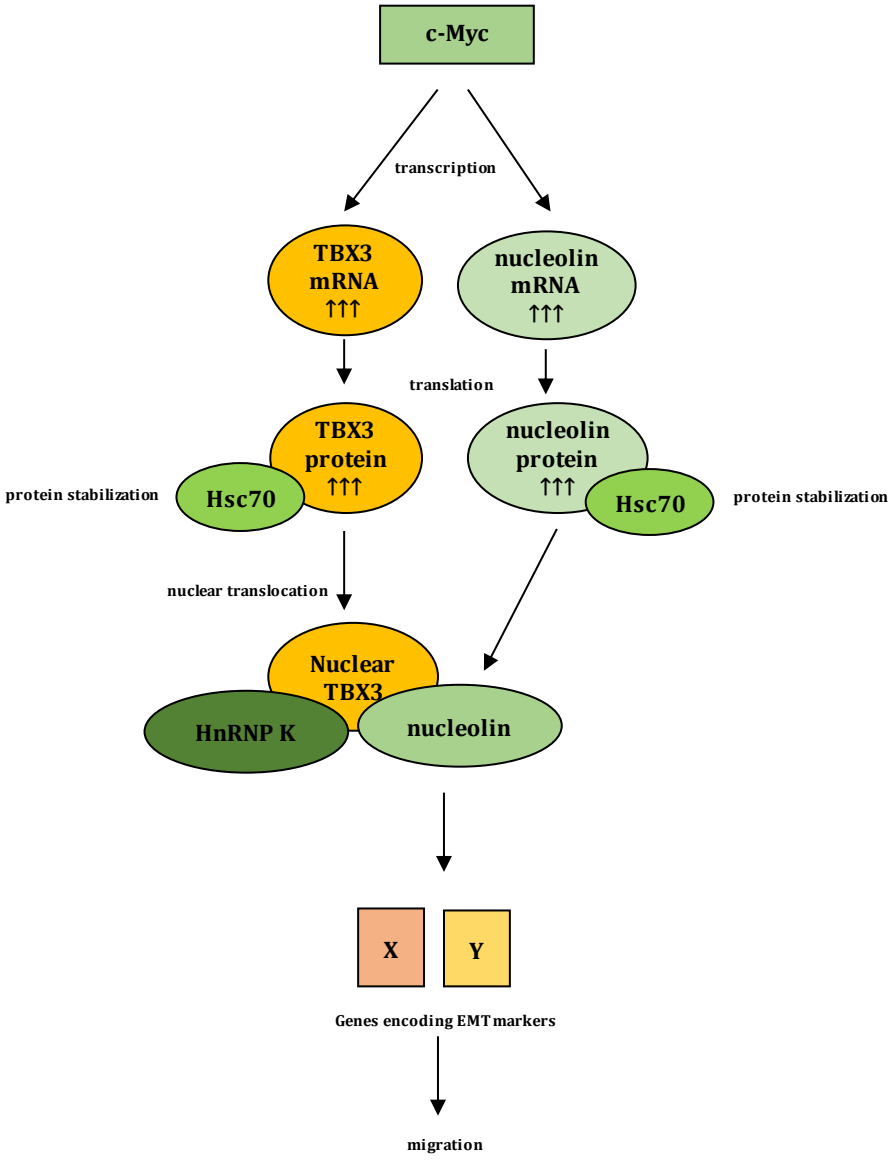

Figure 4 Proposed model for the c-Myc/TBX3/Nucleolin/Hsc70 signalling axis in MCF-7 breast cancer cells

CHAPTER 5

References

Agulnik, S. I., Garvey, N., Hancock, S., Ruvinsky, I., Chapman, D. L., Agulnik, I., Bollag, R., Papaioannou, V. and Silver, L. M. (1996) 'Evolution of mouse T-box genes by tandem duplication and cluster dispersion', *Genetics*, 144(1), pp. 249–254. Available at: https://www.ncbi.nlm.nih.gov/pubmed/8878690.

Andreou, A. M., Pauws, E., Jones, M. C., Singh, M. K., Bussen, M., Doudney, K., Moore, G. E., Kispert, A., Brosens, J. J. and Stanier, P. (2007) 'TBX22 missense mutations found in patients with X-linked cleft palate affect DNA binding, sumoylation, and transcriptional repression.', *American journal of human genetics*. United States, 81(4), pp. 700–712. doi: 10.1086/521033.

Arendt, L. M., St Laurent, J., Wronski, A., Caballero, S., Lyle, S. R., Naber, S. P. and Kuperwasser, C. (2014) 'Human breast progenitor cell numbers are regulated by WNT and TBX3.', *PloS one*. United States, 9(10), p. e111442. doi: 10.1371/journal.pone.0111442.

Ataliotis, P., Ivins, S., Mohun, T. J. and Scambler, P. J. (2005) 'XTbx1 Is a Transcriptional Activator Involved in Head and Pharyngeal Arch Development in Xenopus laevis', (February), pp. 979–991. doi: 10.1002/dvdy.20276.

Atreya, I., Schimanski, C. C., Becker, C., Wirtz, S., Dornhoff, H., Schnurer, E., Berger, M. R., Galle, P. R., Herr, W. and Neurath, M. F. (2007) 'The T-box transcription factor eomesodermin controls CD8 T cell activity and lymph node metastasis in human colorectal cancer.', *Gut*. England, 56(11), pp. 1572–1578. doi: 10.1136/gut.2006.117812.

Bakker, M. L., Boukens, B. J., Mommersteeg, M. T. M., Brons, J. F., Wakker, V., Moorman, A. F. M. and Christoffels, V. M. (2008) 'Transcription Factor Tbx3 Is Required for the Specification of the Atrioventricular Conduction System', pp. 1340–1349. doi: 10.1161/CIRCRESAHA.107.169565.

Ballif, B. C., Theisen, A., Rosenfeld, J. A., Traylor, R. N., Gastier-Foster, J., Thrush, D. L., Astbury, C., Bartholomew, D., McBride, K. L., Pyatt, R. E., Shane, K., Smith, W. E., Banks, V., Gallentine, W. B., Brock, P., Rudd, M. K., Adam, M. P., Keene, J. A., Phillips, J. A. 3rd, Pfotenhauer, J. P., Gowans, G. C., Stankiewicz, P., Bejjani, B. A. and Shaffer, L. G. (2010) 'Identification of a recurrent microdeletion at 17q23.1q23.2 flanked by segmental duplications associated with heart defects and limb abnormalities.', *American journal of human genetics*. United States, 86(3), pp. 454–461. doi: 10.1016/j.ajhg.2010.01.038.

Benson, J. R. (2003) 'The TNM staging system and breast cancer', *The Lancet Oncology*, 4(January), pp. 56–60. doi: 10.1016/S1470-2045(03)00961-6.

Benz, C. C., Scott, G. K., Sarup, J. C., Johnson, R. M., Tripathy, D., Coronado, E., Shepard, H. M. and Osborne, C. K. (1992) 'Estrogen-dependent, tamoxifen-resistant tumorigenic growth of MCF-7 cells transfected with HER2/neu.', *Breast cancer research and treatment*. Netherlands, 24(2), pp. 85–95.

Bollag, R. J., Siegfried, Z., Cebra-Thomas, J. A., Garvey, N., Davison, E. M. and Silver, L. M. (1994) 'An ancient family of embryonically expressed mouse genes sharing a conserved protein motif with the T locus.', *Nature g*Agulnik, S. I., Garvey, N., Hancock, S., Ruvinsky, I., Chapman, D. L., Agulnik, I., Bollag, R., Papaioannou, V. and Silver, L. M. (1996) 'Evolution of mouse T-box genes

by tandem duplication and cluster dispersion', *Genetics*, 144(1), pp. 249–254. Available at: https://www.ncbi.nlm.nih.gov/pubmed/8878690.

Bakker, M. L., Boukens, B. J., Mommersteeg, M. T. M., Brons, J. F., Wakker, V., Moorman, A. F. M. and Christoffels, V. M. (2008) 'Transcription Factor Tbx3 Is Required for the Specification of the Atrioventricular Conduction System', pp. 1340–1349. doi: 10.1161/CIRCRESAHA.107.169565.

Ballif, B. C., Theisen, A., Rosenfeld, J. A., Traylor, R. N., Gastier-Foster, J., Thrush, D. L., Astbury, C., Bartholomew, D., McBride, K. L., Pyatt, R. E., Shane, K., Smith, W. E., Banks, V., Gallentine, W. B., Brock, P., Rudd, M. K., Adam, M. P., Keene, J. A., Phillips, J. A. 3rd, Pfotenhauer, J. P., Gowans, G. C., Stankiewicz, P., Bejjani, B. A. and Shaffer, L. G. (2010) 'Identification of a recurrent microdeletion at 17q23.1q23.2 flanked by segmental duplications associated with heart defects and limb abnormalities.', *American journal of human genetics*. United States, 86(3), pp. 454–461. doi: 10.1016/j.ajhg.2010.01.038.

Bamshad, M., Le, T., Watkins, W. S., Dixon, M. E., Kramer, B. E., Roeder, A. D., Carey, J. C., Root, S., Schinzel, A., Van Maldergem, L., Gardner, R. J., Lin, R. C., Seidman, C. E., Seidman, J. G., Wallerstein, R., Moran, E., Sutphen, R., Campbell, C. E. and Jorde, L. B. (1999) 'The spectrum of mutations in TBX3: Genotype/Phenotype relationship in ulnar-mammary syndrome', *American journal of human genetics*, 64(6), pp. 1550–1562. doi: 10.1086/302417.

Bamshad, M., Lin, R. C., Law, D. J., Watkins, W. C., Krakowiak, P. A., Moore, M. E., Franceschini, P., Lala, R., Holmes, L. B., Gebuhr, T. C., Bruneau, B. G., Schinzel, A., Seidman, J. G., Seidman, C. E. and Jorde, L. B. (1997) 'Mutations in human TBX3 alter limb, apocrine and genital development in ulnar-mammary syndrome.', *Nature genetics*. United States, 16(3), pp. 311–315. doi: 10.1038/ng0797-311.

Benson, J. R. (2003) 'The TNM staging system and breast cancer', *The Lancet Oncology*, 4(January), pp. 56–60. doi: 10.1016/S1470-2045(03)00961-6.

Benz, C. C., Scott, G. K., Sarup, J. C., Johnson, R. M., Tripathy, D., Coronado, E., Shepard, H. M. and Osborne, C. K. (1992) 'Estrogen-dependent, tamoxifen-resistant tumorigenic growth of MCF-7 cells transfected with HER2/neu.', *Breast cancer research and treatment*. Netherlands, 24(2), pp. 85–95.

Bollag, R. J., Siegfried, Z., Cebra-Thomas, J. A., Garvey, N., Davison, E. M. and Silver, L. M. (1994) 'An ancient family of embryonically expressed mouse genes sharing a conserved protein motif with the T locus.', *Nature genetics*. United States, 7(3), pp. 383–389. doi: 10.1038/ng0794-383.

Bongers, E. M. H. F., Duijf, P. H. G., van Beersum, S. E. M., Schoots, J., Van Kampen, A., Burckhardt, A., Hamel, B. C. J., Losan, F., Hoefsloot, L. H., Yntema, H. G., Knoers, N. V. A. M. and van Bokhoven, H. (2004) 'Mutations in the human TBX4 gene cause small patella syndrome.', *American journal of human genetics*. United States, 74(6), pp. 1239–1248. doi: 10.1086/421331.

Boogerd, C. J. J., Wong, L. Y. E., van den Boogaard, M., Bakker, M. L., Tessadori, F., Bakkers, J., 't Hoen, P. A. C., Moorman, A. F., Christoffels, V. M. and Barnett, P. (2011) 'Sox4 mediates Tbx3 transcriptional regulation of the gap junction protein Cx43.', *Cellular and molecular life sciences : CMLS*. Switzerland, 68(23), pp. 3949–3961. doi: 10.1007/s00018-011-0693-7.

Bray, F., Ferlay, J. and Soerjomataram, I. (2018) 'Global Cancer Statistics 2018 : GLOBOCAN Estimates of Incidence and Mortality Worldwide for 36 Cancers in 185 Countries', pp. 394–424. doi: 10.3322/caac.21492.

Braybrook, C., Doudney, K., Marcano, A. C., Arnason, A., Bjornsson, A., Patton, M. A., Goodfellow,

P. J., Moore, G. E. and Stanier, P. (2001) 'The T-box transcription factor gene TBX22 is mutated in X-linked cleft palate and ankyloglossia.', *Nature genetics*. United States, 29(2), pp. 179–183. doi: 10.1038/ng730.

Britten, C. D., Finn, R. S., Bosserman, L. D., Wong, S. G., Press, M. F., Malik, M., Lum, B. L. and Slamon, D. J. (2009) 'A phase I/II trial of trastuzumab plus erlotinib in metastatic HER2-positive breast cancer: a dual ErbB targeted approach.', *Clinical breast cancer*. United States, 9(1), pp. 16–22. doi: 10.3816/CBC.2009.n.003.

Brummelkamp, T. R., Kortlever, R. M., Lingbeek, M., Trettel, F., MacDonald, M. E., van Lohuizen, M. and Bernards, R. (2002) 'TBX-3, the gene mutated in Ulnar-Mammary Syndrome, is a negative regulator of p19ARF and inhibits senescence.', *The Journal of biological chemistry*. United States, 277(8), pp. 6567–6572. doi: 10.1074/jbc.M110492200.

Burgucu, D., Guney, K., Sahinturk, D., Ozbudak, I. H., Ozel, D., Ozbilim, G. and Yavuzer, U. (2012) 'Tbx3 represses PTEN and is over-expressed in head and neck squamous cell carcinoma.', *BMC cancer*. England, 12, p. 481. doi: 10.1186/1471-2407-12-481.

Burness, M. L., Grushko, T. A. and Olopade, O. I. (2010) 'Epidermal Growth Factor Receptor in Triple-Negative and Basal-Like Breast Cancer: Promising Clinical Target or Only a Marker?', *The Cancer Journal*, 16(1). Available at: https://journals.lww.com/journalppo/Fulltext/2010/02000/Epidermal_Growth_Factor_Receptor_in.5.aspx.

Campisi, J. (2013) 'Aging, cellular senescence, and cancer.', *Annual review of physiology*. United States, 75, pp. 685–705. doi: 10.1146/annurev-physiol-030212-183653.

Carlson, H., Ota, S., Campbell, C. E. and Hurlin, P. J. (2001) 'A dominant repression domain in Tbx3 mediates transcriptional repression and cell immortalization: relevance to mutations in Tbx3 that cause ulnar-mammary syndrome', *Human Molecular Genetics*, 10(21), pp. 2403–2413. Available at: http://dx.doi.org/10.1093/hmg/10.21.2403.

Carreira, S., Dexter, T. J., Yavuzer, U., Easty, D. J. and Goding, C. R. (1998) 'Brachyury-related transcription factor Tbx2 and repression of the melanocyte-specific TRP-1 promoter', *Molecular and cellular biology*. American Society for Microbiology, 18(9), pp. 5099–5108. Available at: https://www.ncbi.nlm.nih.gov/pubmed/9710594.

Casey, E. S., O'Reilly, M. A., Conlon, F. L. and Smith, J. C. (1998) 'The T-box transcription factor Brachyury regulates expression of eFGF through binding to a non-palindromic response element.', *Development (Cambridge, England)*. England, 125(19), pp. 3887–3894.

Casey, E. S., Reilly, M. J. O., Conlon, F. L. and Smith, J. C. (1998) 'The T-box transcription factor Brachyury regulates expression of eFGF through binding to a non-palindromic response element The T-box transcription factor Brachyury regulates expression of eFGF through binding to a non-palindromic response element', (November).

Cheng, H. D., Lui, Y. M. and Freimanis, R. I. (1998) 'A novel approach to microcalcification detection using fuzzy logic technique.', *IEEE transactions on medical imaging*, 17(3), pp. 442–450. doi: 10.1109/42.712133.

Coll, M., Seidman, J. G. and Muller, C. W. (2002) 'Structure of the DNA-bound T-box domain of human TBX3, a transcription factor responsible for ulnar-mammary syndrome.', *Structure (London, England : 1993)*. United States, 10(3), pp. 343–356.

Du, H. F., Ou, L. P., Yang, X., Song, X. D., Fan, Y. R., Tan, B., Luo, C. L. and Wu, X. H. (2014) 'A new PKCalpha/beta/TBX3/E-cadherin pathway is involved in PLCepsilon-regulated invasion and migration in human bladder cancer cells.', *Cellular signalling*. England, 26(3), pp. 580–593. doi: 10.1016/j.cellsig.2013.11.015.

Du, W.-L., Fang, Q., Chen, Y., Teng, J.-W., Xiao, Y.-S., Xie, P., Jin, B. and Wang, J.-Q. (2017) 'Effect of silencing the T-Box transcription factor TBX2 in prostate cancer PC3 and LNCaP cells', *Molecular medicine reports*. 2017/08/24. D.A. Spandidos, 16(5), pp. 6050–6058. doi: 10.3892/mmr.2017.7361.

Duo, S., Tiao-Dong, T., Lei, Z., Wei, W., Hong-Li, S. and Xian-Wei, D. (2009) 'Expression and clinical significance of tbx2 in pancreatic cancer.', *Asian Pacific journal of cancer prevention : APJCP*. Thailand, 10(1), pp. 118–122.

English, D. P., Roque, D. M. and Santin, A. D. (2014) 'NIH Public Access', 17(2), pp. 85–99. doi: 10.1007/s40291-013-0024-9.HER2.

Fan, W., Huang, X., Chen, C., Gray, J. and Huang, T. (2004a) 'TBX3 and Its Isoform TBX3+2a Are Functionally Distinctive in Inhibition of Senescence and Are Overexpressed in a Subset of Breast Cancer Cell Lines', *Cancer Research*, 64(15), p. 5132 LP-5139. Available at: http://cancerres.aacrjournals.org/content/64/15/5132.abstract.

Fan, W., Huang, X., Chen, C., Gray, J. and Huang, T. (2004b) 'TBX3 and its isoform TBX3+2a are functionally distinctive in inhibition of senescence and are overexpressed in a subset of breast cancer cell lines.', *Cancer research*. United States, 64(15), pp. 5132–5139. doi: 10.1158/0008-5472.CAN-04-0615.

Farin, H. F., Lüdtke, T. H.-W., Schmidt, M. K., Placzko, S., Schuster-Gossler, K., Petry, M., Christoffels, V. M. and Kispert, A. (2013) 'Tbx2 Terminates Shh/Fgf Signaling in the Developing Mouse Limb Bud by Direct Repression of Gremlin1', *PLOS Genetics*. Public Library of Science, 9(4), p. e1003467. Available at: https://doi.org/10.1371/journal.pgen.1003467.

Feldman, A. M., Lorell, B. H. and Reis, S. E. (2000) 'Trastuzumab in the treatment of metastatic breast cancer : anticancer therapy versus cardiotoxicity.', *Circulation*. United States, 102(3), pp. 272–274.

Ferlay, J., Soerjomataram, I., Dikshit, R., Eser, S., Mathers, C., Rebelo, M., Parkin, D. M., Forman, D. and Bray, F. (2015) 'Cancer incidence and mortality worldwide : Sources , methods and major patterns in GLOBOCAN 2012', 386. doi: 10.1002/ijc.29210.

Ferlay, J., Soerjomataram I, I., Dikshit, R., Eser, S., Mathers, C., Rebelo, M., Parkin, D. M., Forman D, D. and Bray, F. (2014) 'Cancer incidence and mortality worldwide: sources, methods and major patterns in GLOBOCAN 2012.', *Int J Cancer*, 136, pp. E359-86. doi: 10.1002/ijc.29210.

Fernando, R. I., Litzinger, M., Trono, P., Hamilton, D. H., Schlom, J. and Palena, C. (2010) 'The T-box transcription factor Brachyury promotes epithelial-mesenchymal transition in human tumor cells.', *The Journal of clinical investigation*. United States, 120(2), pp. 533–544. doi: 10.1172/JCI38379.

Fillmore, C. M., Gupta, P. B., Rudnick, J. A., Caballero, S., Keller, P. J., Lander, E. S. and Kuperwasser, C. (2010) 'Estrogen expands breast cancer stem-like cells through paracrine FGF/Tbx3 signaling.', *Proceedings of the National Academy of Sciences of the United States of America*.

United States, 107(50), pp. 21737–21742. doi: 10.1073/pnas.1007863107.

Fischer, K. and Pflugfelder, G. O. (2015) 'Putative Breast Cancer Driver Mutations in TBX3 Cause Impaired Transcriptional Repression', *Frontiers in oncology*. Frontiers Media S.A., 5, p. 244. doi: 10.3389/fonc.2015.00244.

Frank, D. U., Emechebe, U., Thomas, K. R. and Moon, A. M. (2013) 'Mouse TBX3 mutants suggest novel molecular mechanisms for Ulnar-mammary syndrome.', *PloS one*. United States, 8(7), p. e67841. doi: 10.1371/journal.pone.0067841.

Garland, L. L., Hidalgo, M., Mendelson, D. S., Ryan, D. P., Arun, B. K., Lovalvo, J. L., Eiseman, I. A., Olson, S. C., Lenehan, P. F. and Eder, J. P. (2006) 'A phase I clinical and pharmacokinetic study of oral CI-1033 in combination with docetaxel in patients with advanced solid tumors.', *Clinical cancer research : an official journal of the American Association for Cancer Research*. United States, 12(14 Pt 1), pp. 4274–4282. doi: 10.1158/1078-0432.CCR-05-2507.

Giuliano, A. E., Connolly, J. L., Edge, S. B. and Mittendorf, E. A. (2017) 'Take free quizzes online at acsjournals . com / ce Breast Cancer — Major Changes in the American Joint Committee on Cancer Eighth Edition Cancer Staging Manual', 67(4). doi: 10.3322/caac.21393.

Gluz, O., Liedtke, C., Gottschalk, N., Pusztai, L., Nitz, U. and Harbeck, N. (2009) 'Triple-negative breast cancer--current status and future directions', *Annals of Oncology*, 20(November), pp. 1913–1927. doi: 10.1093/annonc/mdp492.

Goldenberg, M. M. (1999) 'Trastuzumab, a recombinant DNA-derived humanized monoclonal antibody, a novel agent for the treatment of metastatic breast cancer.', *Clinical therapeutics*. United States, 21(2), pp. 309–318. doi: 10.1016/S0149-2918(00)88288-0.

González, A., Manosalva, I., Liu, T. and Kageyama, R. (2013) 'Control of Hes7 Expression by Tbx6, the Wnt Pathway and the Chemical Gsk3 Inhibitor LiCl in the Mouse Segmentation Clock', *PLOS ONE*. Public Library of Science, 8(1), p. e53323. Available at: https://doi.org/10.1371/journal.pone.0053323.

Gradishar, W. J., Anderson, B. O., Balassanian, R., Blair, S. L., Burstein, H. J., Cyr, A., Elias, A. D., Farrar, W. B., Forero, A., Giordano, S. H., Goetz, M., Goldstein, L. J., Hudis, C. A., Isakoff, S. J., Marcom, P. K., Mayer, I. A., Mccormick, B., Moran, M., Reed, E. C., Salerno, K. E., Schwartzberg, L. S., Smith, K. L., Smith, M. Lou, Soliman, H., Somlo, G., Telli, M., Ward, J. H., Shead, D. A. and Kumar, R. (2015) 'Breast Cancer Clinical Practice Guidelines in Oncology', 13(4), pp. 448–475.

Gray, R., Bhattacharya, S., Bowden, C., Miller, K. and Comis, R. L. (2009) 'Independent review of E2100: a phase III trial of bevacizumab plus paclitaxel versus paclitaxel in women with metastatic breast cancer.', *Journal of clinical oncology : official journal of the American Society of Clinical Oncology*. United States, 27(30), pp. 4966–4972. doi: 10.1200/JCO.2008.21.6630.

Greasley, P. J., Bonnard, C. and Amati, B. (2000) 'Myc induces the nucleolin and BN51 genes : possible implications in ribosome biogenesis', 28(2), pp. 446–453.

Green, M. D., Francis, P. A., Gebski, V., Harvey, V., Karapetis, C., Chan, A., Snyder, R., Fong, A., Basser, R., Forbes, J. F. and Group, on behalf of the A. N. Z. B. C. T. (2009) 'Gefitinib treatment in hormone-resistant and hormone receptor-negative advanced breast cancer', *Annals of Oncology*, 20(11), pp. 1813–1817. Available at: http://dx.doi.org/10.1093/annonc/mdp202.

Habets, P. E. M. H., Moorman, A. F. M., Clout, D. E. W., van Roon, M. A., Lingbeek, M., van Lohuizen, M., Campione, M. and Christoffels, V. M. (2002) 'Cooperative action of Tbx2 and Nkx2.5 inhibits

ANF expression in the atrioventricular canal: implications for cardiac chamber formation.', *Genes & development*. United States, 16(10), pp. 1234–1246. doi: 10.1101/gad.222902.

Hanahan, D. and Weinberg, R. A. (2011) 'Hallmarks of cancer: the next generation.', *Cell*. United States, 144(5), pp. 646–674. doi: 10.1016/j.cell.2011.02.013.

Hansel, D. E., Rahman, A., House, M., Ashfaq, R., Berg, K., Yeo, C. J. and Maitra, A. (2004) 'Met proto-oncogene and insulin-like growth factor binding protein 3 overexpression correlates with metastatic ability in well-differentiated pancreatic endocrine neoplasms.', *Clinical cancer research : an official journal of the American Association for Cancer Research*. United States, 10(18 Pt 1), pp. 6152–6158. doi: 10.1158/1078-0432.CCR-04-0285.

HAYFLICK, L. (1965) 'THE LIMITED IN VITRO LIFETIME OF HUMAN DIPLOID CELL STRAINS.', *Experimental cell research*. United States, 37, pp. 614–636.

He, M.-L., He, M.-L., Chen, Y., Peng, Y., Jin, D., Du, D., Wu, J., Lu, P., Lin, M. C. and Kung, H.-F. (2002) 'Induction of apoptosis and inhibition of cell growth by developmental regulator hTBX5', *Biochemical and biophysical research communications*, 297(2), p. 185—192. doi: 10.1016/s0006-291x(02)02142-3.

Herrmann, B. G., Labeit, S., Poustka, A., King, T. R. and Lehrach, H. (1990) 'Cloning of the T gene required in mesoderm formation in the mouse.', *Nature*. England, 343(6259), pp. 617–622. doi: 10.1038/343617a0.

Higgins, M. J. and Baselga, J. (2011) 'Review series Targeted therapies for breast cancer', 121(10). doi: 10.1172/JCI57152.with.

Hiroi, Y., Kudoh, S., Monzen, K., Ikeda, Y., Yazaki, Y., Nagai, R. and Komuro, I. (2001) 'Tbx5 associates with Nkx2-5 and synergistically promotes cardiomyocyte differentiation.', *Nature genetics*. United States, 28(3), pp. 276–280. doi: 10.1038/90123.

Holash, J., Davis, S., Papadopoulos, N., Croll, S. D., Ho, L., Russell, M., Boland, P., Leidich, R., Hylton, D., Burova, E., Ioffe, E., Huang, T., Radziejewski, C., Bailey, K., Fandl, J. P., Daly, T., Wiegand, S. J., Yancopoulos, G. D. and Rudge, J. S. (2002) 'VEGF-Trap: a VEGF blocker with potent antitumor effects.', *Proceedings of the National Academy of Sciences of the United States of America*. United States, 99(17), pp. 11393–11398. doi: 10.1073/pnas.172398299.

Hoogaars, W. M. H., Barnett, P., Rodriguez, M., Clout, D. E., Moorman, A. F. M., Goding, C. R. and Christoffels, V. M. (2008) 'TBX3 and its splice variant TBX3 + exon 2a are functionally similar', pp. 379–387. doi: 10.1111/j.1755-148X.2008.00461.x.

Hoogaars, W. M. H., Tessari, A., Moorman, A. F. M., de Boer, P. A. J., Hagoort, J., Soufan, A. T., Campione, M. and Christoffels, V. M. (2004) 'The transcriptional repressor Tbx3 delineates the developing central conduction system of the heart.', *Cardiovascular research*. England, 62(3), pp. 489–499. doi: 10.1016/j.cardiores.2004.01.030.

Hsueh, Y. P., Wang, T. F., Yang, F. C. and Sheng, M. (2000) 'Nuclear translocation and transcription regulation by the membrane-associated guanylate kinase CASK/LIN-2.', *Nature*. England, 404(6775), pp. 298–302. doi: 10.1038/35005118.

Huang, B., Cohen, J. R., Fernando, R. I., Hamilton, D. H., Litzinger, M. T., Hodge, J. W. and Palena, C. (2013) 'The embryonic transcription factor Brachyury blocks cell cycle progression and mediates tumor resistance to conventional antitumor therapies', *Cell death & disease*. Nature Publishing Group, 4(6), pp. e682–e682. doi: 10.1038/cddis.2013.208.

Humtsoe, J. O., Koya, E., Pham, E., Aramoto, T., Zuo, J., Ishikawa, T. and Kramer, R. H. (2012) 'Transcriptional profiling identifies upregulated genes following induction of epithelial-mesenchymal transition in squamous carcinoma cells.', *Experimental cell research*. United States, 318(4), pp. 379–390. doi: 10.1016/j.yexcr.2011.11.011.

Hurlin, P. J., Steingrìmsson, E., Copeland, N. G., Jenkins, N. A. and Eisenman, R. N. (1999) 'Mga, a dual-specificity transcription factor that interacts with Max and contains a T-domain DNA-binding motif', *The EMBO journal*, 18(24), pp. 7019–7028. doi: 10.1093/emboj/18.24.7019.

Iqbal, N. and Iqbal, N. (2014) 'Human Epidermal Growth Factor Receptor 2 (HER2) in Cancers : Overexpression and Therapeutic Implications', 2014.

Jacobs, J. J., Keblusek, P., Robanus-Maandag, E., Kristel, P., Lingbeek, M., Nederlof, P. M., van Welsem, T., van de Vijver, M. J., Koh, E. Y., Daley, G. Q. and van Lohuizen, M. (2000) 'Senescence bypass screen identifies TBX2, which represses Cdkn2a (p19(ARF)) and is amplified in a subset of human breast cancers.', *Nature genetics*. United States, 26(3), pp. 291–299. doi: 10.1038/81583.

Jerome, L. A. and Papaioannou, V. E. (2001) 'DiGeorge syndrome phenotype in mice mutant for the T-box gene, Tbx1.', *Nature genetics*. United States, 27(3), pp. 286–291. doi: 10.1038/85845.

Kawamura, A., Koshida, S. and Takada, S. (2008) 'Activator-to-Repressor Conversion of T-Box Transcription Factors by the Ripply Family of Groucho/TLE-Associated Mediators', *Molecular and Cellular Biology*, 28(10), p. 3236 LP-3244. doi: 10.1128/MCB.01754-07.

Khalil, A. A., Sivakumar, S., Lucas, F. A. S., McDowell, T., Lang, W., Tabata, K., Fujimoto, J., Yatabe, Y., Spira, A., Scheet, P., Nemer, G. and Kadara, H. (2017) 'TBX2 subfamily suppression in lung cancer pathogenesis: a high-potential marker for early detection', *Oncotarget*. Impact Journals LLC, 8(40), pp. 68230–68241. doi: 10.18632/oncotarget.19938.

Kispert, A. and Herrmann, B. G. (1993) 'The Brachyury gene encodes a novel DNA binding protein', *The EMBO journal*, 12(8), pp. 3211–3220. Available at: https://www.ncbi.nlm.nih.gov/pubmed/8344258.

Kispert, A., Koschorz, B. and Herrmann, B. G. (1995) 'The T protein encoded by Brachyury is a tissue-specific transcription factor.', *The EMBO journal*, 14(19), pp. 4763–72. Available at: http://www.ncbi.nlm.nih.gov/pubmed/7588606%5Cnhttp://www.pubmedcentral.nih.gov/articlerender.fcgi?artid=PMC394574.

Kispert, A., Ortner, H., Cooke, J. and Herrmann, B. G. (1995) 'The chick Brachyury gene: developmental expression pattern and response to axial induction by localized activin.', *Developmental biology*. United States, 168(2), pp. 406–415. doi: 10.1006/dbio.1995.1090.

Krstic, M., Macmillan, C. D., Leong, H. S., Clifford, A. G., Souter, L. H., Dales, D. W., Postenka, C. O., Chambers, A. F. and Tuck, A. B. (2016) 'The transcriptional regulator TBX3 promotes progression from non-invasive to invasive breast cancer', *BMC Cancer*, 16(1), p. 671. doi: 10.1186/s12885-016-2697-z.

Kuilman, T., Michaloglou, C., Mooi, W. J. and Peeper, D. S. (2010) 'The essence of senescence.', *Genes & development*. United States, 24(22), pp. 2463–2479. doi: 10.1101/gad.1971610.

Kumar P, P., Franklin, S., Emechebe, U., Hu, H., Moore, B., Lehman, C., Yandell, M. and Moon, A. M. (2014) 'TBX3 regulates splicing in vivo: a novel molecular mechanism for Ulnar-mammary syndrome.', *PLoS genetics*. United States, 10(3), p. e1004247. doi:

10.1371/journal.pgen.1004247.

Lamolet, B., Pulichino, A. M., Lamonerie, T., Gauthier, Y., Brue, T., Enjalbert, A. and Drouin, J. (2001) 'A pituitary cell-restricted T box factor, Tpit, activates POMC transcription in cooperation with Pitx homeoproteins.', *Cell*. United States, 104(6), pp. 849–859.

Li, J., Weinberg, M. S., Zerbini, L., Prince, S. and Bronner, M. (2013) 'The oncogenic TBX3 is a downstream target and mediator of the TGF- β 1 signaling pathway', 24, pp. 1–8. doi: 10.1091/mbc.E13-05-0273.

Li, Q. Y., Newbury-Ecob, R. A., Terrett, J. A., Wilson, D. I., Curtis, A. R., Yi, C. H., Gebuhr, T., Bullen, P. J., Robson, S. C., Strachan, T., Bonnet, D., Lyonnet, S., Young, I. D., Raeburn, J. A., Buckler, A. J., Law, D. J. and Brook, J. D. (1997) 'Holt-Oram syndrome is caused by mutations in TBX5, a member of the Brachyury (T) gene family.', *Nature genetics*. United States, 15(1), pp. 21–29. doi: 10.1038/ng0197-21.

Liao, J., Gallas, M., Pegram, M. and Slingerland, J. (2010) 'Lapatinib : new opportunities for management of breast cancer', pp. 79–91. doi: 10.2147/BCTT.S5929.

Lingbeek, M. E., Jacobs, J. J. L. and van Lohuizen, M. (2002) 'The T-box repressors TBX2 and TBX3 specifically regulate the tumor suppressor gene p14ARF via a variant T-site in the initiator.', *The Journal of biological chemistry*. United States, 277(29), pp. 26120–26127. doi: 10.1074/jbc.M200403200.

Liu, J., Lin, C., Gleiberman, A., Ohgi, K. A., Herman, T., Huang, H. P., Tsai, M. J. and Rosenfeld, M. G. (2001) 'Tbx19, a tissue-selective regulator of POMC gene expression.', *Proceedings of the National Academy of Sciences of the United States of America*. United States, 98(15), pp. 8674–8679. doi: 10.1073/pnas.141234898.

Lu, H., Shu, X.-O., Cui, Y., Kataoka, N., Wen, W., Cai, Q., Ruan, Z.-X., Gao, Y.-T. and Zheng, W. (2005) 'Association of genetic polymorphisms in the VEGF gene with breast cancer survival.', *Cancer research*. United States, 65(12), pp. 5015–5019. doi: 10.1158/0008-5472.CAN-04-2786.

Lu, R., Yang, A. and Jin, Y. (2011) 'Dual functions of T-box 3 (Tbx3) in the control of self-renewal and extraembryonic endoderm differentiation in mouse embryonic stem cells.', *The Journal of biological chemistry*. United States, 286(10), pp. 8425–8436. doi: 10.1074/jbc.M110.202150.

MacMurray, A. and Shin, H. S. (1988) 'The antimorphic nature of the Tc allele at the mouse T locus.', *Genetics*, 120(2), pp. 545–550.

Mahlamäki, E. H., Kauraniemi, P., Monni, O., Wolf, M., Hautaniemi, S. and Kallioniemi, A. (2004) 'High-resolution genomic and expression profiling reveals 105 putative amplification target genes in pancreatic cancer', *Neoplasia (New York, N.Y.)*. Neoplasia Press Inc., 6(5), pp. 432–439. doi: 10.1593/neo.04130.

Maira, M., Couture, C., Martelot, G. Le, Pulichino, A., Bilodeau, S. and Drouin, J. (2003) 'The T-box Factor Tpit Recruits SRC / p160 Co-activators and Mediates Hormone Action *', 278(47), pp. 46523–46532. doi: 10.1074/jbc.M305626200.

Majeed, W., Aslam, B., Javed, I., Khaliq, T., Muhammad, F., Ali, A. and Raza, A. (2014) 'Breast cancer: major risk factors and recent developments in treatment.', *Asian Pacific journal of cancer prevention : APJCP*, 15(October 2015), pp. 3353–8. doi: 10.7314/APJCP.2014.15.8.3353.

Masoud, V., Pagès, G., Masoud, V., Pagès, G. and Antipolis, S. (2017) 'World Journal of Clinical Oncology', 8(2), pp. 120–135. doi: 10.5306/wjco.v8.i2.120.

Masuda, H., Zhang, D. and Bartholomeusz, C. (2012) 'Role of epidermal growth factor receptor in breast cancer', pp. 331–345. doi: 10.1007/s10549-012-2289-9.

McCune, K., Bhat-Nakshatri, P., Thorat, M. A., Nephew, K. P., Badve, S. and Nakshatri, H. (2010) 'Prognosis of hormone-dependent breast cancers: implications of the presence of dysfunctional transcriptional networks activated by insulin via the immune transcription factor T-bet.', *Cancer research*. United States, 70(2), pp. 685–696. doi: 10.1158/0008-5472.CAN-09-1530.

Merscher, S., Funke, B., Epstein, J. A., Heyer, J., Puech, A., Lu, M. M., Xavier, R. J., Demay, M. B., Russell, R. G., Factor, S., Tokooya, K., Jore, B. S., Lopez, M., Pandita, R. K., Lia, M., Carrion, D., Xu, H., Schorle, H., Kobler, J. B., Scambler, P., Wynshaw-Boris, A., Skoultchi, A. I., Morrow, B. E. and Kucherlapati, R. (2001) 'TBX1 is responsible for cardiovascular defects in velo-cardio-facial/DiGeorge syndrome.', *Cell*. United States, 104(4), pp. 619–629.

Metherell, L. A., Savage, M. O., Dattani, M., Walker, J., Clayton, P. E., Farooqi, I. S. and Clark, A. J. L. (2004) 'TPIT mutations are associated with early-onset, but not late-onset isolated ACTH deficiency.', *European journal of endocrinology*. England, 151(4), pp. 463–465.

Miller, R. R. and Okkema, P. G. (2011) 'The Caenorhabditis elegans T-Box Factor MLS-1 Requires Groucho Co-Repressor Interaction for Uterine Muscle Specification', *PLOS Genetics*. Public Library of Science, 7(8), p. e1002210. Available at: https://doi.org/10.1371/journal.pgen.1002210.

Miller, S. A., Huang, A. C., Miazgowicz, M. M., Brassil, M. M. and Weinmann, A. S. (2008) 'Coordinated but physically separable interaction with H3K27-demethylase and H3K4-methyltransferase activities are required for T-box protein-mediated activation of developmental gene expression.', *Genes & development*. United States, 22(21), pp. 2980–2993. doi: 10.1101/gad.1689708.

Moasser, M. M. (2011) 'NIH Public Access', 26(45), pp. 6469–6487. doi: 10.1038/sj.onc.1210477.The.

Munagala, R., Aqil, F. and Gupta, R. C. (2011) 'Promising molecular targeted therapies in breast cancer', *Indian journal of pharmacology*. Medknow Publications, 43(3), pp. 236–245. doi: 10.4103/0253-7613.81497.

Mundlos, S. and Horn, D. (2014) 'Small Patella Syndrome BT - Limb Malformations: An Atlas of Genetic Disorders of Limb Development', in Mundlos, S. and Horn, D. (eds). Berlin, Heidelberg: Springer Berlin Heidelberg, pp. 146–147. doi: 10.1007/978-3-540-95928-1_56.

Murakami, M., Nakagawa, M., Olson, E. N. and Nakagawa, O. (2005) 'A WW domain protein TAZ is a critical coactivator for TBX5 , a transcription factor implicated in Holt – Oram syndrome'.

Nahta, R. and Esteva, F. J. (2006) 'HER2 therapy: molecular mechanisms of trastuzumab resistance', *Breast cancer research : BCR*. 2006/11/06. BioMed Central, 8(6), p. 215. doi: 10.1186/bcr1612.

Naiche, L. A., Harrelson, Z., Kelly, R. G. and Papaioannou, V. E. (2005) 'T-box genes in vertebrate development.', *Annual review of genetics*. United States, 39, pp. 219–239. doi: 10.1146/annurev.genet.39.073003.105925.

Nandana, S., Tripathi, M., Duan, P., Chu, C.-Y., Mishra, R., Liu, C., Jin, R., Yamashita, H., Zayzafoon, M., Bhowmick, N. A., Zhau, H. E., Matusik, R. J. and Chung, L. W. K. (2017) 'Bone Metastasis of Prostate Cancer Can Be Therapeutically Targeted at the TBX2-WNT Signaling Axis', *Cancer*

research. 2017/01/20, 77(6), pp. 1331–1344. doi: 10.1158/0008-5472.CAN-16-0497.

Nimmakayalu, M., Major, H., Sheffield, V., Solomon, D. H., Smith, R. J., Patil, S. R. and Shchelochkov, O. A. (2011) 'Microdeletion of 17q22q23.2 encompassing TBX2 and TBX4 in a patient with congenital microcephaly, thyroid duct cyst, sensorineural hearing loss, and pulmonary hypertension.', *American journal of medical genetics. Part A*. United States, 155A(2), pp. 418–423. doi: 10.1002/ajmg.a.33827.

Palena, C., Polev, D. E., Tsang, K. Y., Fernando, R. I., Litzinger, M., Krukovskaya, L. L., Baranova, A. V, Kozlov, A. P. and Schlom, J. (2007) 'The human T-box mesodermal transcription factor Brachyury is a candidate target for T-cell-mediated cancer immunotherapy.', *Clinical cancer research : an official journal of the American Association for Cancer Research*. United States, 13(8), pp. 2471–2478. doi: 10.1158/1078-0432.CCR-06-2353.

Papaioannou, V. E. (2014) 'The T-box gene family: emerging roles in development, stem cells and cancer.', *Development (Cambridge, England)*, 141(20), pp. 3819–33. doi: 10.1242/dev.104471.

Papapetrou, C., Edwards, Y. H. and Sowden, J. C. (1997) 'The T transcription factor functions as a dimer and exhibits a common human polymorphism Gly-177-Asp in the conserved DNA-binding domain.', *FEBS letters*. England, 409(2), pp. 201–206.

Park, J. C., Chae, Y. K., Son, C. H., Kim, M. S., Lee, J., Ostrow, K., Sidransky, D., Hoque, M. O. and Moon, C. (2008) 'Epigenetic silencing of human T (brachyury homologue) gene in non-small-cell lung cancer', *Biochemical and Biophysical Research Communications*, 365(2), pp. 221–226. doi: https://doi.org/10.1016/j.bbrc.2007.10.144.

Paxton, C., Zhao, H., Chin, Y., Langner, K. and Reecy, J. (2002) 'Murine Tbx2 contains domains that activate and repress gene transcription.', *Gene*. Netherlands, 283(1–2), pp. 117–124.

Pearce, E. L., Mullen, A. C., Martins, G. A., Krawczyk, C. M., Hutchins, A. S., Zediak, V. P., Banica, M., DiCioccio, C. B., Gross, D. A., Mao, C.-A., Shen, H., Cereb, N., Yang, S. Y., Lindsten, T., Rossant, J., Hunter, C. A. and Reiner, S. L. (2003) 'Control of effector CD8+ T cell function by the transcription factor Eomesodermin.', *Science (New York, N.Y.)*. United States, 302(5647), pp. 1041–1043. doi: 10.1126/science.1090148.

Peres, J., Davis, E., Mowla, S., Bennett, D. C., Li, J. A., Wansleben, S. and Prince, S. (2010) 'The highly homologous T-Box transcription factors, TBX2 and TBX3, have distinct roles in the oncogenic process', *Genes and Cancer*, 1(3), pp. 272–282. doi: 10.1177/1947601910365160.

Pflugfelder, G. O., Roth, H., Poeck, B., Kerscher, S., Schwarz, H., Jonschker, B. and Heisenberg, M. (1992) 'The lethal(1)optomotor-blind gene of Drosophila melanogaster is a major organizer of optic lobe development: isolation and characterization of the gene', *Proceedings of the National Academy of Sciences of the United States of America*, 89(4), pp. 1199–1203. Available at: https://www.ncbi.nlm.nih.gov/pubmed/1741374.

Prince, S., Carreira, S., Vance, K. W., Abrahams, A. and Goding, C. R. (2004) 'Tbx2 directly represses the expression of the p21(WAF1) cyclin-dependent kinase inhibitor.', *Cancer research*. United States, 64(5), pp. 1669–1674.

Redmond, K. L., Crawford, N. T., Farmer, H., D'Costa, Z. C., O'Brien, G. J., Buckley, N. E., Kennedy, R. D., Johnston, P. G., Harkin, D. P. and Mullan, P. B. (2010) 'T-box 2 represses NDRG1 through an EGR1-dependent mechanism to drive the proliferation of breast cancer cells.', *Oncogene*. England, 29(22), pp. 3252–3262. doi: 10.1038/onc.2010.84.

Reinert, T., Modin, C., Castano, F. M., Lamy, P., Wojdacz, T. K., Hansen, L. L., Wiuf, C., Borre, M., Dyrskjot, L. and Orntoft, T. F. (2011) 'Comprehensive genome methylation analysis in bladder cancer: identification and validation of novel methylated genes and application of these as urinary tumor markers.', *Clinical cancer research : an official journal of the American Association for Cancer Research*. United States, 17(17), pp. 5582–5592. doi: 10.1158/1078-0432.CCR-10-2659.

Renard, C.-A., Labalette, C., Armengol, C., Cougot, D., Wei, Y., Cairo, S., Pineau, P., Neuveut, C., de Reynies, A., Dejean, A., Perret, C. and Buendia, M.-A. (2007) 'Tbx3 is a downstream target of the Wnt/beta-catenin pathway and a critical mediator of beta-catenin survival functions in liver cancer.', *Cancer research*. United States, 67(3), pp. 901–910. doi: 10.1158/0008-5472.CAN-06-2344.

Reyes-Reyes, E. M., Šalipur, F. R., Shams, M., Forsthoefel, M. K. and Bates, P. J. (2015) 'Mechanistic studies of anticancer aptamer AS1411 reveal a novel role for nucleolin in regulating Rac1 activation', *Molecular Oncology*, 9(7), pp. 1392–1405. doi: https://doi.org/10.1016/j.molonc.2015.03.012.

Rodriguez, M., Aladowicz, E., Lanfrancone, L. and Goding, C. R. (2008) 'Tbx3 represses E-cadherin expression and enhances melanoma invasiveness.', *Cancer research*. United States, 68(19), pp. 7872–7881. doi: 10.1158/0008-5472.CAN-08-0301.

Roselli, M., Fernando, R. I., Guadagni, F., Spila, A., Alessandroni, J., Palmirotta, R., Costarelli, L., Litzinger, M., Hamilton, D., Huang, B., Tucker, J., Tsang, K.-Y., Schlom, J. and Palena, C. (2012) 'Brachyury, a driver of the epithelial-mesenchymal transition, is overexpressed in human lung tumors: an opportunity for novel interventions against lung cancer.', *Clinical cancer research : an official journal of the American Association for Cancer Research*. United States, 18(14), pp. 3868–3879. doi: 10.1158/1078-0432.CCR-11-3211.

Rosenbluh, J., Nijhawan, D., Cox, A. G., Li, X., Neal, J. T., Schafer, E. J., Zack, T. I., Wang, X., Tsherniak, A., Schinzel, A. C., Shao, D. D., Schumacher, S. E., Weir, B. A., Vazquez, F., Cowley, G. S., Root, D. E., Mesirov, J. P., Beroukhim, R., Kuo, C. J., Goessling, W. and Hahn, W. C. (2012) 'beta-Catenin-driven cancers require a YAP1 transcriptional complex for survival and tumorigenesis.', *Cell*. United States, 151(7), pp. 1457–1473. doi: 10.1016/j.cell.2012.11.026.

Rowley, M., Grothey, E. and Couch, F. J. (2004) 'The role of Tbx2 and Tbx3 in mammary development and tumorigenesis.', *Journal of mammary gland biology and neoplasia*. United States, 9(2), pp. 109–118. doi: 10.1023/B:JOMG.0000037156.64331.3f.

Sakabe, M., Kokubo, H., Nakajima, Y. and Saga, Y. (2012) 'Ectopic retinoic acid signaling affects outflow tract cushion development through suppression of the myocardial Tbx2-Tgfβ2 pathway', *Development*, 139(2), p. 385 LP-395. doi: 10.1242/dev.067058.

Sarkar, D., Shields, B., Davies, M. L., Muller, J. and Wakeman, J. A. (2012) 'BRACHYURY confers cancer stem cell characteristics on colorectal cancer cells.', *International journal of cancer*. United States, 130(2), pp. 328–337. doi: 10.1002/ijc.26029.

Sawyers, C. (2004) 'Targeted cancer therapy.', *Nature*, 432, pp. 294–297. doi: 10.1038/nature03095.

Scaltriti, M. and Baselga, J. (2006) 'The epidermal growth factor receptor pathway: a model for targeted therapy.', *Clinical cancer research : an official journal of the American Association for Cancer Research*. United States, 12(18), pp. 5268–5272. doi: 10.1158/1078-0432.CCR-05-1554.

Schmitt, E., Paquet, C., Beauchemin, M. and Bertrand, R. (2007) 'DNA-damage response network at the crossroads of cell-cycle checkpoints, cellular senescence and apoptosis.', *Journal of Zhejiang University. Science. B*. China, 8(6), pp. 377–397. doi: 10.1631/jzus.2007.B0377.

Senger, D. R., Galli, S. J., Dvorak, A. M., Perruzzi, C. A., Harvey, V. S. and Dvorak, H. F. (1983) 'Tumor cells secrete a vascular permeability factor that promotes accumulation of ascites fluid.', *Science (New York, N.Y.)*. United States, 219(4587), pp. 983–985.

Shimoda, M., Sugiura, T., Imajyo, I., Ishii, K., Chigita, S., Seki, K., Kobayashi, Y. and Shirasuna, K. (2012) 'The T-box transcription factor Brachyury regulates epithelial-mesenchymal transition in association with cancer stem-like cells in adenoid cystic carcinoma cells.', *BMC cancer*. England, 12, p. 377. doi: 10.1186/1471-2407-12-377.

Sinclair, C. S., Adem, C., Naderi, A., Soderberg, C. L., Johnson, M., Wu, K., Wadum, L., Couch, V. L., Sellers, T. A., Schaid, D., Slezak, J., Fredericksen, Z., Ingle, J. N., Hartmann, L., Jenkins, R. B. and Couch, F. J. (2002) 'TBX2 is preferentially amplified in BRCA1- and BRCA2-related breast tumors.', *Cancer research*. United States, 62(13), pp. 3587–3591.

Singh, M. K., Christoffels, V. M., Dias, J. M., Trowe, M.-O., Petry, M., Schuster-Gossler, K., Burger, A., Ericson, J. and Kispert, A. (2005) 'Tbx20 is essential for cardiac chamber differentiation and repression of Tbx2.', *Development (Cambridge, England)*. England, 132(12), pp. 2697–2707. doi: 10.1242/dev.01854.

Smith, J. C., Price, B. M. J., Green, J. B. A., Weigel, D. and Herrmann, B. G. (1991) 'Expression of a xenopus homolog of Brachyury (T) is an immediate-early response to mesoderm induction', *Cell*, 67(1), pp. 79–87. doi: https://doi.org/10.1016/0092-8674(91)90573-H.

Stennard, F. A., Costa, M. W., Lai, D., Biben, C., Furtado, M. B., Solloway, M. J., McCulley, D. J., Leimena, C., Preis, J. I., Dunwoodie, S. L., Elliott, D. E., Prall, O. W. J., Black, B. L., Fatkin, D. and Harvey, R. P. (2005) 'Murine T-box transcription factor Tbx20 acts as a repressor during heart development, and is essential for adult heart integrity, function and adaptation', *Development*, 132(10), p. 2451 LP-2462. doi: 10.1242/dev.01799.

Stott, D., Kispert, A. and Herrmann, B. G. (1993) 'Rescue of the tail defect of Brachyury mice', *Genes and Development*, 7(2), pp. 197–203. doi: 10.1101/gad.7.2.197.

Tada, M. and Smith, J. C. (2001) 'T-targets: clues to understanding the functions of T-box proteins.', *Development, growth & differentiation*. Japan, 43(1), pp. 1–11.

Takeuchi, J. K., Koshiba-Takeuchi, K., Matsumoto, K., Vogel-Hopker, A., Naitoh-Matsuo, M., Ogura, K., Takahashi, N., Yasuda, K. and Ogura, T. (1999) 'Tbx5 and Tbx4 genes determine the wing/leg identity of limb buds.', *Nature*. England, 398(6730), pp. 810–814. doi: 10.1038/19762.

Toxicity, L. and Management, P. (2007) 'O ncologist', 2, pp. 756–765. doi: 10.1634/theoncologist.12-7-756.

Trempus, C. S., Wei, S.-J., Humble, M. M., Dang, H., Bortner, C. D., Sifre, M. I., Kissling, G. E., Sunman, J. A., Akiyama, S. K., Roberts, J. D., Tucker, C. J., Chun, K.-S., Tennant, R. W. and Langenbach, R. (2011) 'A novel role for the T-box transcription factor Tbx1 as a negative regulator of tumor cell growth in mice.', *Molecular carcinogenesis*. United States, 50(12), pp. 981–991. doi: 10.1002/mc.20768.

Tsuruo, T., Naito, M., Tomida, A., Fujita, N., Mashima, T., Sakamoto, H. and Haga, N. (2003) 'Molecular targeting therapy of cancer : drug resistance , apoptosis and survival signal', 94(1),

pp. 15–21.

Untch, M., Rezai, M., Loibl, S., Fasching, P. A., Huober, J., Tesch, H., Bauerfeind, I., Hilfrich, J., Eidtmann, H., Gerber, B., Hanusch, C., Kuhn, T., du Bois, A., Blohmer, J.-U., Thomssen, C., Dan Costa, S., Jackisch, C., Kaufmann, M., Mehta, K. and von Minckwitz, G. (2010) 'Neoadjuvant treatment with trastuzumab in HER2-positive breast cancer: results from the GeparQuattro study.', *Journal of clinical oncology : official journal of the American Society of Clinical Oncology*. United States, 28(12), pp. 2024–2031. doi: 10.1200/JCO.2009.23.8451.

Vance, K. W., Carreira, S., Brosch, G. and Goding, C. R. (2005) 'Tbx2 is overexpressed and plays an important role in maintaining proliferation and suppression of senescence in melanomas.', *Cancer research*. United States, 65(6), pp. 2260–2268. doi: 10.1158/0008-5472.CAN-04-3045.

Vitelli, F., Viola, A., Morishima, M., Pramparo, T., Baldini, A. and Lindsay, E. (2003) 'TBX1 is required for inner ear morphogenesis.', *Human molecular genetics*. England, 12(16), pp. 2041–2048.

Washkowitz, A. J., Gavrilov, S., Begum, S. and Papaioannou, V. E. (2012) 'Diverse functional networks of Tbx3 in development and disease.', *Wiley interdisciplinary reviews. Systems biology and medicine*. United States, 4(3), pp. 273–283. doi: 10.1002/wsbm.1162.

Weidgang, C. E., Russell, R., Tata, P. R., Kuhl, S. J., Illing, A., Muller, M., Lin, Q., Brunner, C., Boeckers, T. M., Bauer, K., Kartikasari, A. E. R., Guo, Y., Radenz, M., Bernemann, C., Weiss, M., Seufferlein, T., Zenke, M., Iacovino, M., Kyba, M., Scholer, H. R., Kuhl, M., Liebau, S. and Kleger, A. (2013) 'TBX3 Directs Cell-Fate Decision toward Mesendoderm.', *Stem cell reports*. United States, 1(3), pp. 248–265. doi: 10.1016/j.stemcr.2013.08.002.

Weidner, N., Semple, J. P., Welch, W. R. and Folkman, J. (1991) 'Tumor angiogenesis and metastasis--correlation in invasive breast carcinoma.', *The New England journal of medicine*. United States, 324(1), pp. 1–8. doi: 10.1056/NEJM199101033240101.

Willmer, T., Cooper, A., Sims, D., Govender, D. and Prince, S. (2016) 'The T-box transcription factor 3 is a promising biomarker and a key regulator of the oncogenic phenotype of a diverse range of sarcoma subtypes', *Oncogenesis*, 11. doi: 10.1038/oncsis.2016.11.

Willmer, T., Hare, S., Peres, J. and Prince, S. (2016) 'The T - box transcription factor TBX3 drives proliferation by direct repression of the p21 WAF1 cyclin - dependent kinase inhibitor', *Cell Division*. BioMed Central, pp. 1–13. doi: 10.1186/s13008-016-0019-0.

Willmer, T., Peres, J., Mowla, S., Abrahams, A. and Prince, S. (2015) 'The T-box factor TBX3 is important in S-phase and is regulated by c-MYC and cyclin A-CDK2', *Cell Cycle*, 14(19), pp. 3173–3183. doi: 10.1080/15384101.2015.1080398.

Wilson, V. and Conlon, F. L. (2002) 'The T-box family.', *Genome biology*. England, 3(6), p. REVIEWS3008.

Yang, X. R., Ng, D., Alcorta, D. A., Liebsch, N. J., Sheridan, E., Li, S., Goldstein, A. M., Parry, D. M. and Kelley, M. J. (2009) 'T (brachyury) gene duplication confers major susceptibility to familial chordoma.', *Nature genetics*. United States, 41(11), pp. 1176–1178. doi: 10.1038/ng.454.

Yarden Y (2001) 'Biology of HER2 and Its Importance in Breast Cancer', *Oncology*, 61(Suppl 2), pp. 1–13.

Yarosh, W., Barrientos, T., Esmailpour, T., Lin, L., Carpenter, P. M., Osann, K., Anton-culver, H. and Huang, T. (2008) 'TBX3 Is Overexpressed in Breast Cancer and Represses p14 ARF by

Interacting with Histone Deacetylases', (3), pp. 693–700. doi: 10.1158/0008-5472.CAN-07-5012.

Yu, H., Liu, B. O., Liu, A., Li, K. and Zhao, H. (2015) 'T-box 2 expression predicts poor prognosis in gastric cancer', *Oncology letters*. 2015/06/26. D.A. Spandidos, 10(3), pp. 1689–1693. doi: 10.3892/ol.2015.3428.

Yu, J., Ma, X., Cheung, K. F., Li, X., Tian, L., Wang, S., Wu, C. W., Wu, W. K. K., He, M., Wang, M., Ng, S. S. M. and Sung, J. J. Y. (2010) 'Epigenetic inactivation of T-box transcription factor 5, a novel tumor suppressor gene, is associated with colon cancer.', *Oncogene*. England, 29(49), pp. 6464–6474. doi: 10.1038/onc.2010.370.

Yu, J. and Zhang, L. (2005) 'The transcriptional targets of p53 in apoptosis control.', *Biochemical and biophysical research communications*. United States, 331(3), pp. 851–858. doi: 10.1016/j.bbrc.2005.03.189.

Zaragoza, M. V, Lewis, L. E., Sun, G., Wang, E., Li, L., Said-Salman, I., Feucht, L. and Huang, T. (2004) 'Identification of the TBX5 transactivating domain and the nuclear localization signal', *Gene*, 330, p. 9—18. doi: 10.1016/j.gene.2004.01.017.

Zhang, Z., Cerrato, F., Xu, H., Vitelli, F., Morishima, M., Vincentz, J., Furuta, Y., Ma, L., Martin, J. F., Baldini, A. and Lindsay, E. (2005) 'Tbx1 expression in pharyngeal epithelia is necessary for pharyngeal arch artery development.', *Development (Cambridge, England)*. England, 132(23), pp. 5307–5315. doi: 10.1242/dev.02086.

Zong, M., Jia, L. and Li, L. (2013) 'Expression of novel tumor markers of pancreatic adenocarcinomas in intrahepatic cholangiocarcinomas', *OncoTargets and therapy*. Dove Medical Press, 6, pp. 19–23. doi: 10.2147/OTT.S39646.

Zong, M., Meng, M. and Li, L. (2011) 'Low expression of TBX4 predicts poor prognosis in patients with stage II pancreatic ductal adenocarcinoma.', *International journal of molecular sciences*. Switzerland, 12(8), pp. 4953–4963. doi: 10.3390/ijms12084953.

CHAPTER 6

Appendix

6.1. Plasmids and constructs

6.1.1. pCMV-3XFLAG (Addgene):

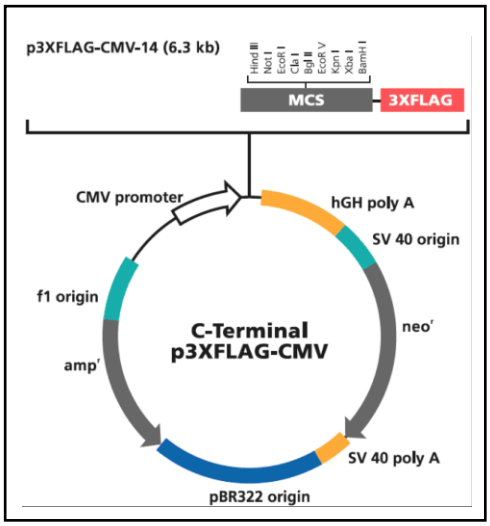

6.1.2. pEGFP-C1 nucleolin (Addgene):

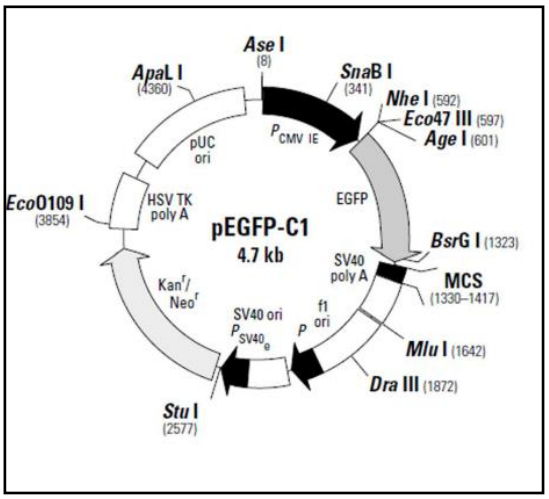

6.2. Cell culture mounting fluid

Mycoplasma test mounting fluid

20 mM Citric acid

55 mM Na2HPO4.2H2O

50% Glycerol

pH to 5.5 and store at 4°C

6.3. Subcellular fractionation

Solution 1:

20mM PIPES pH 6.8

1mM EGTA pH 6.8

1mM MgCl2

25X Proteinase inhibitor cocktail tablets

Phosphatase inhibitors:

1mM NaOrthovanadate

1mM NaF

Solution 2:

100 mM KCl

300 mM Sucrose

10mM PIPES pH 6.8

1mM EGTA pH 6.8

3mM MgCl2

25X Proteinase inhibitor cocktail tablets

Phosphatase inhibitors:

1mM NaOrthovanadate

1mM NaF

6.4. Affinity purification assays

FLAG-lysis buffer

50 mM Tris HCl, pH 7.4

150 mM NaCl

1 mM EDTA

1% TRITON X-100

Protease inhibitors were added before use:

2 µg/ml aprotinin

0.7 µg/ml pepstatin A

2 mM NaF

0.2 mM phenylmethanesulphonyl fluoride (PMSF)

6.5. Protein harvesting and western blotting

2 X Laemmli lysis buffer: 10ml

1M Tris-HCL, pH 6.8

4ml 10% SDS

1ml β-mercaptoethanol

2ml glycerol

1.75ml dH2O

Pinch of bromophenol blue

Store at -20°C or at room temperature

Sodium Dodecyl Sulphate (SDS)-polyacrylamide gels

Acryl-bisacryl-amide mix (30:08)

29 g acrylamide

1g N,N`-methylenebisacrylamide

Make up to 100 ml, heat at 37°C to dissolve chemicals.

Store at 4°C, protected from light

10% Sodium docecyl sulphate (SDS)

100g SDS

Make up to 1L with dH20, pH to 7.2

Store at RT

10% Ammonium persulphate (APS)

0.1g ammonium persulphate

Make solution up to 1ml with dH20

Store at 4°C

Resolving gel:

Acryl-bisacryl-amide mix (30:08) (percentage depending on size of protein of interest)
0.375

M Tris (pH 8.8)

0.1% SDS

0.01% TEMED

141

0.1% Ammonium persulphate

Stacking gel:

5% Acryl-bisacryl-amide mix (30:08)

0.192 M Tris (pH6.8)

0.1% SDS

0.01% TEMED

0.1% Ammonium persulphate

10X running buffer:

10g SDS

30g Tris

144g Glycine pH to 8.3 and make solution up to 1L with dH20

For use dilute to 1 X (100ml 10X PBS; make up to 1L with dH20)

Store at room temperature

10X Transfer buffer:

38g Tris

144g Glycine

Make solution up to 1L with dH20 and store at 4°C

For use dilute 1 X (100ml 10 X Transfer Buffer, 200ml Isopropanol and 700ml dH20)

Store at 4°C

Phosphate buffered saline (PBS)/0.1% Tween

10X PBS:

80g NaCl

26.8g Na2HPO4.12H20

2g KCI

2.4g KH2PO4

Make up to 1L, pH to 6.9 and autoclave

For use dilute to 1 X (100ml 10X PBS; make up to 1L with dH20)

PBS/0.1% Tween:

For membrane washes, add 0.1% Tween to 1X PBS

2 X Protein loading dye:

125 mM Tris-HCl, pH 6.5

0.4% SDS

10% β-mercaptoethanol

20% glycerol

5 X Protein loading dye:

10% glycerol

1% SDS

0.25M Tris-Cl, pH 6.8

3mg Bromophenol blue

5% PBS/T milk

5% powder milk (w/v)

Make up to 100ml with 1 XPBS/0.1% Tween-20

Store at 4°C

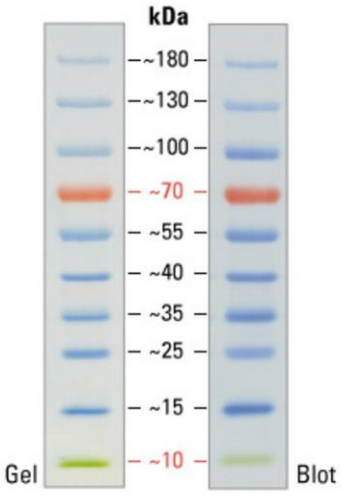

Figure 6.1: PageRuler Pre-stained Protein Marker

6.6. Filter aided sample preparation (FASP*)*

UT buffer

8 M urea

0.1 M Tris, pH 8.5

ABC buffer

50 mM ammonium bicarbonate buffer, pH 8

SHARON PRINCE
MSC SUPERVISOR
22nd FEBRUARY 2019

ncbste003:TURNITIN_VER1.pdf

ORIGINALITY REPORT

28%	15%	7%	18%
SIMILARITY INDEX	INTERNET SOURCES	PUBLICATIONS	STUDENT PAPERS

PRIMARY SOURCES

1	Submitted to University of Cape Town Student Paper	14%
2	www.cansa.org.za Internet Source	1%
3	Wansleben, Sabina, Jade Peres, Shannagh Hare, Colin R. Goding, and Sharon Prince. "T-box transcription factors in cancer biology", Biochimica et Biophysica Acta (BBA) - Reviews on Cancer, 2014. Publication	1%
4	Clemens Hermann, Alexander D. Giddey, Andrew J.M. Nel, Nelson C. Soares, Jonathan M. Blackburn. "Gel-free sample preparation techniques and bioinformatic enrichment analysis to in depth characterise the cell wall proteome of mycobacteria", MethodsX, 2018 Publication	1%
5	open.uct.ac.za Internet Source	<1%
	effiloop.com	